PLASTICITY IN THE RAPID ESCAPE REFLEX OF THE ANNELID WORM,

Lumbriculus variegatus

A Dissertation

by

ZANE RYAN LYBRAND

Submitted to the Office of Graduate Studies of
Texas A&M University
in partial fulfillment of the requirements for the degree of

DOCTOR OF PHILOSOPHY

August 2012

Major Subject: Zoology

Plasticity in the Rapid Escape Reflex of the Annelid Worm, *Lumbriculus variegatus*

PLASTICITY IN THE RAPID ESCAPE REFLEX OF THE ANNELID WORM,

Lumbriculus variegatus

A Dissertation

by

ZANE RYAN LYBRAND

Submitted to the Office of Graduate Studies of
Texas A&M University
in partial fulfillment of the requirements for the degree of

DOCTOR OF PHILOSOPHY

Approved by:

Chair of Committee,	Mark J. Zoran
Committee Members,	Duncan S. MacKenzie
	Robyn Lints
	William H. Griffith
Head of Department,	U.J. McMahan

August 2012

Major Subject: Zoology

ABSTRACT

Plasticity in the Rapid Escape Reflex of the Annelid Worm, *Lumbriculus variegatus*.

(August 2012)

Zane Ryan Lybrand, B.S., Texas A&M University

Chair of Advisory Committee: Dr. Mark J. Zoran

Neural plasticity is the process by which anatomical (structural) and physiological (functional) changes in the nervous system of an organism lead to alterations in behavior. This dissertation examines the structural and functional changes that occur during neural morphallaxis, a rare form of neural plasticity, in the annelid worm, *Lumbriculus variegatus*. Neural morphallaxis involves the reorganization of the animal's nervous system during segmental regeneration following injury. Here, I have examined neural morphallaxis of the giant fiber pathway, which mediates rapid escape reflex behaviors in *Lumbriculus*. Electrophysiological recording techniques, immunohistochemistry, and transmission electron microscopy were used to demonstrate that prior to injury and neural morphallactic regeneration, activation of the escape reflex neural circuitry is nonfunctional in specific regions of the worm's nervous system. Following body fragmentation, neural circuits underlying specific escape responses rapidly become functional. The speed of functional changes in sensory-to-giant interneuron physiology, less than 24 hours, did not coincide with significant anatomical changes to sensory afferent synapses, suggesting a role for the unsilencing of existing

sensory synapses. Furthermore, I have discovered and described a sensory interneuron system that mediates sensory inputs via electrical synapses onto the giant interneuron pathway. This finding led to my hypothesis that the site of sensory plasticity during neural morphallaxis is not at the giant axon, but rather at the glutamatergic synapses between sensory neurons and their sensory interneuron targets. Results from this dissertation demonstrate that sensory inputs onto the giant interneuron pathway are functionally silent prior to neural morphallaxis and the awakening of ineffective synapses occurred rapidly, within hours, following injury. Neural morphallactic plasticity was determined to occur at glutamatergic synapses onto bilaterally paired sensory interneurons that were coupled to the giant interneuronal pathway. The early phase of morphallaxis is then followed by gradual structural and functional changes to enhance aspects of the escape response network. This research provides a foundation for future studies of the mechanisms underlying neural morphallactic regeneration in *Lumbriculus variegatus* and provides comparative insight into the evolution and plasticity of neural circuit underlying discrete animal behavior.

If you done it, it ain't bragging.

– Walt Whitman

ACKNOWLEDGEMENTS

I would like to thank a number of people for the support and guidance through my graduate studies. First and foremost I want to thank my advisor, Dr. Mark Zoran. Your guidance, support, and constructive criticisms have made me the scientist that I am today. I also would like to thank the members of my advisory committee, Dr. Duncan MacKenzie, Dr. Robyn Lints, and Dr. William Griffith, for the feedback and direction in my dissertation research from the very beginning of my graduate studies.

Acknowledgements must be made to Dr. Veronica Martinez-Acosta. She prepared many of the preparations that proved critical for the anatomy of this project. Thank you, Veronica. Without you, it would have taken me forever to finish these experiments. I would also like to acknowledge Rick Littleton at the Texas A&M Microscopy and Imaging Center for his guidance on use of imaging equipment. Thank you to the expertise of the lab of Dr. Jack McMahan. Dr. Joseph Szule and Mr. Robert Marshall have been fundamental in my expedition through the ultrastructure of the ventral nerve cord. I am so fortunate to have advice from world experts on synaptic morphology.

During all my journeys and adventures, I have had three stalwart companions that have remained tried and true, Alisa, Jarret, and Jeffrey. I consider y'all colleagues, but more so, my closest friends. Through late night Prelim Training Sessions (PTS), countless conference meetings, and deep philosophical discussions on pop-culture and

Jim Rome shenanigans, I have countless experiences that I will take with me for the rest of my life.

To my family, I'd like to thank you for your support. I hope I've made you proud. Your love has given me the confidence and freedom to achieve my dreams. For that, I can not thank you enough. Because of you, I am the man I am today.

Last but certainly not least, I owe so much to Mary-Colette. Sweetheart, I know I've been difficult. Without you though, I could not have finished this dissertation. Your unconditional love, support, and encouragement, has kept me going. You have pushed me further than I could ever push myself. Thank you and I love you.

TABLE OF CONTENTS

CHAPTER Page

LIST OF FIGURES

LIST OF TABLES

CHAPTER I

INTRODUCTION

Originally coined by the psychologist and philosopher William James, "neural plasticity" was used to define alterations in the nervous system to explain changes in behavior (James, 1890). Fundamental studies, in the late 19th century, detailing the microanatomy, development, and regeneration of the nervous system by Santiago Ramon y Cajal attributed these changes to the communication between two neurons (DeFelipe, 2006). Since then neural plasticity has been studied with respect to countless aspects of neural development, learning and memory, and neural regeneration (Baudry et al., 1999). Some of the most extensively studied examples of neural plasticity are the long-term cellular and molecular changes in synaptic strengthening and weakening, or long-term potentiation (LTP) and depression (LTD). These phenomena are now commonly accepted as a basis for synaptic changes associated with long-term memory formation (Kullmann and Lamsa, 2007). Development of the visual cortex uses a form of activity-dependent synaptic plasticity. Seminal experiments on kittens demonstrated that, during a critical period of development, ocular deprivation causes structural changes in striate cortex (V1) organization (Hubel and Wiesel, 1970). Ineffective synapses were pruned away leaving only those capable of relaying functional signals (Bourne, 2010). Neural plasticity is also paramount to mammalian spinal cord

regeneration. A number of morphogens, or secreted proteins, that aid in axon guidance have also been implicated in spinal cord synaptic plasticity (Onifer et al., 2011). Neural plasticity, in many forms, is a fundamental aspect of nervous system function, development, and repair.

A rare form of neural plasticity has been identified in the aquatic annelid worm *Lumbriculus variegatus* (Drewes and Fourtner, 1990). In response to injury or asexual reproduction, *Lumbriculus* will undergo a form of regeneration called neural morphallaxis, which involves the reorganization of the giant fiber pathways that mediate rapid escape reflexes. During neural morphallactic regeneration, the structure (anatomy) and function (physiology) of sensory inputs to the giant fibers rapidly change their functional communication. I have hypothesized that neural morphallactic plasticity involves the awakening of non-functional synapses, a class of neural connections in vertebrates and invertebrates know as silent synapses.

Silent synapses and neural plasticity

A pervasive mechanism of neural plasticity is the recruitment of silent synapses. By definition, a silent synapse is an ineffective synapse that is structurally present yet physiologically nonfunctional. Originally identified by Patrick Wall and Eugene Merrill, stimulation of primary afferent sensory fibers failed to activate postsynaptic spinal cord neurons in cats. These sensory afferent synapses were identified as “ineffective synapses” because after transection of a subset of presynaptic fibers the previously silenced fibers became functional (Merrill and Wall, 1972; Wall, 1977). Since then

evidence for silent synapses has been identified in a wide range of animal systems (Atwood and Wojtowicz, 1999).

One of the earliest definitive examples of silent synapses was found in the motor neurons of the crayfish, *Procambarus clarkii.* Ultrastructural reconstruction of the crayfish neuromuscular junction identified a large number of synaptic boutons (Jahromi and Atwood, 1974; Wojtowicz et al., 1994; Cooper et al., 1995). Quantal analysis of synaptic transmission indicated that quantal content (i.e., amount of neurotransmitter released) was low. However, following high frequency stimulation, the quantal content was increased (Wojtowicz et al., 1994) from an unsilencing of nonfunctional synapses. These and other classic studies in invertebrates demonstrated that silent synapses could be awakened in an activity-dependent manner.

Around the same time, silent synapses were identified in the central nervous system (CNS) of a vertebrate. In goldfish, a powerful escape reflex is mediated by a pair of neurons in the hindbrain, called Mauthner cells (M cells), each receiving inputs from glycinergic interneurons. Paired recordings demonstrated a high percentage of postsynaptic failures of synaptic transmission (Faber et al., 1991). Following iontophoresis of cAMP into the lateral dendrite of the M cell, the glycinergic interneuron was functionally awakened and excitatory postsynaptic potentials were increased (Wolszon and Faber, 1989). These were critical studies that not only identified silent synapses within in the CNS, but also demonstrated for the first time a postsynaptic mechanism for unsilencing these synapses.

Possibly the most notorious silent synapse was found within the CA1 subfield of the rat hippocampus. Pyramidal neurons of the CA1 are activated by excitatory glutamatergic inputs from Schaffer collaterals. Both NMDA receptors (NMDAR) and AMPA receptors (NMDAR) are expressed on the postsynaptic dendritic spines of the CA1. These receptors are both activated by the binding of glutamate. However, NMDA receptors have slower activation kinetics. Due to a voltage-dependent magnesium plug mechanism, the NMDAR requires a synchronous depolarization and binding of glutamate (Kerchner and Nicoll, 2008). Therefore, silent synapses appear abundant in a diverse range of taxa, from the neural muscular junction of crustaceans to specialized regions governing special memory in the mammalian brain.

Postsynaptic mechanisms for silent synapses

A paramount feature of hippocampal long-term potentiation (LTP) is the postsynaptic recruitment of new AMPAR to dendritic spines and this mechanism is the cellular basis of physiological gain-of-function at hippocampal silent synapses. Furthermore, the recruitment of AMPAR mediated excitatory postsynaptic currents (EPSCs) is completely abolished by the NMDAR antagonist, APV. Taken together, these studies suggest that at rest silent synapses lack significant numbers of functional AMPA receptors and via an LTP-mediated mechanism are unsilenced by the emergence of AMPAR-mediated electrical signaling (Liao et al., 1995; Isaac et al., 1999).

The most direct evidence for silent synapses supports this mechanism based on postsynaptic modifications. The emerging AMPA receptor mediated currents recorded in

unsilenced synapses have been shown to coincide with the rapid appearance of immunostained AMPARs on dendritic spines of hippocampal cultured neurons (Liao et al., 2001; Lu et al., 2001; Pickard et al., 2001), as well as in intact CA1 spines using electron microscopy (Takumi et al., 1999; Racca et al., 2000). Thus, silent synapses are, in part, mediated by the absence of functional postsynaptic AMPA receptors and these hippocampal synapses become functional upon the recruitment of these postsynaptic signaling molecules.

Presynaptic mechanisms of silent synapses

While the identification of silent synapses in numerous systems is well accepted, there remains a debate on the mechanism by which a synapse is silenced and subsequently unsilenced. It is supposed that presynaptic mechanisms of silent synapses are a product of a disruption to the process of synaptic transmission (Voronin and Cherubini, 2004). By releasing a reduced amount of neurotransmitter (NT), likely by lowering quantal content, the concentration of NT available for postsynaptic membrane depolarization in response to presynaptic activation is insufficient. In whole-cell patch-clamp recordings of hippocampal neuron cell cultures, glutamate was iontophoretically released at either a slow, long duration or a short, fast duration. Following a quick application of glutamate, AMPA receptor-mediated EPSCs emerged, suggesting that the speed and concentration at which glutamate is delivered to the synapse mediates its unsilencing (Renger et al., 2001). A popular presynaptic mechanism by which glutamate concentrations change synaptically is known as a “glutamate spillover”. NMDA-

mediated EPSCs recorded from hippocampal silent synapses are thought to be a result of glutamate "spilling over" from neighboring functional synapses. Following a high frequency stimulus, AMPA receptor currents emerge (Kullmann et al., 1996). While there appears to be no direct evidence of extracellular glutamate from neighboring synapses, it remains a compelling idea. While little direct evidence supports a mechanism by which synapses are presynaptically silenced, it is clear that modifications to the release of neurotransmitter have direct affects on the recruitment of AMPA-mediated postsynaptic currents.

Regeneration in *Lumbriculus variegatus* as a model for neural plasticity

Lumbriculus variegatus is an aquatic oligochaete that inhabits the shallows of freshwater lakes, ponds and marshes of temperate climates. Commonly known as the California mudworm, it can typically be found with its head burrowed into the mud leaving its tail extended up into the water column. The tail will be crooked to lie along the air-water boundary line, which will aid in respiration due to modifications for gas exchange in the tail (Brinkhurst and Jamieson, 1971). This behavior increases exposure to predatory attacks. Thus, *Lumbriculus* has evolved rapid escape reflexes, which consist of neural circuits that trigger anterior and posterior shortening (i.e., head and tail withdrawal behaviors), allowing the quick withdrawal of its body away from potential threats of segmental injury or death. The tail withdrawal reflex is elicited by a tactile stimulus to body segments within a sensory field comprising approximately 70% of the posterior region. Another sensory field for head withdrawal reflex activation exists in

the anterior 40% portion of the worm. There is also a small region of sensory field overlap located at approximately the 1/3-2/3 body segment boundary (Drewes and Fourtner, 1990).

Neural morphallaxis in *Lumbriculus* involves changes in these sensory fields. Tactile stimulation to fragments cut from the posterior segments of the worm will initiate a tail withdrawal reflex. During neural morphallactic regeneration, segments that will become the new head transform their nervous system such that a tactile stimulus will then activate a head withdrawal behavior. I hypothesized that shifts in sensory fields during neural morphallaxis are mediated by silent synapses. Therefore, to further understand the studies conducted to test this hypothesis, a basic understanding of *Lumbriculus* neuroanatomy, neurophysiology, and regeneration following injury is required.

Neural anatomy of *Lumbriculus variegatus*

The oligochaete nervous system consists of two main parts: the brain and the ventral nerve cord. The brain is a complex bilobed cerebral ganglion of higher order neurons located just dorsal to the buccal cavity (Brinkhurst and Jamieson, 1971). Running along the anterior-posterior axis, the ventral nerve cord (VNC) contains three giant fibers, one medial giant fiber (MGF) that is flanked by two lateral giant fibers (LGF). Other than the giant fiber cell bodies, the VNC is composed of other interneurons, sensory and motor neuron cell bodies and the neuropile, a complex entanglement made up of dendrites, axons, synapses and their supportive glial cells

(Jamieson, 1981). At each segment, four pairs of lateral nerves project from the VNC and innervate the body wall. Giant fibers themselves are composed of individual interneurons located in each segment linked together to form a "chain of giant axons" (Günther and Walther, 1971; Zoran and Drewes, 1987). The axon of each giant interneuron is linked at a septum to neighboring axons via gap junctions forming a through-conducting pathway. Cell bodies for the MGF are located ventral to the giant fibers and extend their axons dorsally to expand into a giant axon. The cell bodies for the LGFs are located on opposite sides of the nerve cord and send axons into the contralateral neuropile. The LGFs are interconnected by cross-bridges, which result in a bilateral synchronization of interneuronal action potentials (Drewes, 1984).

The ultrastructure of the giant fibers is fundamentally different in anterior versus posterior regions of the animal. *Eisenia foetida* and *Lumbricus terrestris*, two terrestrial oligochaetes, have three to four collaterals that project from the giant interneuron through a myelin-like sheath into the neuropile. It is at these collaterals that connections from sensory afferents (inputs) and to motor efferents (outputs) are thought to exist (Gunther and Schurmann, 1973; Drewes, 1984). Unmyelinated nodes in *Lumbricus terrestris* and collaterals identified on the LGF of the tubificid worm *Branchiura sowerbyi,* are thought to aid in saltatory conduction of action potentials down the giant fiber (Gunther, 1976; Zoran et al., 1988). Sensory inputs onto the MGF are restricted to the anterior region of the animal and constitute the MGF sensory field, which governs the head withdrawal reflex. Conversely, sensory inputs onto the LGFs are restricted to the posterior 2/3 of the animal and constitute the LGF sensory field (see Figure 1). In *L.*

variegatus, the axonal diameter of the MGF in the anterior portion of the worm is larger and decreases in size posteriorly, while the converse is true for the LGF axonal diameter. Little histology has been done on the ultrastructure of the giant fibers in *L. variegatus*; however, the neuroanatomy appears highly conserved within the Class Oligochaeta, so one could speculate on the homology between the different species.

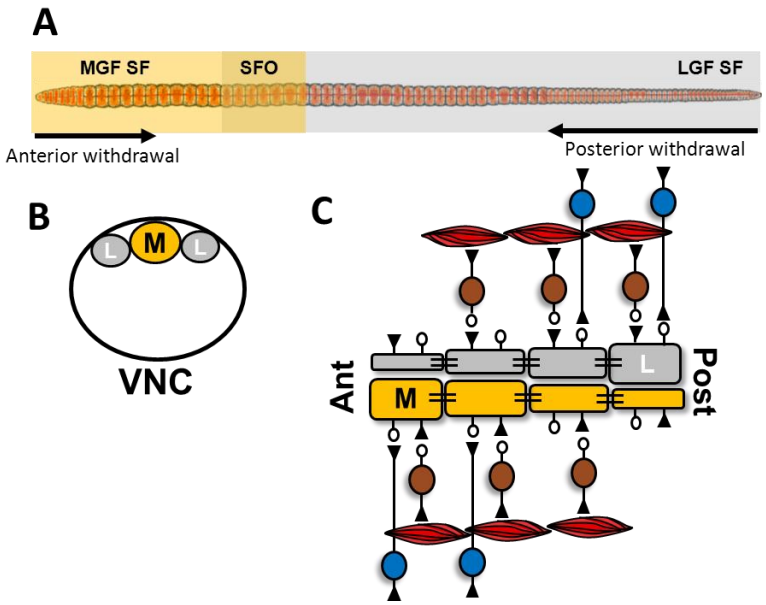

Figure 1. Neuroanatomy of sensory fields in *Lumbriculus variegatus.* A) Touch stimulation of segments in the anterior 1/3 of the worm activates the medial giant fiber sensory field, driving an anterior withdrawal behavior (MGF SF). Similarly stimulation of the posterior 2/3 activates the lateral giant fiber sensory fields driving a posterior withdrawal behavior (LGF SF) and there is a small region of sensory field overlap (SFO) where stimulation activates both MGF and LGF sensory fields and simultaneous withdrawal of anterior and posterior ends. B) Cross section of the ventral nerve cord (VNC) shows the location of the MGF flanked by two LGF. C) A schematic of the neural circuitry underlying the sensory fields. Sensory inputs in the anterior (Ant) regions activate the MGF interneuron. Similarly sensory inputs in the posterior region activate the LGF interneuronal pathway Adapted from Zoran and Martinez, 2009.

Regeneration and neural morphallaxis

The capacity for regeneration is widespread among species of the phylum Annelida. *Lumbriculus* in particular has been shown to regenerate a completely new animal from a fragment of only a few segments (Berrill, 1952) and is known to regenerate a new head of approximately 8 segments when the fragment is taken from anywhere along the body axis (Drewes and Fourtner, 1990). Regeneration of lost body parts occurs in two separate modes: epimorphosis and morphallaxis (Morgan, 1901). Epimorphosis is described as the dedifferentiation of cells at the site of injury followed by stem cell population activation and the formation of a blastema and eventually new bud tissues. Morphallaxis on the other hand, involves the reorganization of extant tissue without the differentiation of stem cell populations. Both modes work in concert with each other in order to ensure the survival of the organism. For instance, in the case of an anterior amputation from a predatory attack, the epimorphic budding of newly formed head segments is accompanied by a morphallactic shift of segments, with a segmental identity previously posterior taking on a new anterior position and identity.

Over the past two decades, *L. variegatus* has been an ideal model for studying neural morphallaxis. Drewes and Fourtner (1990) originally described neural morphallaxis in *Lumbriculus* through the definition of three characteristic features of the regenerative process. First, in fragments of 30 segments taken from the posterior quarter of the worm, they monitored the shifting of giant fiber sensory fields. The LGF sensory field slowly shifted posteriorly as the newly organized MGF sensory field emerged in the anterior regions of a regenerating fragment. This behavioral characteristic of

morphallaxis was attributed to changes in neural pathways, although these circuits and their plasticity remained undefined. A second characteristic they described was a functional change in the conduction velocity of the giant fibers. Using an extracellular recording grid to monitor action potentials through the body wall of posterior fragments, the conduction velocity was recorded for both the MGF and LGF over the course of neural morphallaxis. At 7 days after injury there was no significant difference between conduction velocities of the MGF and LGF, however between days 7 and 28 there was a gradual increase in MGF conduction velocity and decrease in LGF conduction velocity. No evaluation of the first week of morphallaxis was conducted with respect to changes in conduction velocity or sensory fields were performed. Therefore, the timeframe for first emergence of neurophysiological changes during neural morphallaxis remained unknown. The third characteristic of morphallaxis that Drewes and Fourtner (1990) described was a structural change in giant fiber diameter. Histological cross-sections taken from control animals indicated that the MGF had a larger caliber in the anterior region and the LGF had a larger caliber in the posterior region. In sections taken from posterior morphallactic fragments, there was a noticeable change in caliber to more intermediate values, indicative of the new positional identity of that fragment's segments. No other ultrastructural features of the escape neural circuit were examined prior to or following neural morphallaxis. Therefore, one aspect of the current work is to fill some of these gaps in our existing knowledge of this worm's morphallactic neural plasticity.

Molecular changes during neural morphallaxis

More recent work has investigated additional cellular and molecular changes during neural morphallaxis in *Lumbriculus*. Martinez et al., (2005), using a monoclonal antibody generated against a leech glycoepitope (i.e., the Lan 3-2 epitope; Zipser and McKay, 1981), demonstrated that multiple proteins possessing this epitope are differentially altered in their expression during neural morphallaxis. One such protein, named morphallaxis protein 66 (MP66) due to its approximate size of 66 kDa, was markedly upregulated during the exact time frame of neural morphallaxis, both following injury and in advance of asexual fission (Martinez et al., 2005; Martinez et al., 2006). Furthermore, hot spots of Lan3-2 immunostaining were identified along the giant axons, which were regularly spaced at intervals that correlated with those of the giant axon collaterals identified with Lucifer yellow dye injection. This observation was of particular interest because the Lan3-2 glycoepitope is a surface marker of sensory afferent neurons in leech and is required for their appropriate developmental collateral branching and synaptogenesis in the CNS (Tai and Zipser, 1998).

The chemical structure of the Lan3-2 glycoepitope consists of a beta-(1,4)-linked mannopyranose (Huang et al., 2008) and in the leech nervous system the Lan3-2 epitope has been shown to be an *N*-linked glycosylation of the ectodomain of the protein tractin (Bajt et al., 1990; Xu et al., 2003). Tractin is the leech homologue of the phylogenetically conserved family of L1-like neural cell adhesion molecules (L1CAMs). L1CAMs are immunoglobulin superfamily cell adhesion molecules that, as transmembrane molecules, participate in connecting their extracellular binding with the

intracellular cytoskeleton via adaptor molecules. The Lan3-2 glycoepitope is also expressed on the cell surface of neurons in nematode worms, suggesting the ancient nature of this epitope in neural function (Vansteenhouse et al., 2010). In *Lumbriculus*, Lan 3-2 labeled periaxonal regions on the extracellular surface of the giant axons and glial-like sheaths. Still, it remained to be determined whether or not the Lan3-2 epitope is expressed at synapses of the escape neural circuit.

Nervous system reorganization

Neural morphallaxis in *Lumbriculus*, with respect to the shift of giant fiber sensory fields, involves the reorganization of the two disparate escape neural pathways. Prior to neural morphallaxis, posterior fragments are governed entirely by the LGF escape neural pathway. During neural morphallaxis, sensory activation of the LGF is lost in the anterior portion of the fragment and activation of the MGF pathway emerges (Drewes and Fourtner, 1990). Still, the cellular mechanism of nervous system remodeling is unknown for neural morphallaxis. Synaptogenesis, silent synapses and neural pathway inhibition are just a few examples of neural mechanisms that might underlie this rare form of regenerative plasticity in *Lumbriculus.*

Wiring or rewiring a nervous system, whether vertebrate or invertebrate, requires an orchestration of diffusible extracellular matrix-associated and surface-bound factors that enable the presynaptic growth cone to seek out and connect to its proper postsynaptic target. Once a potential site is chosen, synapse formation begins. Presynaptic molecules are secreted (e.g., agrin, glutamate, acetylcholine) and with the

appropriate receptors in place, a signaling cascade is activated clustering postsynaptic receptors and scaffolding proteins forming a mature synapse (Munno and Syed, 2003). Early in the development of neural pathways, growth cones release neurotransmitter to find appropriate target sites. Prior to synapse formation, the growth cone of a motor neuron synthesizes and releases neurotransmitter before it contacts a target cell (Fischbach et al., 1978). Thus, during synaptogenesis, synapses are functional hours, days, or even weeks prior to the structure of the synapse emerges (Kullberg et al., 1977; Dennis et al., 1981). Therefore, 'silent' synapses are prevalent during nervous system development and, perhaps, are largely restricted to events of adult neural plasticity. In the case of segmental regeneration in *Lumbriculus*, the process of neural morphallaxis itself is quite rare, and thus this system provides a unique opportunity to study the cellular mechanisms underpinning the silencing and unsilencing of mature synapses (Fig. 2A). In principle, a silent synapse is deficient in either presynaptic or postsynaptic machinery, as mentioned earlier, and is unable to effectively communicate information at these connections (Voronin and Cherubini, 2004). Several examples have identified the role of silent synapses in animal behavior and the mechanisms underlying their neural circuit modulation, from crustaceans (Jahromi and Atwood, 1974), fish (Faber et al., 1991), to mammals (Isaac et al., 1995; Liao et al., 1995), suggesting that silent synapses are a highly conserved mechanism of neural plasticity (Fig. 2 B and C).

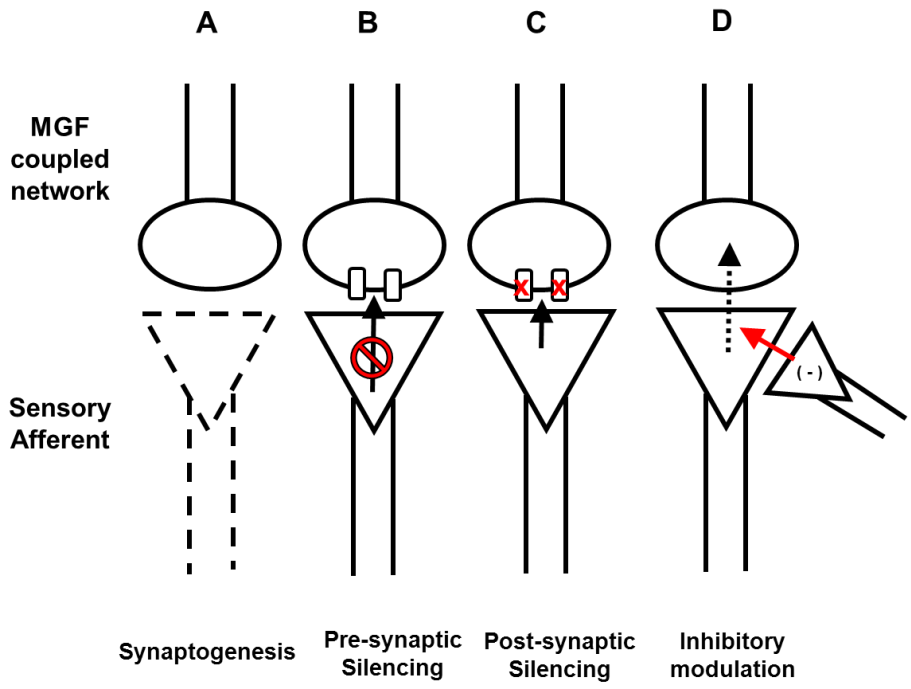

Figure 2. Possible mechanisms for silent synapses. A) Synaptogenesis, or the formation of new synapses, can lead to the silencing of non-functional synapses. B) Presynaptic silencing of a synapses stems from a failure to release sufficient neurotransmitter. C) Similarly, postsynaptic mechanisms for silent synapses result from a lack of receptors on the postsynaptic neuron. D) A modulatory interneuron can inhibit the presynaptic neuron, preventing the synapse from sufficiently communicating.

I have hypothesized that silent sensory synapses of *Lumbriculus* are present throughout the worm's life, but in a vast number of segments these synapses are ineffective.

Another potential mechanism by which synapses of the *Lumbriculus* nervous system could be silent and subsequently awakened is by the presence of an opposing inhibitory neuron onto the sensory inputs of the giant fiber pathways. Neural morphallaxis might be a process that selectively removes this inhibition. A similar mechanism has been identified during metamorphosis of many holometabolans (e.g.,

tobacco hornworm moth, *Manduca sexta*), where motor neurons are born during embryogenesis and persist through the worm-like larval stage to function in the adult moth. Lateral movements of the caterpillar are in part controlled by the ipsilateral stretch receptor (SR-3) that innervates the ipsilateral motor neuron. Prior to metamorphosis, this synapse is inhibitory. However, after metamorphosis, the inhibition is removed and the motor neurons are able to coordinate abdominal muscle movements (Levine and Truman, 1982). Thus, other inhibitory interneurons could prevent the activation of giant fiber pathways and it is the silencing of these modulatory interneurons that function to modify the neural circuitry that mediates the escape reflexes (Fig. 2D)

Objectives of the dissertation research

Plasticity in the rapid escape reflex of *Lumbriculus variegatus* was originally described as a functional reorganization of neural pathways following segmental fragmentation (Drewes and Fourtner, 1990). Cellular and molecular studies of neural morphallaxis suggested that this type of regeneration is a rare form of synaptic plasticity (Martinez et al., 2005; Martinez et al., 2006). Nonetheless, no studies of the modulation of synaptic physiology in this species have been conducted. The focus of this study, therefore, was to characterize the functional and structural changes in the neural pathways of *Lumbriculus variegatus* that are reorganized during neural morphallactic plasticity. The general hypothesis of this thesis is that neural morphallaxis is mediated by the unsilencing of sensory inputs of the giant interneuronal circuits that govern the rapid escape reflex.

Specific aims of chapters

Chapter II

Neural morphallaxis is characterized by a functional remodeling in the activation of the giant fiber pathways. Extracellular and intracellular electrophysiological recordings demonstrated changes in the functional activation of the giant fibers mediating the neurobehavioral changes underlying neural morphallaxis. Functional synaptic transmission at the sensory-to-giant interneuron was undetected prior to segmental amputation, but rapidly emerged following one day of morphallactic regeneration. Neural morphallactic regeneration varied along the anterior-posterior axis and activation of MGF pathway emerged more rapidly in more anterior segments of the tail. Simultaneous activation of the medial giant fiber and lateral giant fiber occurred for a transient period of time. Therefore, neural morphallaxis of the sensory-to-medial giant interneuron is mediated by synaptic plasticity. Data from this chapter has been accepted for publication in *Developmental Neurobiology* (Lybrand and Zoran, 2012).

Chapter III

To further understand the anatomy and physiology of the medial giant fiber pathway, synaptic changes of the sensory input to the MGF pathway were characterized during neural morphallaxis. Current-clamp electrophysiology demonstrated that sensory activation of the MGF pathway was inhibited by a specific glutamate receptor

antagonist. Fluorescent dye fills and transmission electron microscopy analysis identified a network of sensory interneurons coupled to the MGF. Glutamate receptors were located on the periaxonal regions of the giant fibers and sensory interneurons of both anterior and posterior segments. Colocalized with these glutamate receptors was a molecular marker for neural morphallactic plasticity, Lan3-2. Together, these results suggest that neural morphallaxis of the giant fiber pathway is mediated by synaptic unsilencing of glutamatergic inputs onto the sensory interneurons rather than directly onto the MGF. Data from this chapter are being reformatted for submission to the *Journal of Comparative Neurology* (Lybrand et al., 2012).

Chapter IV

Changes to giant fiber morphology and physiology during neural morphallaxis have been characterized to be a gradual change over several weeks. I have demonstrated using extracellular grid recordings there is a rapid reduction in the speed of spike propagation along the MGF that occurs within the first few days of neural morphallaxis. The reduced MGF conduction velocity is transient and recovers by the end of the first week of regeneration. Dye injections and electrophysiological recordings demonstrated that electrical coupling between electrical segmental elements of the medial giant axons changed during a late phase but not an early phase of neural morphallaxis.

CHAPTER II

RAPID NEURAL CIRCUIT SWITCHING MEDIATED BY SYNAPTIC PLASTICITY DURING NEURAL MORPHALLACTIC REGENERATION*

Introduction

The nervous system integrates extrinsic (environmental) and intrinsic (organismal) signals to manifest appropriate behavioral responses and to promote survival. Multiple forms of neural plasticity have evolved to regulate this neurobehavioral integration. Neural development (Bourne, 2010), learning and memory (Redondo and Morris, 2011) and neural regeneration (Harel and Strittmatter, 2006) are inherently plastic biological processes that involve relatively rapid cellular and molecular changes in nervous system structure and function. Alterations in the functional properties of synapses, broadly termed synaptic plasticity, are often key events underlying rapid neural circuit changes. For example, some synapses are incapable of neurotransmission during long periods in developing and mature nervous systems and are, therefore, functionally silent. However, these silent synapses act as reserve connections that can quickly become functional upon appropriate activation (Kerchner and Nicoll, 2008).

Silent synapses can be narrowly defined as synapses in which excitatory postsynaptic signaling is absent at the resting membrane potential, but emerges as the postsynaptic cell is depolarized. This usage of the term has its origin in studies of

---

*Reprinted with permission from "Rapid neural circuit switching mediated by synaptic plasticity during morphallactic regeneration" by Lybrand ZR and Zoran MJ, 2012. Developmental Neurobiology, in press, doi: 10.1002/dneu.20993. Copyright [2012] by Wiley Periodicals, Inc.

hippocampal plasticity, where functional unsilencing mediates aspects of long-term potentiation (LTP) of pyramidal synapses (Isaac et al., 1995; Liao et al., 1995). In a broader sense, silent synapses are ineffective synapses that have a structural presence, but are physiologically nonfunctional. The knowledge that synapses exist structurally, but not functionally, goes back over four decades (Merrill and Wall, 1972) and such ineffective synapses are known to exist in multiple brain regions (Kerchner and Nicoll, 2008). In fact, it has been suggested that the awakening of previously silent synapses might be a form of neural plasticity common to a wide range of animal nervous systems (Atwood and Wojtowicz, 1999).

The nervous system of *Lumbriculus variegatus*, an aquatic oligochaete, undergoes rapid physiological changes in response to injury-induced fragmentation and in anticipation of asexual fission. Fragmentation leads to the formation of two body fragments, or zooids, and the developmental growth of the new head and tail buds occurs by the regenerative process of epimorphosis. Epimorphosis requires the dedifferentiation of extant tissue, activation of stem cell populations, cellular proliferation and the differentiation of cells to replace the lost body parts. This results in a new worm, with eight new head segments and extensive numbers of new tail segments. The complete regeneration and maturation of new heads and tails occurs in a few weeks (Zoran and Martinez, 2009).

Accompanying this epimorphosis following fragmentation is a rare form of regenerative plasticity, called neural morphallaxis, which involves the remodeling of original segments, including their escape circuits, as take on new positional identities

(Drewes and Fourtner, 1990). This novel developmental plasticity involves the sensory-to-giant fiber pathways that mediate head withdrawal, governed by a medial giant (interneuronal) fiber (MGF) in anterior segments, and tail shortening, mediated by lateral giant fibers (LGF) in posterior segments (Martinez et al., 2005). Furthermore, this rapid switching of giant fiber sensory fields occurs within days of injury as posterior segments adopt more anterior functionality (Drewes and Fourtner, 1990; Zoran and Martinez, 2009).

We have tested the hypothesis that an emergence of functional synaptic transmission at sensory-to-MGF fiber synapses underlies the rapid switching of escape neural circuits in this regenerating annelid worm. Using non-invasive extracellular and conventional intracellular recordings of giant interneuronal synaptic and spiking activities, we demonstrate the nature and speed of sensory-to-interneuron synaptic transformation and that morphallactic plasticity involves the emergence of functional neurotransmission.

Materials and methods

Animals and maintenance

Aquatic oligocheate worms, *L. variegatus*, were purchased from Flinn Scientific (Batavia, IL). Worms were housed in plastic bins containing aerated, aged freshwater and squares of brown paper toweling. A constant temperature of 16^{o}C was maintained. Worms were fed powdered Algae-Feast™ Spirulina (Aquatic Eco-Systems Inc., Apoka, FL) weekly. Amputation of tail segments was conducted using microdissection scissors

to generate fragments of desired segmental identity. To create fragments within the LGF sensory field, a cut was made either 10 segments posterior (10SP) or 30 segments posterior (30SP) to the center of the region of sensory field overlap (SFO, see Fig. 1). The region of overlap in *Lumbriculus* is centered at the one-third anterior to two-thirds posterior segment boundary and is restricted to approximately 12% of the body segments (Martinez et al., 2005). Since worms between 100 and 120 total segments were used in these studies, the region of sensory field overlap consisted of 12 to 13 segments. Thus, cuts at 10 segments posterior to the center of the overlap zone were 3-4 segments into the LGF sensory field. Following amputation, worm fragments were maintained in fresh spring water (Ozarka, Oklahoma City, OK) until used for experiments.

Electrophysiological recording

Non-invasive electrophysiology

Giant fiber action potentials were detected extracellularly through the animal body wall using non-invasive electrode grid recordings (O'Gara et al., 1982). The large currents produced by annelid giant interneurons allow for the recording of spike voltages and the identification of specific fiber units based on waveform characteristics, such as size and shape. Medial giant fiber (MGF) and lateral giant fiber (LGF) action potential waveforms were distinguished based on previously reported spike characteristics (Zoran and Drewes, 1988; Zoran et al., 1988; Drewes and Fourtner, 1990; Rogge and Drewes, 1993). MGF spikes are monophasic in waveform, whereas LGF spikes are diphasic and typically twice the amplitude and duration of MGF spikes (Drewes and Fourtner, 1990).

A hand-held plastic probe was used to deliver touch stimuli to the body wall (Zoran and Drewes, 1987). Segments of specific identity (e.g., segment number 30) were marked with a spot of water-insoluble ink and individual segments at a known distance from the marked segment were touched. Extracellular voltages, recorded using a printed circuit-board grid of electrode pairs (1 mm spacing between positive and negative electrodes), were preamplified with differential recording amplifiers (100 x gain, AC-coupled differential inputs). Analog spike voltages were digitized with a Powerlab A-D conversion system (ADInstruments, Inc., Colorado Springs, CO) at a sampling rate of 40k/s, with 20kHz lowpass filtering. Waveforms were analyzed on a PowerMac G4 computer (Apple, Inc., Cupertino, CA) using the Powerlab Chart v4.1 software.

Invasive electrophysiology

Current-clamp intracellular recordings were performed on reduced preparations of *L. variegatus*. Worms were immobilized by submersion in worm saline solution (Zoran et al., 1988) containing 0.25 mM nicotine and the body wall was opened with a mid-dorsal surgical incision. Gastrointestinal and nephridial tissues were removed so that the ventral nerve cord (VNC) and the MGF could be visualized under a dissecting microscope. The MGF was then penetrated with a borosilicate glass microelectrode (tip resistance of 10-25MΩ) filled with 1.5M KCl, only preparations with a stable resting membrane potential of -60mV (or more negative) were used for analysis. Postsynaptic potentials were amplified using the Axoclamp200B (Molecular Devices, Sunnyvale, CA), filtered at 10 kHz, digitized and recorded on a Dell computer using pClamp10

software. Amplitude and frequency of spontaneous miniature events were analyzed using a semi-automated protocol within pClamp10. Evoked potentials were generated by electrical stimulation of the body wall, using a suction electrode that was positioned adjacent to the VNC within the recorded segment. In non-regenerating worms, an electrical stimulus at a constant duration of 0.2ms was applied to the suction electrode, using a Stimulus Isolation Unit (direct coupled mode; Grass, West Warwick, RI) with increasing voltage amplitude (2-5 V) until 100% of all stimuli activated postsynaptic potentials. These parameters were used in all consecutive recordings to activate sensory inputs to the MGF. The amplitude of evoked potentials was analyzed using Clampfit 10.0 software (Molecular Devices, Sunnyvale, CA). Electrophysiological recordings were only collected from the MGF pathway. The medial giant axon is approximately 10-20μm in diameter in mid-body segments were recording were made. Due to the significantly smaller size of the LGF in these segments (<5μm), stable resting membrane potentials were difficult to maintain and electrophysiological data on neural morphallaxis could not be collected. To test statistical significance, Student's t-test (two tailed) or chi-square analyses (Microsoft Excel 2010) were used where indicated. Statistical significance was $p<0.05$. Data are presented as the mean plus or minus the standard error of the mean (SEM).

Results

Anterior-posterior variation in sensory field plasticity

We tested whether or not the escape neural circuit in segments adjacent to the region of sensory field overlap (SFO; segments where tactile stimulation evokes both MGF-mediated and LGF-mediated withdrawal) is transformed more rapidly than the same circuits in more posterior segments (Fig. 3A). Tactile stimulation of the most anterior body segments of a tail fragment 1 h after the amputation at 10 segments posterior (10SP) to the center of the SFO generated only LGF-mediated posterior shortening (Fig. 3B). By 1 day (1d) post-amputation, similar touch stimuli activated MGF-mediated anterior shortening in approximately 40% of fragments tested (Fig. 3B and D). In contrast, tactile stimulation did not evoke anterior shortening in tail fragments at 1d after amputation at 30 segments posterior (30SP) to the center of the SFO (Fig. 3C and D). By 1d of regeneration, wound healing had begun at amputation sites, but no head buds were observed in either experimental group.

Both the 10SP and 30SP groups were tested for morphallactic changes during 1 d, 2-4 d and 5-7 d post-cut. Between days 2-4 post amputation, as head bud formation was being initiated, 50% of the regenerating worms tested in both groups responded to touch stimuli with anterior withdrawal (Fig. 3D). Most fragments in both the 10SP and 30SP groups responded to tactile stimulation with head withdrawal by days 5-7 post-cut (Fig. 3D). Thus, segments closer to the SFO shifted their sensory fields more rapidly than segments located 20 segments more distal to the SFO, but only in the 1d following amputation.

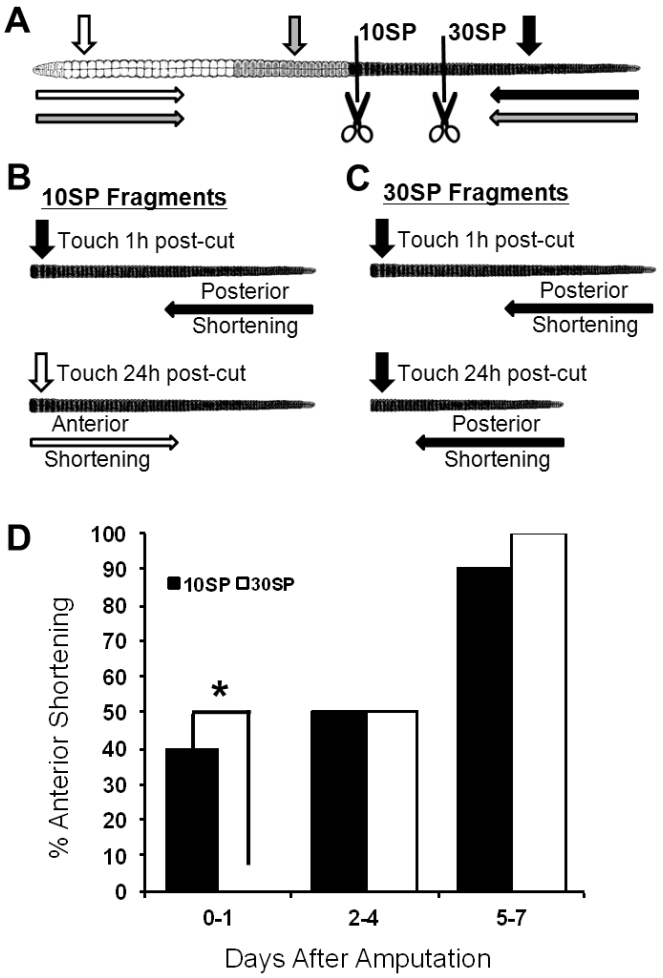

Figure 3. Behavioral plasticity along the anterior-posterior axis following segmental amputation. A. This schematic of sensory fields in *L. variegatus* indicates the location of the MGF sensory field (white anterior segments, left portion of diagrammatic worm). A tactile stimulation (white downward arrow) produces an anterior shortening behavior (white horizontal arrow). The grey segments represent the region of sensory field overlap (SFO) and tactile stimulation of these segments (grey downward arrow) results in simultaneous anterior and posterior shortening (grey horizontal arrows). Black segments represent the LGF sensory field and tactile stimulation here (black downward arrow) results in only posterior shortening (black horizontal arrow). Worms were segmentally amputated at locations within the LFG sensory field, 10 segments posterior to the center of the SFO (10SP) and 30 segments posterior to the center of the SFO (30SP). B. When fragments from the 10SP group were stimulated tactilely on the anterior end (black downward arrow) only posterior shortening behavior was observed. After 1 day (1d), some fragments responded to stimulation (white downward arrow) with an anterior shortening behavior. C. Fragments from the 30SP group, at 1 h and 1d post-cut, only responded to stimulation with posterior shortening. D. At one day or less after amputation, 40% of 10SP fragments (black bars) displayed anterior shortening behavior. This percentage was significantly greater than the 30SP group (open bars), none of which responded to stimulation with anterior withdrawal (*, $p<0.01$; Chi-square analysis). By day 4, 50% of fragments in both groups displayed anterior shortening behavior and, by days 5-7, nearly all of the fragments had developed anterior escape responses.

Using non-invasive electrophysiological recordings, MGF spikes were activated by anterior touch in 65-70 % of 10SP and 30SP fragments 1 day post-amputation (Fig. 4). Furthermore, 100 % of these regenerating worms by days 2-4 produced MGF spikes. Still, all 30SP fragments with MGF pathway activation on 1d post-cut failed to generate detectable anterior shortening, as shown in the previous experiment (Fig. 4B). Thus, neurobehavioral plasticity during neural morphallaxis involved the initial emergence of sensory-to-giant interneuronal pathway activation, followed by coupling of giant fiber excitation to overt segmental shortening. Most giant fiber spikes in the first days following fragmentation, whether medial or lateral interneuron action potentials, were single spiking events (Fig. 4B and C). As previously reported (Drewes and Fourtner, 1990), MGF spikes had monophasic waveforms, while LGF spikes were diphasic and longer in duration. Since multiple closely spaced spikes are required to generate facilitated muscle potentials and body shortening in lumbriculid worm species, including L. variegatus (Zoran and Drewes, 1987; Fig. 4A), it was not surprising that single spikes during early morphallaxis did not elicit motor responses. Since the majority of touch stimuli evoked MGF spikes by 1d post-amputation, we examined responses within the first hours after cut. MGF spikes and head withdrawal responses were present in some 10SP fragments within several hours of fragmentation, but no MGF-mediated events were detected in 30SP fragments tested by 6 h post-cut.

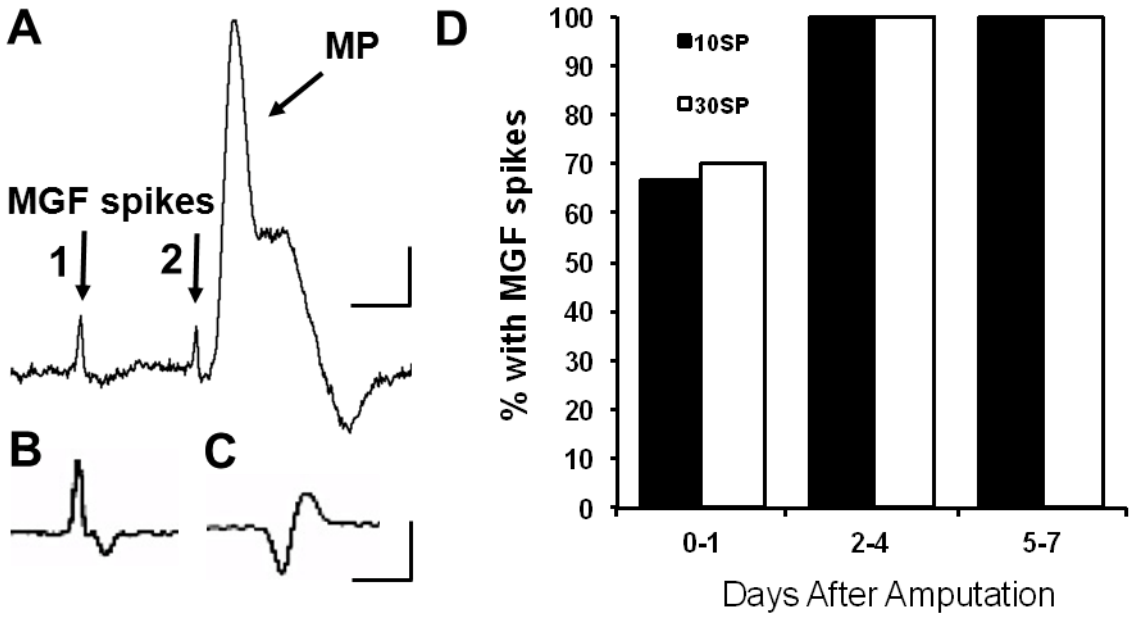

Figure 4. Sensory field plasticity along the anterior-posterior axis following segmental amputation. A. This non-invasive electrophysiological recording from an intact worm illustrates the neural reflex activity associated with stimulation of the MGF sensory field. A tactile stimulus to an anterior body segment activated multiple medial giant fiber action potentials (MGF spikes, 1 and 2 arrows), which drove activation of large muscle potentials (MP) that resulted in anterior shortening behavior. In the first days following amputation in 30SP fragments, only single MGF spikes (B) or LGF spikes (C) were elicited by anterior tactile stimulation. No muscle activity or shortening accompanied these single spikes. D. In regenerating fragments, MGF spikes were activated by tactile stimulation in almost 70% of both 10SP (black bars) and 30SP (white bars) groups. No significant differences in the percentage of preparations with touch-evoked MGF spiking were detected between groups on any days after amputation. Scale bar equals 5 mV, 2 ms (A) and 3 mV, 1 ms (B and C).

In fact, at 6 h post-amputation, single MGF spikes were activated in only 6 % of 10SP fragments, while 74 % of the responses in these fragments were solely LGF spike-associated. Furthermore, the remaining 20 % of responses involved mixed spiking, with combined MGF and LGF activity, similar to the dual pathway activation seen at the

region of SFO in intact animals. Thus, morphallaxis of the rapid escape neural pathway consists of an extended period (several days) where giant fiber action potentials were activated, but these spikes failed to generate segmental shortening. Additionally, morphallaxis of GF neural circuits likely involved a rapid and transitory period of dual pathway activation.

Sensory-to-giant interneuron synaptic transmission emerges by 1d after amputation

Although tactile stimulation of tail segments does not elicit MGF spikes in L. variegatus (Zoran and Drewes, 1987), there is no evidence of synaptic transmission within LGF sensory fields at sensory-to-medial giant interneuron synapses prior to neural morphallaxis. Therefore, synaptic transmission at MGF interneurons was recorded using intracellular current-clamp recordings and body wall electrical stimulation before and during neural morphallaxis. Intact worms were opened with a dorsal midline incision at two segmental levels: between 10 and 30 segments anterior to the SFO (10-30SA), which includes only segments within the MGF sensory field and between 10 and 30 segments posterior to the SFO (10-30SP), which includes only segments within the LGF sensory field. In uncut control animals, spontaneous, miniature postsynaptic potentials (mPSP) were recorded in MGF interneurons at region 10-30SA (MGF SF, Fig. 5A), but not region 10-30SP (LGF SF; Fig. 5B). mPSPs within the MGF SF averaged 1.3 ± 0.2 mV in amplitude (n=4), with a frequency of 9.4 ± 2.6 Hz (n=4). However, 1 day following amputation within the LGF SF, mPSPs were detected at a low frequency (0.5 ± 0.3 Hz; Fig. 5C and E) and low amplitude (0.5 ± 0.3 mV; Fig. 5D).

Both of these synaptic properties were significantly lower ($p<0.05$) than those recorded from MGF interneurons of intact animals. Over the course of the first week of

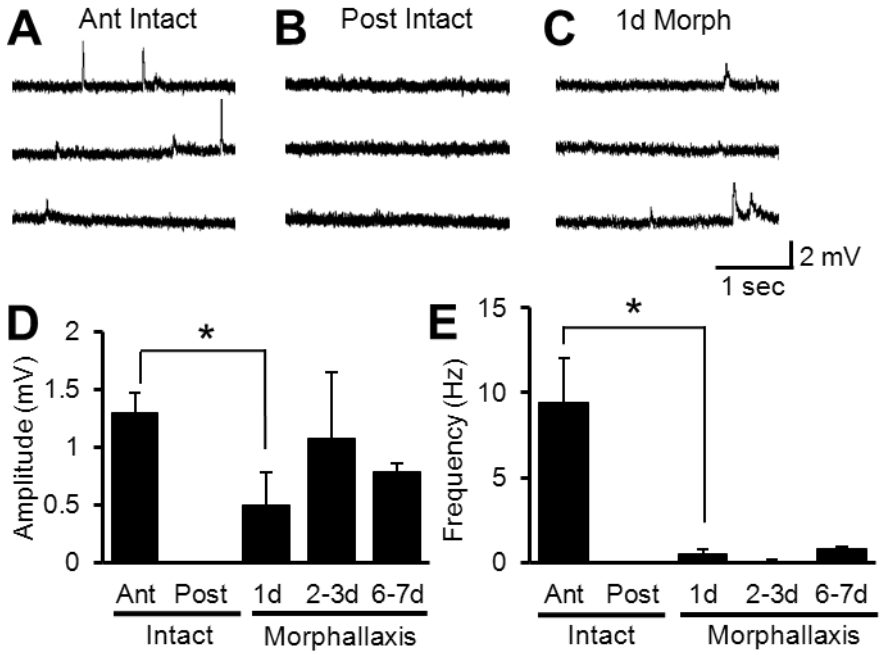

Figure 5. Spontaneous synaptic potentials are not detected at nascent synapses prior to morphallaxis. A. Spontaneous postsynaptic potentials from the MGF were recorded using intracellular current clamp recordings. Upward deflections in the three representative voltage traces recorded from MGF interneurons of anterior segments of intact animals (Ant Intact) are miniature postsynaptic potentials (mPSPs). B. No mPSPs were detected in MGF recordings from posterior segments of intact animals (Post Intact). C. Following 1 day of regeneration, mPSPs were detected in segments of posterior fragments undergoing morphallaxis (1d Morph). D. The amplitude of MGF mPSPs on day 1 of morphallaxis was significantly lower than that of mPSPs recorded in anterior segments of intact worms (*, $p<0.05$). mPSP amplitude did not increase significantly over the first week of morphallaxis. E. The frequency of MGF mPSPs on day 1 of morphallaxis was significantly lower than that of mPSPs recorded in anterior segments of intact worms (*, $p<0.05$). mPSP frequency did not increase significantly over the first week of morphallaxis.

regeneration, neither mPSP amplitude nor frequency increased significantly (Fig. 5D and E). Evoked synaptic transmission was also assessed by electrical stimulation of the body wall. Stimulating region 10-30SA within the MGF sensory field of intact worms elicited a large spike (LS) in 54% of all preparations (n=11; Fig. 6A and C). However, when region 10-30SP within the LGF sensory field was stimulated no postsynaptic responses or evoked action potentials were recorded (n=4; Fig. 6B and C). Although no MGF electrophysiological responses were evoked by body wall stimulation within the LGF sensory field of intact animals, synaptic potentials were recorded in MGF interneurons of transforming segments during the first day (1d) of neural morphallaxis.

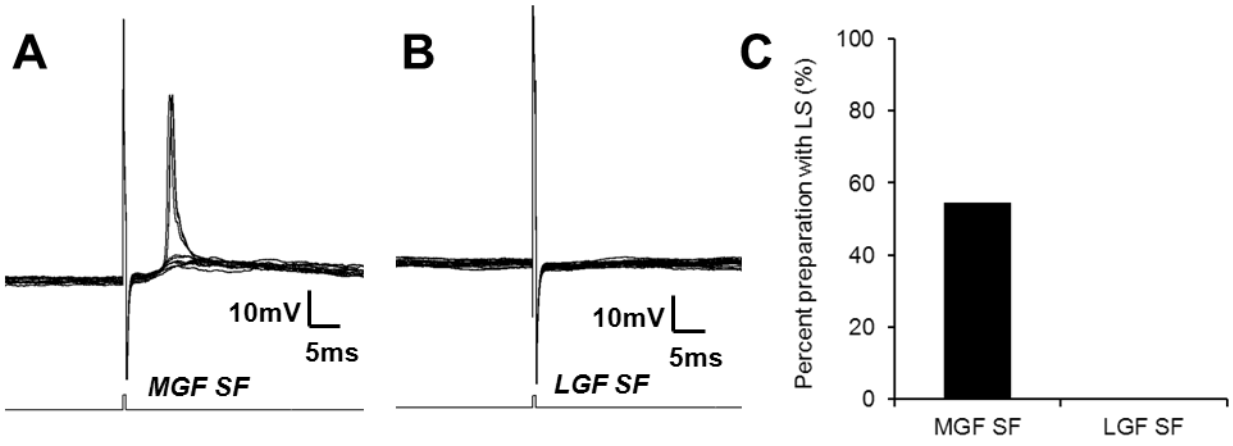

Figure 6. Electrically-evoked MGF activity is not detected within the LGF sensory field of intact animals A. Intracellular MGF recordings from an intact worm within the MGF sensory field (MGF SF) demonstrate that both graded postsynaptic potentials and large GF spikes (LS) are evoked by body wall stimulation (Stim). B. Body wall stimulation within the LGF sensory field (LGF SF) evoked no postsynaptic potentials in the MGF interneuron and no MGF spikes. C. Quantification of the evoked GF activity showed that 54% of worms exhibited large spikes when stimulated in MGF sensory field, as compared to none in the LGF sensory field.

Approximately 52.0 ± 9.5 % of stimuli evoked only subthreshold, graded PSPs in the MGF (n=11; Fig. 7A and B). Less frequently evoked events were PSPs associated with small amplitude, all-or-none action potentials. These small spike (SS) events were elicited in response to 19.8 ± 6.1 % of the electrical stimuli (Fig. 7A and B). The generation of these small spikes is not understood, however, one possibility is that they represent electrically coupled action potentials generated in other interneurons. The function of these small spikes has not been further investigated here. Another 31.0 ± 11.9 % of stimuli evoked PSPs associated with large amplitude MGF spikes (LS; Fig. 7A and B). These large MGF spikes had a classical action potential waveform and amplitudes greater than 50 mV. Small spikes typically had less than half the amplitude of large MGF spikes (Fig. 7B), often characterized by multiple peaks or plateau-like potentials.

Electrical stimulation of 10-30SP fragments with emerging MGF sensory fields evoked subthreshold PSPs (43.4 ± 12.3 % of stimuli, n = 10) and PSPs with associated small spikes (29.6 ± 10.7 % of events) at 1d post-cut (Fig. 7C and D). In contrast, no large MGF spikes were evoked at this stage of regeneration (Fig. 7D). Thus, segments with an initial posterior identity, with no evidence of MGF sensory input, gained functional sensory-to-giant interneuron synaptic transmission within 1d of head amputation, where graded PSPs and small spikes first emerge, followed by subsequent recruitment of large amplitude MGF spikes. Taken together, these electrophysiological studies demonstrate that functional synaptic transmission emerges at sensory-to-MGF connections in transforming segments during neural morphallaxis.

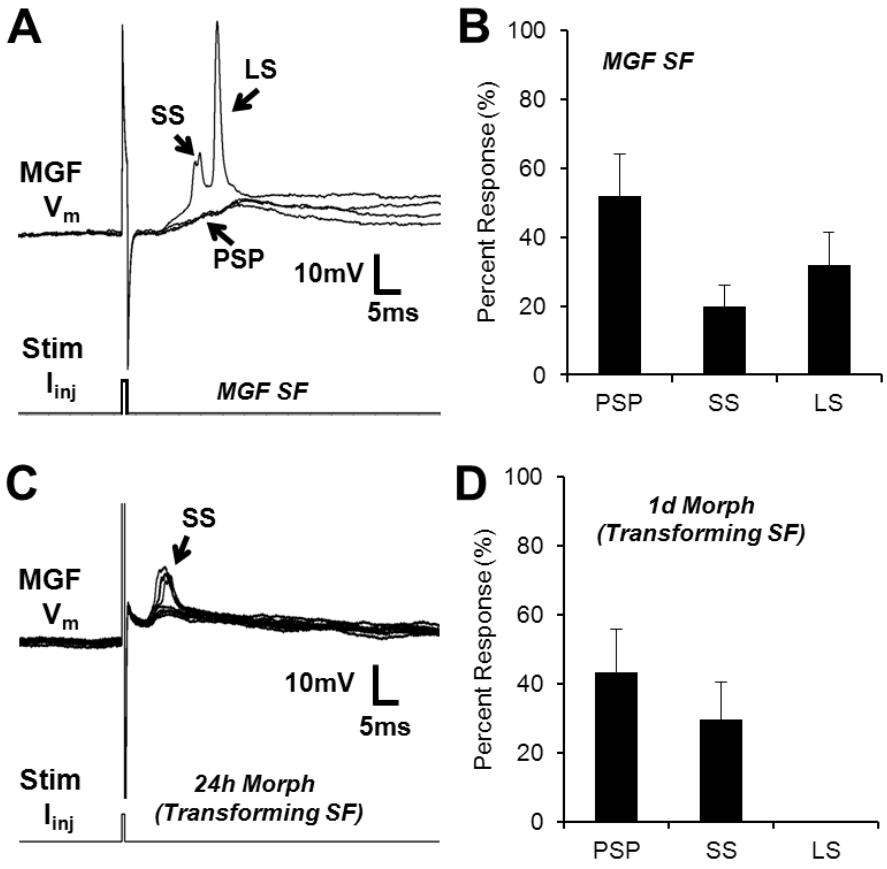

Figure 7. Functional synaptic transmission emerges in MGF interneurons during neural morphallaxis
A. Electrical stimulation (Stim) of the body wall of an intact worm within the MGF sensory field (MGF SF) resulted in graded postsynaptic potentials (PSP), evoked small amplitude spikes (SS), and large amplitude spikes (LS) recorded in the MGF interneuron. B. A majority of the evoked events in the MGF sensory field of intact animals were subthreshold graded PSPs. Small amplitude spikes (SS) were the least frequent events recorded in these uninjured worms. C. Evoked synaptic transmission emerged in MGF interneurons in the transforming LGF sensory field of regenerating fragments (Transforming SF). D. Although graded PSPs and small spikes (SS) were equally frequent in transforming segments following 1d of morphallaxis (1d Morph), no large MGF spikes (LS) were evoked by electrical stimulation of the body wall.

MGF spikes can be generated hours after fragmentation

Although large amplitude MGF spikes could not be detected at 1d post-amputation in reduced preparations using intracellular recordings, non-invasive recordings had demonstrated that MGF spikes and anterior shortening were possible during this time frame. If our hypothesis is correct that escape circuit plasticity involves the unsilencing of nonfunctional synapses, then neural morphallaxis of synaptic connectivity should be a rapid process. Therefore, we used non-invasive recordings within the first 6 h post-amputation to determine how quickly MGF sensory fields can emerge. MGF and LGF spike activation was quantified in response to tactile stimulation of 10-30SP fragments.

A single tactile stimulation to this region in an intact worm typically produced only trains of LGF spikes, which ranged from spike pairs to trains of >20 LGF spikes (LL; Fig. 8A). Similarly, only trains of MGF spikes were recorded in intact animals within the MGF sensory field (MM; Fig. 8B). Tactile stimulation of the region of sensory field overlap (SFO) resulted in both the MGF and LGF spikes that typically occurred as doublet spikes (i.e., one MGF and one LGF spike). Approximately 16.7 % of the stimuli that activated dual pathway firing in the SFO zone involved doublets with an initial LGF spike followed by a MGF spike (LM) and 83.3 % of doublets were the reverse with MGF followed by LGF (ML; Fig. 8C).

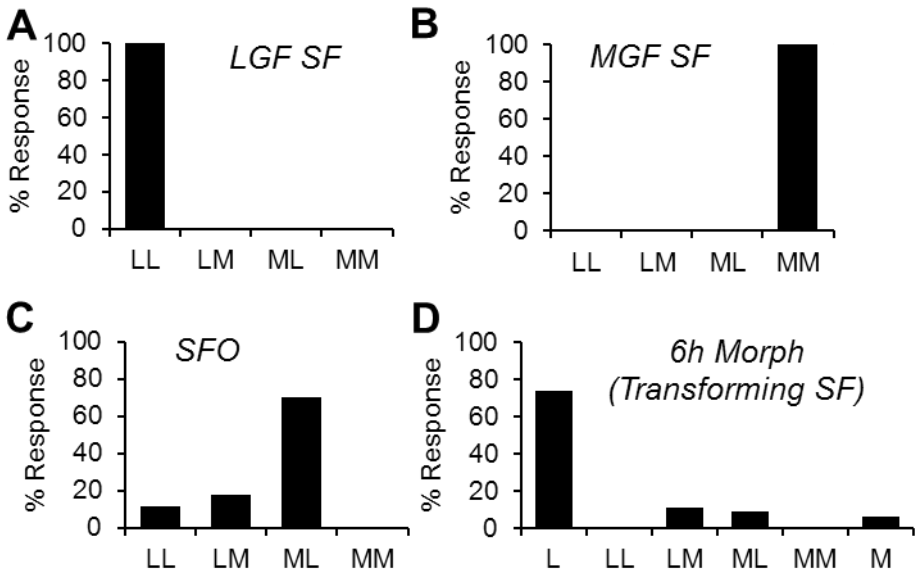

Figure 8. Sensory field transformation involves a transient period of dual giant fiber pathway activation. A. Tactile stimulation of body segments within the LGF sensory field of intact worms activated only trains of LGF spikes (LL), as detected by non-invasive extracellular recordings. B. Similarly, stimulation of the MGF sensory field activated only trains of MGF spikes (MM). C. In the region of sensory field overlap (SFO), stimulation of body segments activated doublets of LGF and MGF giant fiber action potentials, with the LGF spike first in the pair (LM) or the MGF spike first (ML). Trains of LGF spikes (LL) were rare and MM spike trains (MM) were not detected following stimulation in the SFO. D. Tactile stimulation to transforming posterior segments (previously entirely LGF SF), after 6 h of morphallaxis (6h Morph), activated predominately single LGF spikes (L). However, even at 6 h of regeneration, some MGF spikes were detectable either as single spikes (M) or as doublets of LGF and MGF spikes (LM or ML pairs).

Between two to six hours post-amputation, only 74 % of the stimuli activated LGF spiking, indicating that neural circuit transformation had been initiated in a quarter of these 10-30SP fragments. However, unlike intact worms, GF spikes in regenerating fragments were single action potential events or heterogeneous spike pairs. No GF spike trains were activated by touch of the anterior most segments of regenerating fragments during these early hours of morphallaxis. Furthermore, 6 % of the responses to tactile

stimulation involved a single MGF spike, confirming that complete pathway transformation in some fragments occurred within several hours. Interestingly, 20 % of the responses involved doublets of LGF and MGF spikes, similar to the intact region of overlap, with 11.1 % ML responses and 8.9 % LM responses (Fig. 8D). Although single or doublet GF spikes were not sufficient to induce overt behavioral shortening within hours of amputation, these spikes were detected in response to body wall stimulation. Thus, synaptic changes within escape neural circuits must occur within hours of body injury.

Interspike intervals (ISI) were calculated for intact worms and for fragments with ongoing neural morphallaxis. ISI for LL and MM responses in intact worms were 16.7 ± 6.5 and 15.0 ± 6.0 ms, respectively. Within the region of sensory field overlap, the ISI for ML was 9.2 ± 2.4ms and LM was 7.6 ± 5.5ms. These ISI values were significantly greater than those calculated for GF doublet spikes recorded from fragments in the process of neural morphallaxis ($p<0.05$). ISI for ML and LM responses in 10-30SP fragments at 2-6 h post-amputation were 3.3 ± 1.1 and 2.8 ± 0.9 ms, respectively. These short ISI values might be indicative of simultaneous activation of the LGF and MGF interneuronal pathways by a single tactile stimulus. Thus, transitional sensory-to-giant interneuron plasticity likely involves a period of dual system activation that exists transiently at the earliest stages of neural circuit transformation.

Discussion

Two giant fiber pathways, constructed of segmental linkages of interneuronal axons, mediate independent escape circuits. The medial giant fiber (MGF) pathway regulates head withdrawal and the lateral giant fiber (LGF) pathway regulates tail withdrawal. Sensory inputs that activate the MGF pathway are restricted to the anterior 1/3 of the worm's body segments. In contrast, the LGF sensory field constitutes the posterior 2/3 of the body segments. At the interface of the MGF and LGF sensory fields, a region of sensory field overlap exists, where touch stimuli activate simultaneous anterior and posterior shortening (Drewes, 1984; Zoran and Drewes, 1987; Drewes and Fourtner, 1990). Regenerating posterior body fragments that previously responded to tactile stimulation with only LGF activation and tail shortening reorganize their touch sensory fields such that MGF activation emerges within the first week of regeneration after fragmentation (Drewes and Fourtner, 1990; Lesiuk and Drewes, 2001a). In the present studies, touch stimuli activated MGF-mediated anterior shortening in regenerating fragments within hours of amputation, but only in segments nearest the sensory field overlap zone. More posterior fragments, although capable of coupling sensory stimuli to giant fiber spike activation within 1d of injury, were incapable of generating touch-activated tail shortening until several days post-amputation. Therefore, segments closer to the original region of sensory field overlap mount neural morphallactic transformation more readily than segments more posterior.

Neural circuit switching in Lumbriculus

Escape neural circuits, at least those in segments close to regions of giant fiber sensory field overlap, rapidly switched such that body wall touch elicited new and opposing neurobehavioral events (i.e., MGF responses where only LGF had existed) within hours of anterior segment amputation. It has long been known that disruption of sensory pathways can lead to the awakening of ineffective synapses connecting sensory and spinal interneurons (Merrill and Wall, 1972). Although some synapses do not respond to stimulation with postsynaptic activation, after ablation of a subset of afferent fibers, these silent synapses gain reliable neurotransmission. While aspects of LGF to MGF circuit transformation in *Lumbriculus* are similar to this sensory-spinal synaptic unsilencing, morphallactic pathway switching is triggered by body fragmentation and involves a more developmental process of synaptic maturation.

We used extra- and intracellular electrophysiological approaches to determine the mechanistic nature of giant fiber pathway switching. Neuromorphallactic plasticity involved an initial emergence of sensory-to-giant interneuronal synaptic function. That is, the first step in morphallactic plasticity was the acquisition of functional synaptic transmission (i.e., sensory-stimulus evoked synaptic activity). Subsequent to the emergence of stimulus-dependent giant fiber excitation, fragments gained the capacity to couple GF spiking to overt behavioral shortening. MGF spikes are necessary, but not sufficient, for rapid withdrawal, even in intact lumbriculid worms, since multiple action potentials in close temporal proximity are required to trigger facilitated muscle potentials (Zoran and Drewes, 1987). Therefore, although morphallaxis involved an increased

ability of giant interneurons to effectively drive motor outputs, increases in synaptic transmission and efficacy were fundamental features of this regenerative plasticity. Neither spontaneous nor evoked synaptic transmission was detectable at sensory-to-MGF connections prior to anterior segment amputation. After amputation, stimulation of regenerating posterior fragments evoked subthreshold PSPs incapable of triggering tail withdrawal. This acquisition of functional synaptic transmission was followed by the emergence of sensory-evoked MGF action potential generation and, subsequently, the capacity for MGF spiking to activate behavioral shortening.

Silencing and unsilencing in synaptic plasticity

Since sensory-to-giant interneuronal synaptic function is recruited within hours of body fragmentation, it is possible that these synapses were extant, but non-functional prior to amputation. Such recruitment of silent synapses has been demonstrated in the nervous systems of crustaceans (Jahromi and Atwood, 1974), insects (Atwood et al., 1993), fish (Faber et al., 1991) and mammals (Wall, 1977; Isaac et al., 1995; Malenka and Nicoll, 1997) and, if not for the difficulty in their demonstration, they might be considered a pervasive mechanism of neural plasticity (Atwood and Wojtowicz, 1999). In the classic model for synapse unsilencing during LTP at hippocampal synapses, mobilization of AMPA-receptors in postsynaptic membranes mediates activity-dependent gain-of-function. The strengthening of lumbriculid sensory to MGF physiological performance described here involves a sequence of electrophysiological events consistent with synaptic unsilencing. Furthermore, morphallactic plasticity entails

a transient stage of simultaneous MGF and LGF spike activation. This period of dual pathway activation suggests that loss of LGF circuit function is mechanistically linked to the gain of MGF circuit function.

Multiple cellular and molecular mechanisms are involved in neural morphallaxis (Lesiuk and Drewes, 1999, 2001a, 2001b; Martinez et al., 2005; Martinez et al., 2006; Martinez et al., 2008), including the transformation of giant fiber axonal morphology, a process that requires several weeks for completion (Drewes and Fourtner, 1990; Zoran and Martinez, 2009). In contrast, circuit switching occurs in several hours. Nonetheless, it remains quite possible that sensory field transformations involve new synapse formation rather than unsilencing of extant synapses, as it is difficult to distinguish physiological emergence from de novo formation. Two criteria, physiological insufficiency and structural presence, must both be satisfied before synaptic unsilencing is established (Atwood and Wojtowicz, 1999). Each segmental axon element of a *Lumbriculus* giant fiber pathway has 4 ventrally projecting collaterals that are the sites of sensory synaptic inputs (Martinez et al., 2005), making the quest for individual synapses with electron microscopy and the structural evidence of silent synapses difficult to obtain. Therefore, we cannot demonstrate a role for synaptic unsilencing in neural morphallaxis. Still, it is clear that postsynaptic inactivity of the MGF pathway rapidly gives way to subthreshold inputs that mature into suprathrehold PSPs within a matter of hours, a timeframe perhaps too brief for wide spread axonal growth and de novo synapse formation.

Adaptive nature of escape circuit switching

The ability of lumbriculid giant fiber pathways to rapidly switch provides these annelids' nervous systems with behavioral flexibility that seems highly adaptive. *Lumbriculus variegatus* is an oligochaete worm that lives in shallow bodies of freshwater and reproduces both sexually and asexually (Zoran and Martinez, 2009). Asexual reproduction is by architomic fission, where fragments regenerate lost segments. Additionally, lumbriculid worms are capable of self-amputation by autotomy (Lesiuk and Drewes, 1999). After architomic or autotomic fragmentation, a constant number of head segments and varying lengths of tail segments are regenerated (Berrill, 1952; Drewes and Fourtner, 1990; Martinez et al., 2005). Regeneration of limited numbers of head segments requires positional transformation as posterior fragments become more anteriorly located. This need for future and rapid change in positional identity has likely favored the evolution of neural morphallactic plasticity, particularly in regions of sensory field overlap where architomic fission planes consistently form (Martinez et al., 2006).

It has been argued that the evolutionary origins of asexual reproduction and regeneration in annelids are linked (Bely, 1999; Alvarado, 2000; Bely and Wray, 2001; Bely, 2006) and that the cellular mechanisms underlying neural morphallaxis in *Lumbriculus* have been co-opted to mediate both reproductive and regenerative developmental events (Zoran and Martinez, 2009). Reorganization of neural circuits is achieved in anticipation of reproductive fragmentation and in compensation for injury-induced amputation. Like the highly plastic silent synapses in the mammalian CNS

(Isaac et al., 1999; Philpot and Zukin, 2010), the sensory-to-interneuronal synapses within the escape neural circuits of *Lumbriculus* are primed to undergo rapid electrophysiological strengthening following fragmentation. Although silent synapses are present in many animal phyla, the mechanisms mediating them vary widely. For example, the unsilencing of synapses between inhibitory interneurons and Mauthner cells of the goldfish brainstem involves a nonfunctional postsynaptic membrane becoming functional (Faber et al., 1991). In contrast, silent synapses at the crayfish neuromuscular junction are presynaptically nonfunctional (Wojtowicz et al., 1991; Wojtowicz et al., 1994). Although it remains to be determined whether pre- or postsynaptic mechanisms mediate escape circuit morphallaxis, a central characteristic of this neural plasticity is the progressive, albeit rapid, physiological maturation of functional synaptic transmission, a common developmental feature of gain-of-function at many silent synapses. We hypothesize that nonfunctional synapses exist throughout the *Lumbriculus* nervous system positioned and poised for activation when needed. It has been proposed that a majority of synapses in the neural pathways of animals are effectively silent and are recruited at particular times by appropriate physiological triggers, including neuronal activity, neuromodulators or hormones (Atwood and Wojtowicz, 1999). The critical reserve of putative silent synapses along lumbriculid giant fiber systems might be aroused by developmental or morphallactic signals associated with fragmentation, regeneration or the acquisition of new positional identity.

CHAPTER III

GLUTAMATERGIC SYNAPTIC PLASTICITY MEDIATES RAPID ESCAPE REFLEX TRANSFORMATION DURING MORPHALLACTIC REGENERATION IN THE ANNEILD WORM *Lumbriculus variegatus*

Introduction

Neural plasticity alters the anatomy (structure) and physiology (function) of an organism's nervous system and these neural transformations occur during development, in response to environmental stimuli or as a result of changes in behavior. For example, during neural development of the visual system, synaptic pruning eliminates inappropriate neural circuits, leaving pathways appropriate for bilateral organization of the primary visual cortex (Hensch, 2005). Following damage due to injury or stroke, neural circuits of the somatosensory cortex remap during the recovery of motor function (Wittenberg, 2010). Additionally, long term potentiation (LTP) and long term depression (LTD) are cellular correlates of neural plasticity that involve synaptic changes, which either enhance or diminish, respectively, communication between neurons of the mammalian hippocampus (Kullmann and Lamsa, 2007), sensorimotor circuits of the marine mollusk, *Aplysia* (Roberts and Glanzman, 2003) and the sensory P-AP synapse and the central T-S synapse in leech *Hirudo* (Burrell and Li, 2008; Grey and Burrell, 2010). Furthermore, a nervous system's ability to change, both anatomically and

physiologically, is adaptive, presumably giving an organism enhanced survivability and fitness.

Neural morphallaxis is a type of regeneration deployed in the nervous system of the aquatic annelid, *Lumbriculus variegatus*, after the loss of body segments due to injury. During neural morphallaxis, neural circuits that mediate escape behaviors rapidly transform into circuits for alternative escape responses, switching from tail to head withdrawal responses to a tactile stimulus. In intact worms, tactile stimulation of anterior segments activates the medial giant fiber (MGF), whereas stimulation of posterior segments activates the lateral giant fibers (LGF) (Drewes and Fourtner, 1990; Lybrand and Zoran, 2012). Each of these dorsal giant fiber axons is part of a chain of electrically coupled and segmentally arranged giant axons that constitute the giant fiber pathways (Drewes, 1984; Zoran and Drewes, 1987). Transformation of giant fiber pathways is thought to involve plasticity at the sensory-to-medial giant interneuron synapse and perhaps the giant interneuron gap junctional coupling (Zoran and Martinez, 2009). Functional synaptic transmission onto the MGF emerges in posterior segments within 6 hours following body segment amputation (Lybrand and Zoran, 2012). Still, the specific changes in structure and function of the sensory-to-MGF pathway during neural morphallaxis have not been determined and constitute a critical gap in our understanding of this rapid form of neural plasticity.

In this study, we have investigated the role of chemical and electrical synaptic plasticity during the transformation of the giant interneuronal escape neural circuit during morphallactic regeneration. We have demonstrated that glutamatergic synapses,

located in domains surrounding the giant interneurons, mediate the rapid escape reflex in *Lumbriculus variegatus*. Stimulation of sensory afferents activated a giant interneuronal network within the VNC that was coupled electrically to the medial giant fiber pathway. However, electrophysiological recording and dye coupling studies demonstrated that plasticity at glutamatergic synapses, and not electrical synapses, mediate transformations in the escape neural circuit. A molecular marker of neural morphallaxis, the Lan3-2 glycoepitope, is colocalized with glutamate receptors and changes in the intensity of Lan3-2 immunoreactivity correlated with changes in glutamate synapse function during the first week of neural morphallaxis.

Materials and methods

Animal cultures

Lumbriculus variegatus cultures were purchased from Flinn Scientific (Batavia, IL) and housed in bins filled with aerated fresh water at a temperature of 16ºC. Brown paper towels were cut into one inch squares and used as substrate material. The worms were fed a weekly diet of powdered Algae-Feast™ Spirulina (Aquatic Eco-Systems Inc., Apoka, FL). For regeneration experiments, worms were immobilized in a 0.25 μM nicotine and spring water (Ozarka, Oklahoma City, OK) solution and body segments were amputated using microdissection scissors to generate tail fragments. To ensure that tail fragments were within the LGF sensory field, amputation cuts were made 10-30 segments posterior to the region of sensory field overlap. Regenerating tail fragments were cultured in spring water until used for experiments.

Electrophysiology and pharmacology

Current clamp recordings were performed on reduced preparations of *Lumbriculus variegatus*. These preparations consisted of body segments opened with a dorsal incision and pinned with the outer body wall against the body of the silicone dish. Following removal of gut tissue, the ventral nerve cord and body wall musculature was visualized. Once the preparation was dissected, it was treated for 5 minutes with worm saline (Zoran et al., 1998), 25μM 6-Cyano-7-nitroquinoxaline-2,3-dion (CNQX; Sigma-Aldrich) in <0.1% DMSO and worm saline, or 100μM D-2-Amino-5-phosphonophentanoic acid (AP5; Sigma-Aldrich) in worm saline. At the end of the 5-minute treatment, one minute of electrophysiological recording was performed. Because MGF microelectrode penetrations were difficult to maintain and sustained resting membrane potential recordings during media exchange were not feasible, independent preparations were used to treat, washout, and then record MGF electrophysiological data. Thus, for washout data, preparations were treated for the 6 minutes with drugs and the treatment solution was then replaced with worm saline for an additional 5 minutes before the washout recordings were performed (see Fig. 7A).

Spontaneous and evoked post synaptic potentials (PSP) were recorded from anterior segments within the medial giant fiber sensory field, using the same procedures as previously described (Lybrand and Zoran, 2012). Amplitudes of evoked PSPs were measured using Clampfit 10.0 software (Molecular Devices, Sunnyvale, CA). A semi-

automated event-detection protocol within Clampfit 10.0 was used to analyze spontaneous events. A template waveform was generated from >100 events recorded from the MGF in anterior segments of non-regenerating worms. In pharmacology experiments, stable resting membrane potential (-60mV) were maintained in reduced preparations for as long as possible. Once a stable recording was achieved, synaptic physiology was assessed for one minute.

Dye injections

For giant fiber injections, worms were immobilized in nicotine, dissected and pinned to silicone dishes as described above. MGF axons were injected using micropipettes filled with 3% lucifer yellow, fastgreen, and rhodamine dextran (3%; Molecular Probes) or Neurobiotin (1:1000; Vector Laboratories, Burlingame, CA) using a picospritzer (General Valve). Once injected, preparations were incubated in worm saline for 30 minutes at room temperature to allow dye diffusion. For Neurobiotin fills, injected fragments were incubated in Fluorescein Avidin D (1:1000; Vector Labs) in phosphate buffered saline (PBS) overnight at 4ºC, followed by an extensive PBTD (PBS + 0.1% DMSO + 0.1% Tween ®20; Sigma Aldrich) wash, and a secondary incubation in anti-avidin conjugated to fluorescein (1:1000; Vector Labs) overnight at 4ºC. Prior to imaging, fragments were dehydrated with a series of five ethanol baths (70%, 80%, 95%, 95%, and 100% EtOH) at 10 min each and were cleared by emersion in methyl salicylate prior to being mounted on glass slides.

Immunohistochemistry and image analysis

Worms were immobilized in 0.25μM nicotine in spring water, pinned on a silicone dish, and fixed with a 4% paraformaldehyde solution for 30 minutes at room temperature. Fixed preparations were washed in PBS. Fragments were placed in a 30% sucrose solution for 12 hours before being embedded in Tissue Freezing Medium (TFM™; Triangle Biological Solutions, Durham, NC) and were frozen at -80°C. Blocks were cut using a cryostat (Leica) and cross-sections were mounted on Colormark™ Plus slides (Erie Scientific Company, Portsmouth, NH) and dried overnight. Dried slides were washed with PBTD for 30 minutes before blocking for 2h in a solution of PBS and 5% fetal goat serum was applied. Sections were treated with primary antibodies diluted in blocking serum overnight at 4°C. Primary antibodies used were GluR5-7 (1:50; BD Pharmigen), GluR2, 3 (1:33; Abcam), NR1(1:33; BD Pharmigen), Lan3-2 (1:50; previously provided by Jørgen Johansen). After wash with PBTD, sections were treated with fluorescent secondary antibodies, Alexa Fluor® 488 goat anti-mouse IgM, Alexa Fluor® 488 goat anti-rabbit IgG, and Alexa Fluor® 568 goat anti-mouse IgG (1:1000; Invitrogen). DAPI (4',6-Diamidino-2-Phenylindole, Dihydrochloride) was included in the secondary incubation for nuclear staining in all preparations (1:1000; Invitrogen). Slides were then washed and ProLong® Gold Antifade reagent (Invitrogen) was added. Imaging was done on an Olympus IX70 inverted microscope and CoolSnapHQ camera (Actimetrics, Wilmette, IL). Fluorescent intensity was measured by selecting regions of

interest (ROI) using Simple PCI6.0 imaging software (Compix, Inc., Cranberry Township, PA). For each image, four ROI around each giant fiber, four randomly selected neuropile and four background values were measured. An average value for LGF, MGF, VGF, neuropile and background were calculated and statistically analyzed with the same ROI values from all other images. For all fluorescent intensity data presented, the average background intensity was subtracted from all average ROI values.

Electron microscopy

Anterior and posterior fragments from non-regenerating worms were fixed by immobilizing in 25μM nicotine solution and immersed in 3% glutaraldehyde/worm saline (500 mOsM total) overnight. Anterior fragments consisted of 6-10 segments from the first quarter of the worm and posterior fragments were 30 segments from the posterior quarter. Fragments were then washed hourly in worm saline for 5 hours and post fixed in 2% osmium tetroxide and worm saline for 2 hours. Following post fixation, fragments were rinsed in 33mM PBS for 30 minutes and washed 20 minutes in deionized water. Fixative and buffer solutions were maintained at ±4°C with a pH around 7.2 (Kensler et al., 1979). Fragments were dehydrated in an acetone series (10, 20, 30…90, 95, 100, 100, and 100%) on ice with care to prevent exposure to air and stored at 0°C overnight.

Prior to embedding, fixed fragments were transferred into propylene oxide. In order to ensure proper infiltration of plastic resin, fragments were placed in increasing percentages of Epon-Araldite mixture over 24 hours. Samples were then flat embedded

in a small aluminum dish with fresh Epon-Araldite and baked at 60°C for 48 hours. Ultra-this sections (about 70nm) from anterior and posterior blocks were stained with uranyl acetate in methanol and aqueous lead citrate. Conventional transmission electron microscopy with JOEL1200 EX equipped with a 3kx3k SIA lens-coupled CCD slow-scan camera was used to examine sections.

Statistics

Statistical significance was analyzed using a Student's t-test (Excel 2010, Microsoft) and presented as $p<0.01$ or $p<0.05$ where indicated. Variation was presented as standard error of the mean (SEM).

Results

Medial giant fiber activation is inhibited by AMPA/kainate receptor antagonist

Touch- and pressure-sensitive neural pathways in some annelids are mediated by glutamatergic sensory input onto interneuronal targets of the ventral nerve cord (Baccus et al., 2000; Burrell and Sahley, 2004; Grey and Burrell, 2010; Li and Burrell, 2011). To determine if glutamate is the neurotransmitter that mediates sensory afferent activation of the medial giant fiber pathway in *Lumbriculus*, glutamate receptor antagonists were applied to reduced preparations, where giant interneuron electrophysiogical responses to sensory pathway stimulation were accessed (Lybrand and Zoran, 2012). Medial giant fiber (MGF) post synaptic potentials (PSP) and spike activation were recorded in anterior body segments following a 5 min treatment with 25μM CNQX (an

AMPA/kainate receptor antagonist), 100µM AP5 (a NMDA receptor antagonist) or physiological saline control (Fig. 9A). A variety of evoked events (graded PSPs, small

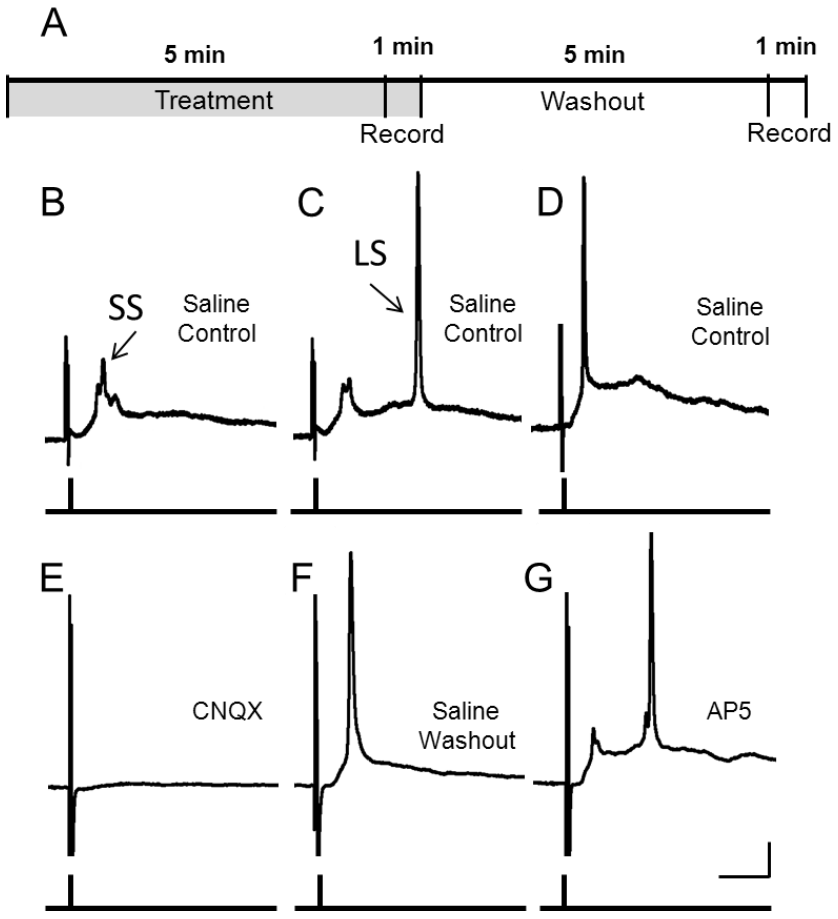

Figure 9. Glutamate antagonism of MGF pathway activation. A) Dissected preparations were treated for 5 minutes prior to penetration of the MGF with an intracellular microelectrode and during one minute of electrophysiological recording. Preparations treated with pharmacological agents were then washed with saline for 5 minutes before a one-minute recording to assess recovery of function following drug washout. B-C) Three examples of saline control recording are shown. Brief electrical stimulation of the body wall (lower traces) elicited PSPs that generated small spikes (SS) that were detected alone (B), were recorded along with large spikes (LS) that were temporally separated (C), or were activated in apparent synchrony with large spikes (D). Activities simultaneous with the onset of stimulation are electrical artifacts. E) Treatment with CNQX abolished stimulus evoked MGF spike activation. F) After 5 minutes of CNQX treatment and a subsequent 5 minutes of saline washout, activation of the MGF was coupled to body wall stimulation. (G) AP5 treatment had no effect on MGF activation. Scale bars equal 10mV (vertical) and 10ms (horizontal).

spikes and large spikes; Fig. 9B) were recorded in anterior MGFs of saline control preparations. Small spikes were either recruited alone (Fig. 9B), in temporal separation from large spikes (Fig. 9C), or in presumed synchrony with large spikes (Fig. 9D). No PSPs or MGF action potentials were detected in response to stimulation following application of CNQX (Fig. 9E). However, in preparations treated with CNQX and subsequently washed for 5 min with saline, graded PSPs, small spikes, and large spikes were each present (Fig. 9F). In contrast, preparations treated with AP5 responded to body wall stimulation with electrophysiological events that were not different from those in preparations treated with saline alone (Fig. 9G).

Further analysis of postsynaptic potentials demonstrated that CNQX treatment reduced the amplitude of evoked PSPs from 8.2±1.1 mV (n=4) to 0.5±0.2mV (n=11; $p<0.01$; Fig. 10A and B). In contrast, the suppression produced by AP5 treatment on evoked PSP amplitude was less than that of CNQX (5.0±0.4mV; n=6) and was not significantly different from that seen in preparations following saline washout (5.0±1.3 mV, n=7; Fig. 10A and B). CNQX treatment also reduced the amplitude of spontaneous (miniature) PSPs as compared to saline controls, where mPSP amplitudes were 1.9±0.2 mV and 0.8±0.3 mV, ($p<0.01$) in control and treated preparations, respectively (Fig. 10C and D). No significant reduction in mPSP amplitude was seen in AP5-treated preparations, nor were the amplitudes of miniature synaptic events recorded during AP5 treatment different from those of washout preparations (2.2±0.2mV; n=7). In contrast,

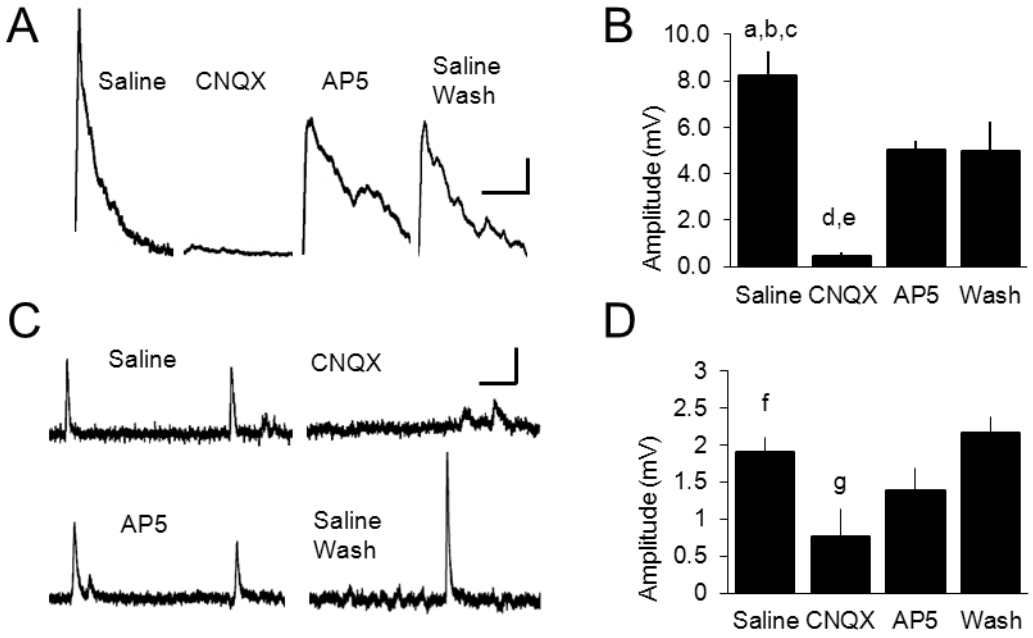

Figure 10. Glutamate antagonism of MGF evoked and spontaneous PSPs. A) Evoked PSPs were abolished by CNQX, but not AP5 treatment. Preparations treated with the antagonist for 5 minutes and subsequently washed for 5 minutes with saline possessed PSP amplitudes that were greater than those in CNQX. B) Quantification of evoked PSP amplitudes demonstrated significant reductions following CNQX treatment as compared to control and washout preparations. a: saline-CNQX ($p<0.01$), b: saline-AP5 ($p<0.01$), c: saline-washout ($p<0.05$), d: CNQX-AP5 ($p<0.01$), e: CNQX-washout ($p<0.01$). C) Representative traces of spontaneous PSPs recorded in presence of glutamate receptor antagonists or saline. D) Quantification of spontaneous PSP amplitudes demonstrated significant reductions following CNQX treatment as compared to control and washout preparations. f: saline-CNQX ($p<0.01$), g: CNQX-washout ($p<0.01$). Error bars presented as SEM. Saline, n=4; CNQX, n=11; AP5, n=7; Washout, n=5. Scale bars equal (A) 2mV (vertical) and 2ms (horizontal) and (C) 1mV (vertical) and 0.1ms (horizontal).

mPSP amplitudes recorded in CNQX-treated preparations were significantly different from washout values ($p<0.01$, n=5; Fig. 10C and D). Thus, MGF PSPs, as well as small

and large spikes, activated by electrical stimulation of sensory afferents were completely abolished by CNQX, but not AP5, treatment, suggesting that sensory-to-giant fiber synapses are exclusively glutamatergic and sensitive to AMPA/kainate receptor antagonism. Furthermore, small spikes recorded in the MGF were indicative of electrically coupled interneuronal inputs, rather than direct electrical coupling from sensory neurons.

Medial giant fiber coupled network

Synaptic inputs to, and outputs from, the giant interneurons of oligochaetes are thought to occur at small unmyelinated collaterals ventrally located along the length of these myelinated giant axons (Drewes 1984, Zoran et al., 1988). In order to visualize these collaterals, the fluorescent dye Lucifer yellow (LYCH; 450 Da) was injected into the MGF of anterior (n=6 preparations) and posterior (n=3 preparations) segments and imaged with fluorescence microscopy. LYCH diffused along the medial giant axon, passing through the septal boundaries (SB) between neighboring axons. In fixed preparations, the septal boundary was identifiable as a chevron shaped apposition of axonal membranes (Fig. 11A), which are the site of gap junction plaques that couple the segmentally arranged giant fiber pathway (Gunther, 1975). Within each segment of giant axon, LYCH accumulated at four collateral projections that were equally spaced (~100 μm) along the axon (Fig. 11A and F). In addition to collaterals, a single medial giant interneuron cell body was present in each body segment and was consistently located at a segment position similar to that of the autofluorescent setae (Fig 11A).

Electrophysiological recordings of small amplitude MGF spikes were indicative of electrically coupled neuronal inputs, yet LYCH injections revealed no dye coupling to neurons other than adjacent medial giant axons. Therefore, neurobiotin (NB; 320 Da), a smaller neuronal tracer molecule, was injected into medial giant axons of anterior (n=20 preparations) and posterior (n=8 preparations) body segments. In these NB-injected preparations, multiple neuronal cell bodies and axon tracts were labeled within the ventral nerve cord. Besides the cell body of the medial giant interneuron, four laterally located cell bodies and four medially located cell bodies were visible in each body segment, within both the MGF sensory field (anterior; Fig. 11B) and the LGF sensory field (Fig. 11C). Along with these NB-labeled cells, a pair of intermediate giant fibers (IGF) was dye coupled to the MGF. The IGFs were smaller in diameter and located ventrolaterally with respect to the MGF. Two cross-bridges connected the paired IGFs (Fig. 11B and D). Interestingly, neither LYCH nor NB injected into the MGF labeled processes outside of the VNC, in control or regenerating worm fragments (Fig. 11E).

The cellular structure of the MGF coupled network was confirmed in NB-filled preparations using serial cross-sections of anterior and posterior body segments. These preparations again demonstrated that a pair of bilateral axons within the IGF bundles was dye coupled to the dorsal MGF (Fig. 12A and B). Furthermore, lateral cell bodies with axons projecting to the IGFs and ventromedial cell bodies had strong fluorescent signals. Thus, a consensus structure of the MGF dye-coupled network includes a total of nine cells and three intersegmental giant fiber pathways: the dorsal MGF and two IGFs (Fig. 12C and D). Dye coupling within this network was restricted to the ventral nerve

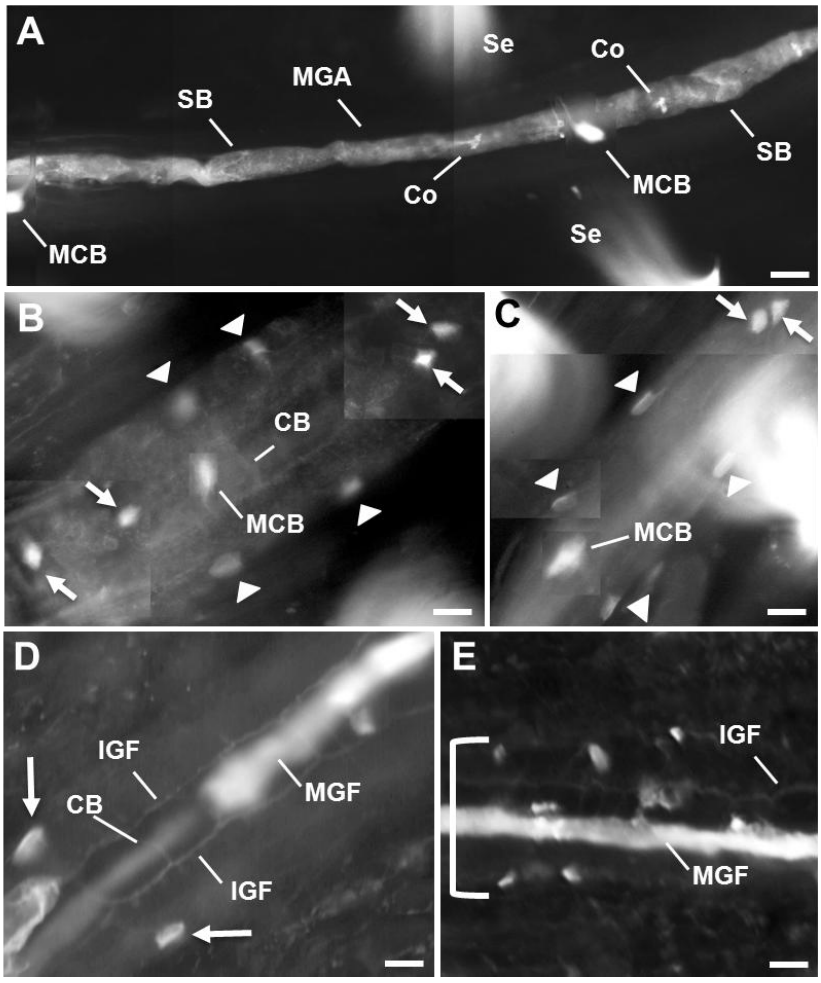

Figure 11. Dye coupling within the MGF network for anterior escape. A) A fluorescent dye, Lucifer yellow, spread both anteriorly and posteriorly along the giant fiber when injected into one of the segmentally-arrange medial giant axons (MGA). A single medial giant cell body (MCB) accumulated the fluorescent dye in each body segment at the level of the bilateral pairs of setae (Se), which are autofluorescent and positioned within the body wall adjacent to the ventral nerve cord. Lucifer yellow readily diffused across septal boundaries (SB), which are the sites of gap junctional coupling between neighboring MGAs. Lucifer yellow also accumulated in multiple giant fiber collaterals (Co) in each segment. Injected anterior preparations; n=6. B) The neurotracer dye, neurobiotin (NB), was injected into a medial giant axon (out of the plane of focus in this image) of an anterior body segment. NB dye diffused along the medial giant fiber as well as into several other neurons and processes within anterior segments of the ventral nerve cord (n=20 preparations). Besides the MCB, eight other neuronal cell bodies became visible following NB immunocytochemical staining. Four dye-coupled cell bodies were positioned laterally within the cord (arrowheads) and four cell bodies were located in the medial cord (arrows). C) This arrangement of strongly dye-coupled medial (arrows) and lateral (arrowheads) neurons along the length of animal's body was indicated by the presence of a similar set of NB stained cells in posterior body segments (n=8 preparations). D) In this anterior body segment, the NB-injected medial giant fiber (MGF) was clearly dye-coupled to the smaller diameter intermediate giant fibers (IGF) and their paired cell bodies (arrows). E) The dye transfer within the MGF/IGF coupled system was restricted to the ventral nerve cord (bracket indicates the edges of the VNC). No processes of dye-coupled neurons extended from the VNC into the peripheral body wall tissues. Scale bars in A and E equal 30 µm. Scale bars in B, C and D equal 15 µm.

cord, indicating that neither sensory afferent, nor motor efferent neurons were directly coupled to the MGF network. Furthermore, the MGF coupled network was metameric and appeared identical in anterior and posterior segments, as well as in body segments undergoing neural morphallaxis.

Synaptic ultrastructure of the MGF coupled network

As mentioned earlier, the synaptic inputs and outputs of the oligochaete giant interneurons are thought to occur at unmyelinated axon collaterals, yet convincing ultrastructural evidence exists for only the latter. Therefore, we conducted transmission electron microscopy of MGF collaterals from both anterior and posterior segments of *Lumbriculus*. Collaterals in *L. variegatus* were identified as protrusions through the myelin-like sheathing of the giant axon. In axon collaterals of both anterior and posterior segments, clusters of synaptic vesicles were localized on the lateral edges of the protruding collaterals (Fig. 13A and B). Synaptic vesicle clusters were associated with numerous mitochondria, as well as pre- and postsynaptic densities, features similar to collateral synaptic architecture identified in other oligochaete worms (Jamieson, 1981).

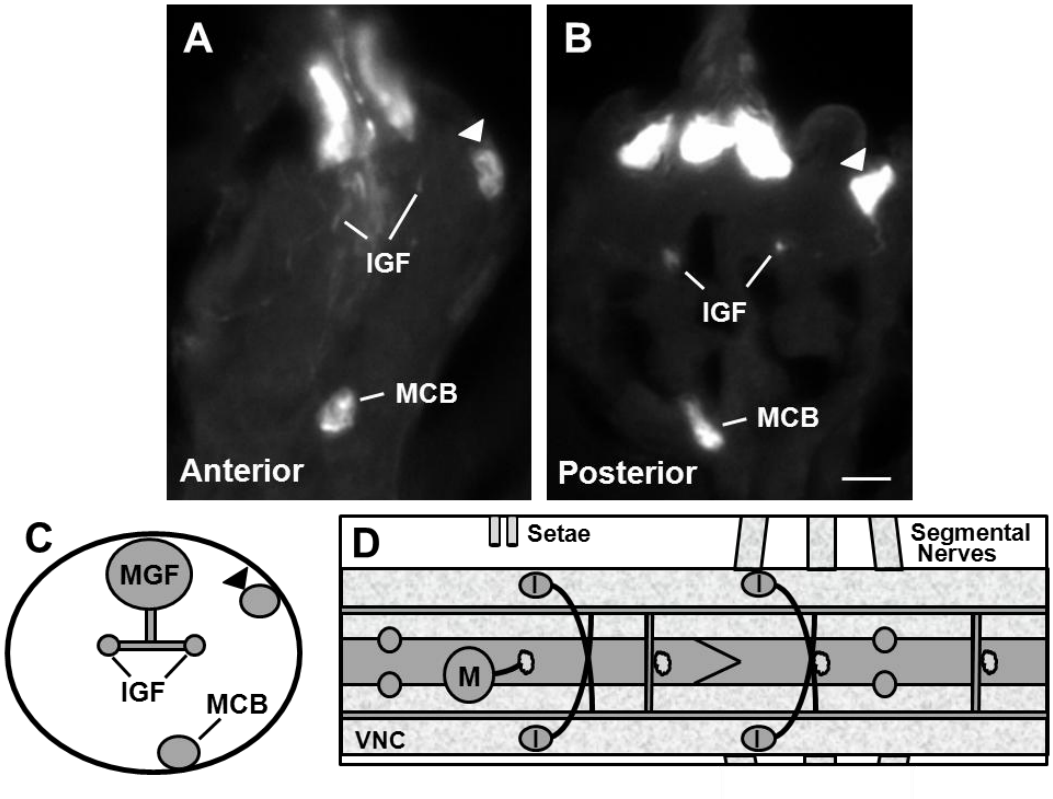

Figure 12. Cellular organization of the MGF coupled network. A) Cross section of the VNC of an anterior segment with neurobiotin injected into the MGF (asterisks). Neurobiotin labeled a medial cell body (MCB), a bilaterally paired intermediate giant fiber (IGF), a lateral cell body (arrow head). B) In posterior segments, NB similarly labeled a medial cell body (MCB), paired IGF, a laterally located cell body (arrow head. C) A summary schematic of a cross section through the VNC identifying the relative size and location of the NB labeled cells as shown in the immunohistochemistry images. D) This horizontal longitudinal illustration of one segment of ventral nerve cord (VNC) summarizes the dye-coupled elements of the MGF coupled network for anterior escape and their position in the VNC relative to two landmarks: the segmentally-arranged body wall setae and the segmental nerves. Each body segment (anterior and posterior) contained nine dye-coupled cell bodies, including one medial giant interneuron (M) and four intermediate giant interneurons (I). Four medial giant axon collaterals (lightly shaded), two intermediate giant axon cross-bridges and one medial giant interneuron septal boundary (chevron) were stereotypically arranged within each segment.

The organization of these synaptic sites, likely interneuronal outputs onto motor neurons (Gunther and Schurmann, 1973), was similar in anterior and posterior segments of the MGF pathway (Fig. 13C and D). However, ultrastructure evidence for the presence of synaptic inputs onto the MGF collaterals, for either anterior or posterior segments, was not observed during the complete serial-section analysis of multiple MGF collaterals.

Electrophysiology and neurobiotin dye fills suggested that the intermediate giant fibers were electrically coupled to the MGF pathway. These intermediate giant interneurons, therefore, constitute potential sites of synaptic input onto the MGF pathway. Bundles of unmyelinated axons located ventrolaterally to the MGF collateral were identified in transmission electron micrographs (Fig. 14A and B) and these IGF bundles were continuous with axonal cross-bridges that connected the IGF to the ventrally projecting MGF collateral (Fig. 14B). The IGFs, and other unmyelinated giant interneuronal bundles, were located adjacent to cellular processes containing clusters of synaptic vesicles associated with plasma membrane thickenings, reminiscent of pre- and postsynaptic densities (Fig. 14C and D). Thus, while no synaptic inputs onto the giant fiber collaterals were discovered, putative synaptic inputs onto intermediate interneuronal giant fibers might constitute an alternative and indirect pathway for sensory activation of the MGF pathway.

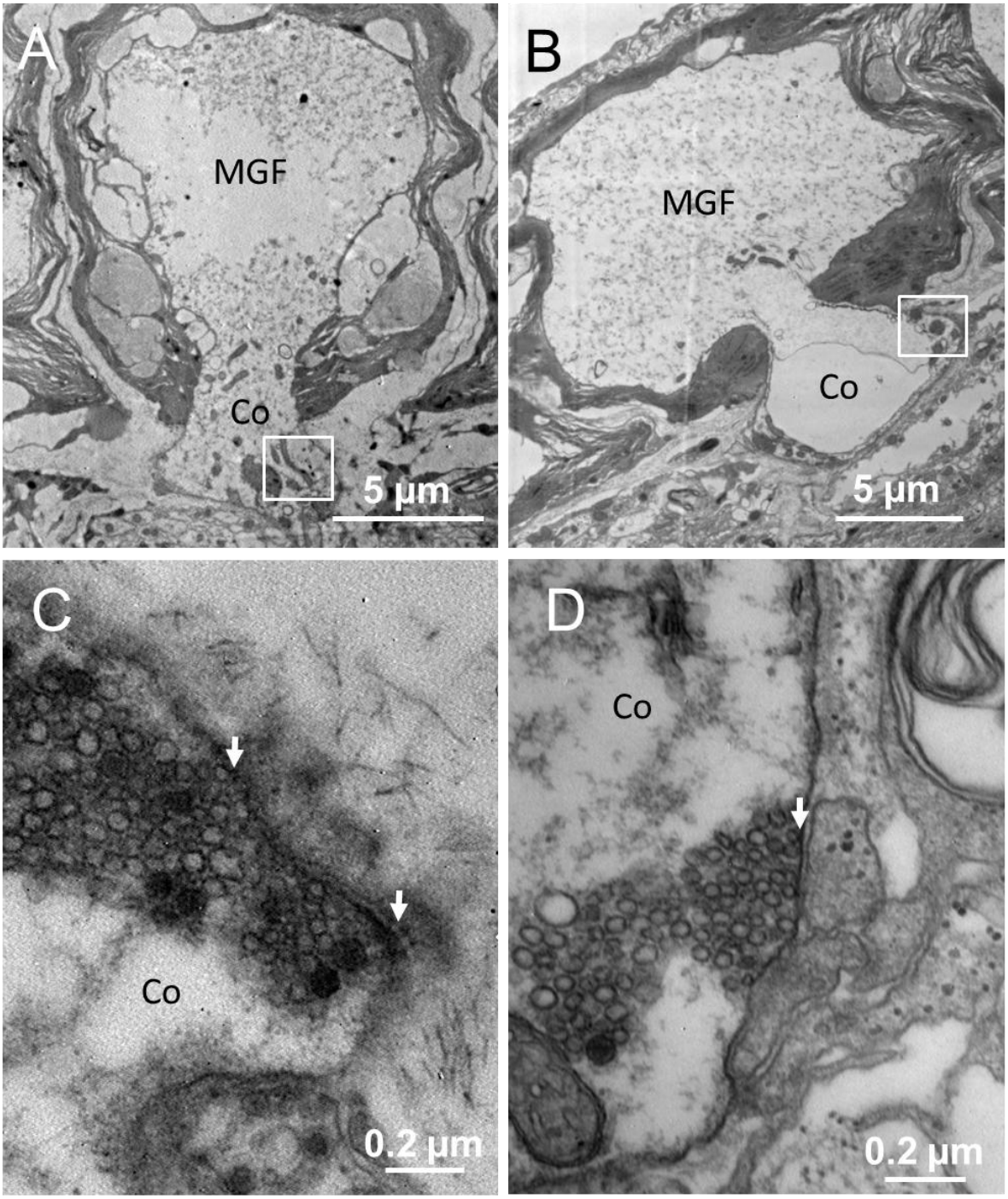

Figure 13. Ultrastructure of MGF collaterals imaged with TEM. A) Cross-section of the MGF from an anterior body segment with a collateral (Co) protruding ventrally through an opening in the loose myelin-like sheath. A region of densely clustered synaptic vesicles was located in the lateral region of collateral (white box). B) Cross-section of the MGF from a posterior body segment with a collateral (Co) protruding through the myelin-like sheath. A region of densely clustered synaptic vesicles was located in the lateral region of collateral (white box). C) Higher magnification of collateral region indicated by box in (A). Both translucent and dense-core vesicles within the collateral cytoplasm were aggregated into a cluster. The plasma membranes of neighboring cells possessed dense thickening in regions adjacent to the vesicle clusters (white arrows). D) Higher magnification of collateral region indicated by box in (B). Vesicle clusters were aggregated within the MGF collateral cytoplasm at regions of plasma membrane thickening (white arrow).

Ionotropic glutamate receptor immunoreactivity at periaxonal regions

Since our ultrastructural studies revealed evidence for synaptic outputs of the dorsal giant interneurons at axon collaterals and synaptic inputs to the intermediate giant interneurons at the axon bundles, we conducted immunocytochemical staining to VNC cryosections to determine if periaxonal regions of MGF collateral and IGF bundles are sites of glutamate receptor (GluR) clustering. Three ionotropic GluR antibodies, which have previously been shown to cross-react with annelid (leech) nervous system (Thorogood et al., 1999), were used as potential synaptic markers because neurotransmission onto the MGF was abolished by CNQX, an AMPA/kainate receptor antagonist. We first tested the immunoreactivity of an antibody to GluR5-7, which specifically recognizes subunits 5, 6 and 7 of kainate receptors in vertebrates and labels putative glutamate receptors in the leech nervous system (Thorogood et al., 1999). We found extensive immunoreactivity of the GluR5-7 antibody within the *L. variegatus* VNC (Fig 15A; n=25) and weak immunoreactivity of the GluR2-3 antibody, which recognizes subunits 2 and 3 of vertebrate AMPA receptors (Fig. 15B; n=2). A third

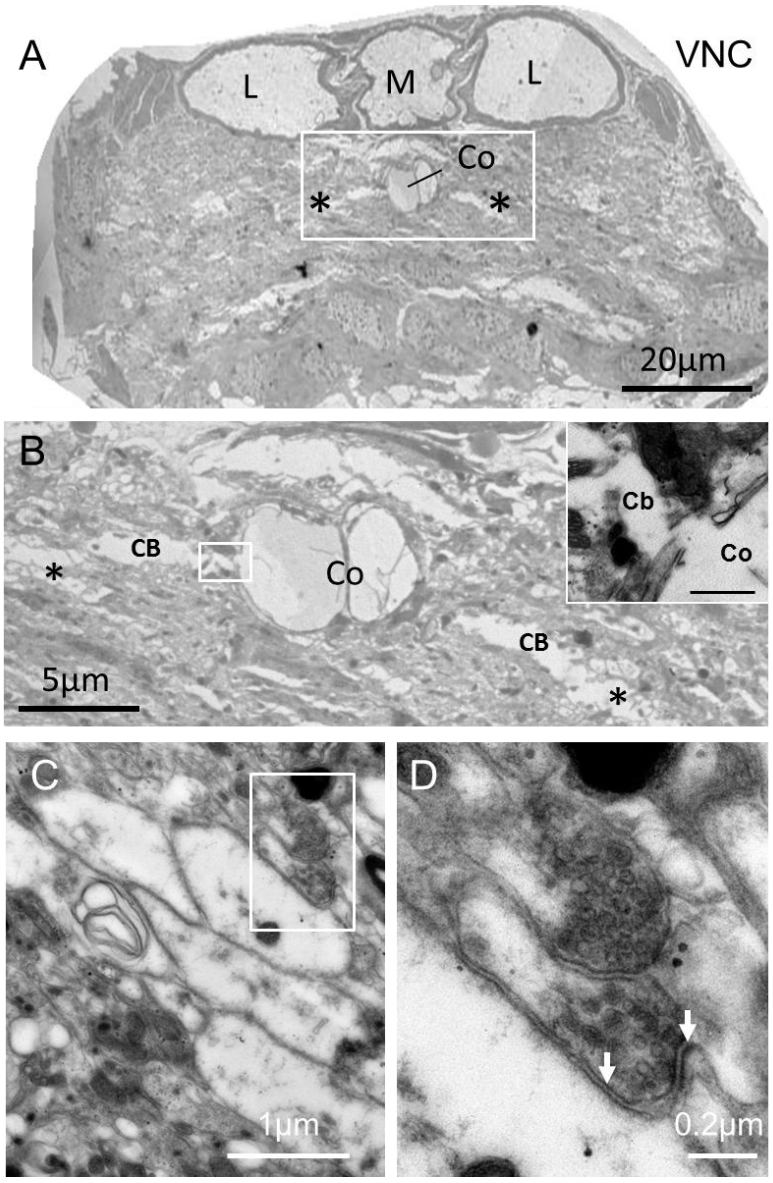

Figure 14. Ultrastructure of intermediate giant interneuron bundles imaged with TEM. A) Cross-section through the ventral nerve cord (VNC) of a posterior body segment shows the three myelinated dorsal giant axons: a medial giant fiber (M) flanked by two lateral giant fibers (L). The MGF collateral (Co) extends ventrally into the neuropile (Ne) of the VNC. Intermediate giant fiber (IGF) bundles, indicated by asterisks (*), are located ventrolaterally to the MGF collateral. B) Higher magnification of MGF collateral, IGF bundles and neuropile region indicated in panel A (white box) illustrates the IGF cross-bridge (CB) that extends from the IGF bundle to the MGF collateral. The inset shows a higher magnification of the site of collateral-cross-bridge contact. C) Cross-section through an IGF bundle shows 4-5 axons of giant interneurons. Synaptic profiles of vesicle clusters with neighboring processes were frequently observed. D) Higher magnification of synaptic region marked in panel C. White arrows indicate sites of pre- and postsynaptic densities, presumed to be synaptic inputs onto IGF bundle.

glutamate receptor antibody, NR1, which recognizes subunit 1 of NMDA receptors, did not immunoreact with the VNC of *Lumbriculus* (Fig. 15C; n=4). GluR5-7 staining was present at longitudinal muscle fibers and in gut tissues (not shown), but was most obvious as punctate labeling within the neuropile of the VNC (Fig. 15D). This GluR5-7 staining was intensely localized to periaxonal regions of the giant fibers, including the medial and lateral dorsal fibers (MGF and LGF; Fig. 15E and F), the ventral giant fibers (VGF; Fig. 15G) and the intermediate giant fibers (IGF; Fig. 15H). Similarly expressed at MGF network synaptic sites in both anterior and posterior segments VNC sections, we compared GluR5-7 immunoreactivity at these pathway periaxonal regions. Punctate GluR5-7 antibody staining intensity at regions surrounding the MGF and IGF axons, as well as LGF and VGF axons, was quantified and compared between anterior and posterior segments. GluR5-7 immunofluorescence was significantly greater in intensity than the general intensity of the neuropile (Fig. 16A and C; $p < 0.01$, n=7), particularly in anterior segments. In posterior sections, the intensity of GluR5-7 immunoreactivity was only significantly greater than the neuropile at VGF periaxonal regions (Fig. 16B and C; $p<0.01$, n=3).

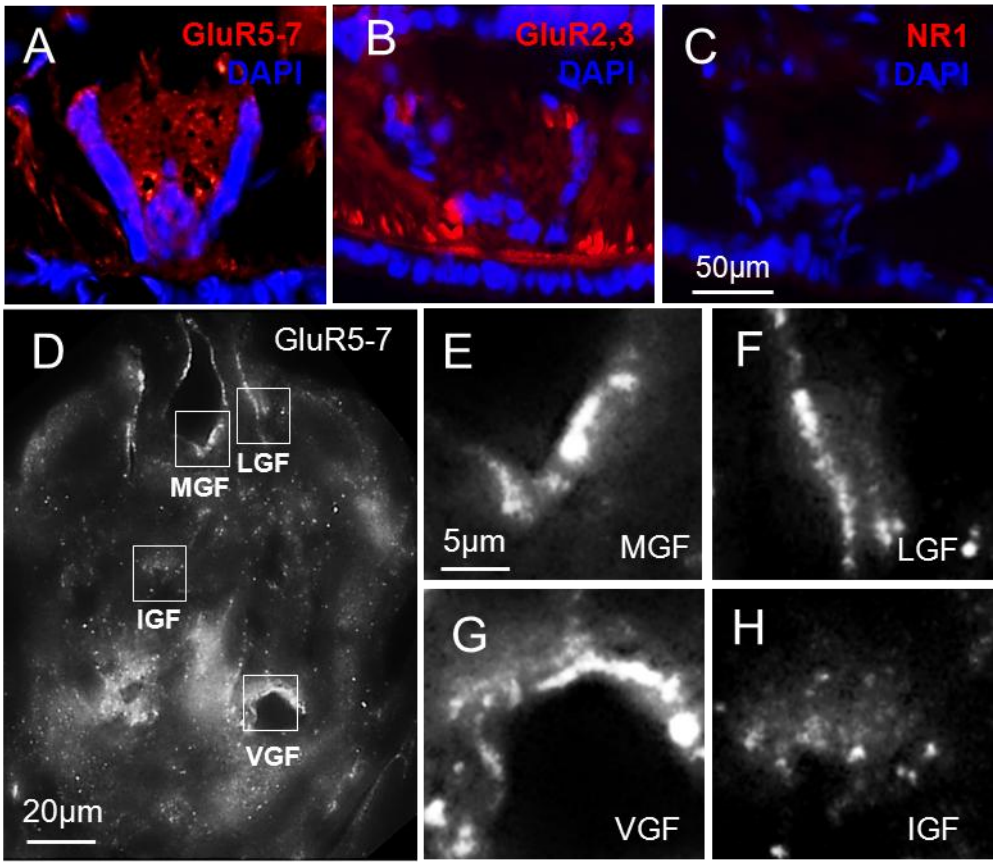

Figure 15. Glutamate receptor immunoreactivity of the VNC. A) VNC from anterior body segments was densely labeled with a GluR5-7 monoclonal antibody, particularly in with the neuropile. B) GluR2-3 immunoreactivity was weak in the VNC neuropile, although staining outside the VNC was present. C) VNC from anterior body segments was not labeled with a NR1 monoclonal antibody. Sections in A-C were co-labeled with DAPI to visualize the nuclei of cell bodies. D) GluR5-7 immunoreactivity was localized to periaxonal regions of the giant interneurons. Higher magnification images of GluR5-7 immunoreactivity illustrate punctate GluR staining at region adjacent to the MGF (E), LGF (F), VGF (G) and IGF (H) axons. Scale for A-C is 50µm (in panel C); E-H is 5µm (in panel E).

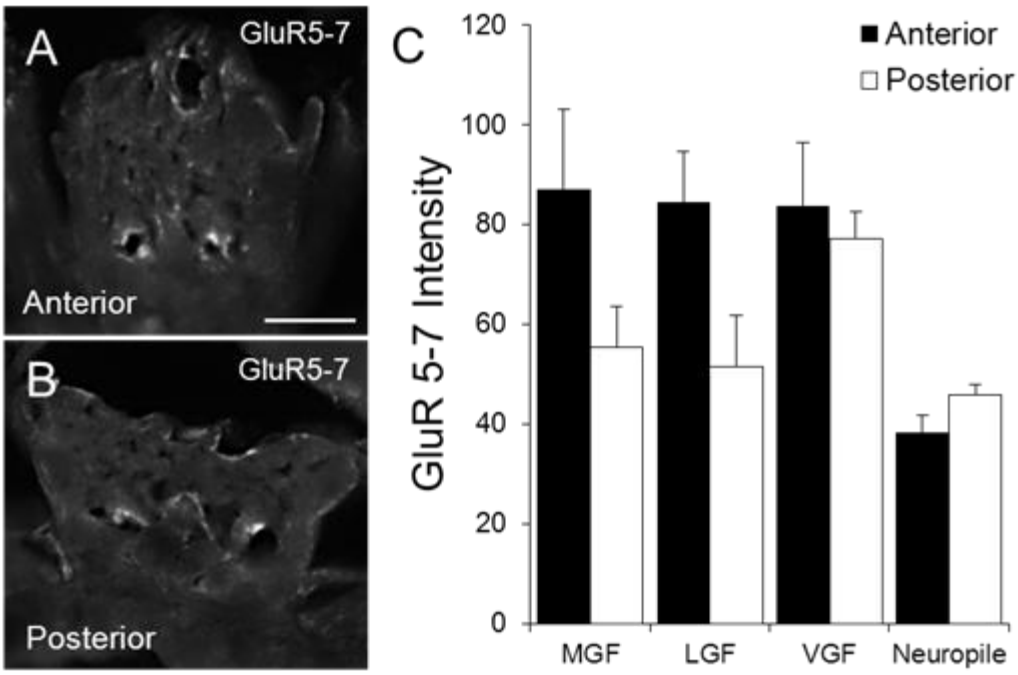

Figure 16. Anterior-posterior differences in giant fiber pathway GluR5-7 immunofluorescence. A) Cryosections of anterior segments showed a significantly higher intensity of GluR5-7 fluorescence around the LGF, MGF and VGF compared to the overall intensity of the neuropile. B) Posterior segments were only statistically greater in immunofluorescent intensity in the periaxonal region of the VGF. C) Quantification of immunofluorescence intensity of periaxonal regions compared to general neuropile intensity. All values are presented as background intensity subtracted. Statistical significance is compared to neuropile ($p < 0.01$). Scale bare shown is 50μm.

Although functional neurotransmission onto the MGF coupled network was absent in posterior segments, GluR5-7 glutamate receptors are not dramatically different along the length of the worm VNC, suggesting that glutamatergic synapses might not be unsilenced by the new expression of significant numbers of postsynaptic receptor molecules. Thus, GluR5-7 antibody stained periaxonal regions associated with MGF coupled networks, implicating these sites as potential locations of sensory afferent

inputs. Furthermore, GluR colocalization to IGF bundles was not different between anterior and posterior pathway regions.

Glutamate receptor co-localization with a marker of neural morphallaxis

Lan3-2 is a monoclonal antibody that recognizes a mannose-rich epitope on sensory afferent tracts of the leech, *Hirudo medicinalis* (Peinado et al., 1987; Zipser et al., 1994). In *Lumbriculus variegatus*, the Lan3-2 antibody has been used as a molecular marker for neural morphallaxis following injury and during asexual reproduction, as the expression of this glycoepitope on multiple proteins changes markedly during this form of regeneration (Martinez et al., 2005). Cross-sections of the VNC in anterior segments of non-regenerating worms were stained with the Lan3-2 antibody to identify where this glycoepitope was expressed (Fig. 17A). Lan3-2 immunoreactivity was high at the periaxonal regions of the medial (Fig. 17B), intermediate (Fig. 17H) giant axons. Co-immunostaining with the GluR5-7 antibody revealed considerable co-localization of the glutamate receptors with the Lan3-2 glycoepitope, particularly at these periaxonal regions (Fig. 17C-D and F-G). To confirm glutamate receptor localization around IGF, cross-sections of preparations with neurobiotin (NB) filled MGF coupled network stained with GluR5-7, showed GluR5-7 staining in the periaxonal region of the IGF. Because GluR5-7 localizes around NB labeled IGF and Lan3-2 glycoepitope colocalizes with the GluR5-7 antibody, suggests that synaptic input of the MGF coupled sensory interneurons to be potential sites of neural morphallactic plasticity during regeneration in *Lumbriculus*.

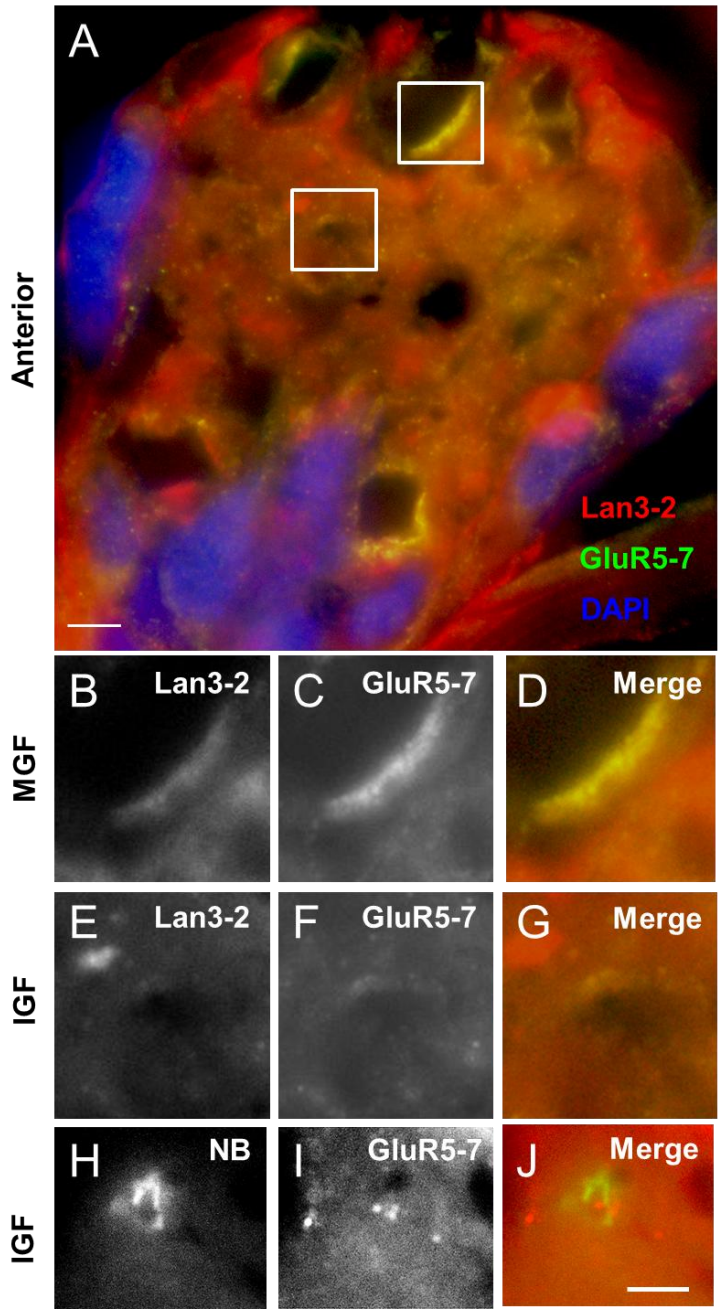

Figure 17. Anti-GluR stained synapses co-label with a neural morphallaxis marker. A) Merged image of VNC labeled with the Lan3-2 antibody (red), which labels a glycoepitope associated with several proteins upregulated during neuromorphallaxis, and anti-GluR5-7 (green) and DAPI (blue). Periaxonal regions around dorsal (B-D) and intermediate (E-G) giant axons show Lan3-2 and GluR5-7 colocalization. (H-J) show intermediate giant fiber filled with Neurobiotin (NB) and labeled with GluR5-7. Scale in (A) is 20µm and B-J is 10µm.

Discussion

Neural morphallaxis, as originally described for the aquatic annelid worm *Lumbriculus variegatus*, is a rare form of regenerative neural plasticity that involves structural and functional changes to the worm's nervous system as segmental fragments take on new positional identities following body amputation (Drewes and Fourtner, 1990; Martinez et al., 2005). One component of neural morphallaxis is the rapid transformation of sensory fields, which underpins the conversion of tail withdrawal responses to tactile stimulation into head withdrawals. This sensory field transformation occurs in 24h or less, as sensory inputs gain the ability to activate the giant interneurons mediating rapid head escape behaviors, while simultaneously losing the ability to activate the tail escape interneurons (Lybrand and Zoran, 2012). In the present study, we have defined the escape neural circuit, anatomically and physiologically, that mediates rapid head withdrawal in *Lumbriculus*, with the goal of determining the neurological nature of this rare form of neurobehavioral plasticity.

Escape reflexes in *Lumbriculus* are mediated by giant fiber pathways that are arranged in segmental fashion along the length of the worm's body. Anterior shortening (head withdrawal behavior) is evoked by stimulation of sensory neurons within segments of the anterior 1/3 of animal's body, which lead to activation of the medial giant fiber (MGF) pathway (Drewes, 1984; Zoran and Drewes, 1987; Drewes and Fourtner, 1990; Lybrand and Zoran, 2012). Stimulation of any other body segment, outside of this MGF sensory field, will fail to activate MGF spikes or head withdrawal. Rather, stimuli to these body segments activate the lateral giant fiber (LGF) pathway and tail withdrawal.

However, following amputation of the anterior body segments, the LGF sensory fields of tail fragments quickly transform, such that stimulation of the anterior portion of the fragment drives MGF pathway activation and anterior escape behavior.

An understanding of the sensory-to-giant interneuron connectivity has existed for decades in the context of several escape neural circuits. For example, the neural circuits that mediate wind current-activated evasion in cockroaches (Dagan and Parnas, 1974; Westin et al., 1988), tactile initiation of tail-flip escape in crayfish (Wine and Krasne, 1972; Zucker, 1972) and statoacoustic activation of Mauthner cell-mediated startle in fishes (Korn and Faber, 1975; Zottoli, 1977) are all well understood. Still, little is known about how sensory neurons of oligochaete worms, including earthworms and *Lumbriculus*, connect to giant fiber pathways, thereby coupling environmental stimuli to escape circuit activation.

Synaptic inputs to the dorsal giant fiber pathways

Neurons involved in the excitation of giant fibers in earthworms consist of segmentally arranged mechanosensory neurons, including both touch- and pressure-sensitive cells (Gunther, 1970; Gunther, 1971). Activation of touch-sensitive neurons evokes small PSPs in both MGF and LGF interneurons, with PSP amplitude largest in the MGF of anterior segments and in the LGF of posterior segments (Smith and Mittenthal, 1980). Electrical stimulation of the body wall in anterior segments of *Lumbriculus*, presumably activating multiple sensory neuron classes, evoked several

electrophysiological responses in the MGF, including small and large spikes and PSPs of graded amplitude. However, stimulation of posterior segments did not activate detectable MGF responses (Fig. 18A and D). We hypothesize that large MGF spikes were the action potentials responsible for activating motor efferents and thus driving neuromuscular synapses and muscle contraction. The small MGF spikes were hypothesized to be the product of action potentials in intermediate interneurons electrically coupled to the MGF pathway (Lybrand and Zoran, 2012) and this prediction was strongly supported by the discovery of Neurobiotin dye coupling between medial giant interneurons and smaller, unmyelinated interneurons (intermediate giant fibers; IGF) of the *Lumbriculus* VNC. The structural organization of these IGFs was similar to that described in the earthworm, where intermediate giant interneurons form electrical synapses with the medial giant interneuron (Walther, 1971; Gunther and Schurmann, 1973; Drewes, 1984). The current structural and functional demonstration of a medial giant fiber coupled network is consistent with the prediction from electrophysiological studies in earthworms that sensory processing interneurons might be interposed between touch-sensitive neurons and the dorsal giant interneurons they activate (Smith and Mittenthal, 1980).

Lucifer yellow and Neurobiotin, but not rhodamine dextran, injected into the *Lumbriculus* MGF, passed readily through putative gap junctions located at the septal boundary between adjacent segments of medial giant axon. In contrast, only Neurobiotin diffused from the MGF into the coupled IGFs, suggesting that gap junctions present at MGF-to-MGF and IGF-to-MGF connections within the coupled network are

functionally, if not structurally, distinct. Interestingly, no dye-filled processes were found to exit the VNC within the segmental nerves, demonstrating that neither sensory neurons nor motoneurons are dye-coupled to the network, ruling out the possibility that small MGF spikes were the product of antidromic motor neuronal spike propagation following body wall stimulation. Furthermore, synaptic transmission and MGF activation, including the small spikes, were abolished by treatment with CNQX, an antagonist of specific glutamate receptors. Thus, MGF pathway activation was exclusively driven, directly or indirectly, by glutamatergic chemical neurotransmission and small spikes recorded in the MGF were likely the product of IGF action potential currents spread through electrical synapses at sites of contact between the intermediate and dorsal fibers of the MGF coupled network.

Dye coupling between IGF and MGF axonal pathways suggested that activation of the coupled network by sensory afferents might occur at glutamatergic synapses onto the IGF (Fig 18A). Serial transmission electron microscopy identified synaptic outputs at axon collaterals of the MGF in both posterior and anterior segments, but failed to generate any evidence of synaptic inputs at these same locations. However, synaptic inputs were identified at intermediate giant interneuronal bundles. These TEM results are reminiscent of those from earthworm studies, where no chemical synapses onto giant fiber collaterals could be identified and where touch- and pressure-sensitive neurons activated by body wall stimulation did not likely activate the MGF directly (Gunther, 1971). Rather, sensory afferents are likely transmitted via electrical synapses at contacts between cross-bridges of intermediate giant interneurons and MGF collaterals.

Furthermore, glutamate receptors, as determined by immunocytochemical staining with a GluR5-7 antibody, were enriched at periaxonal regions of the MGF, likely associated with glutamatergic outputs, and at IGF bundles, the putative sites of glutamatergic sensory inputs.

Rapid synaptic plasticity during escape circuit sensory field transformation

Sensory field transformation associated with neural morphallaxis in *Lumbriculus* involves a change in functional synaptic transmission that emerges during the first 6-24h of segmental regeneration (Lybrand and Zoran, 2012). This rapid synaptic plasticity suggests a concerted unsilencing of existing, but non-functional, sensory afferents onto the MGF coupled network. Synapses that are incapable of neurotransmission during long periods, and therefore functionally silent, may be quite common in a wide range of nervous systems and possess the ability to quickly become functional in the appropriate context (Atwood and Wojtowicz, 1999; Kerchner and Nicoll, 2008). We suggest that the initial unsilencing of sensory afferents in *Lumbriculus* begins with the emergence of functional synaptic transmission at the IGF sensory bundles, since both PSPs and small spikes are the earliest events recorded in MGFs of transforming segments during neural morphallaxis (Fig. 18B and E; Lybrand and Zoran, 2012). Presumably, within the next seven days of regeneration, the MGF becomes sufficiently excitable such that large spikes are activated by electrical inputs from the IGFs of the coupled network. This emerging excitability may, in part, be a product of the increased synaptic communication

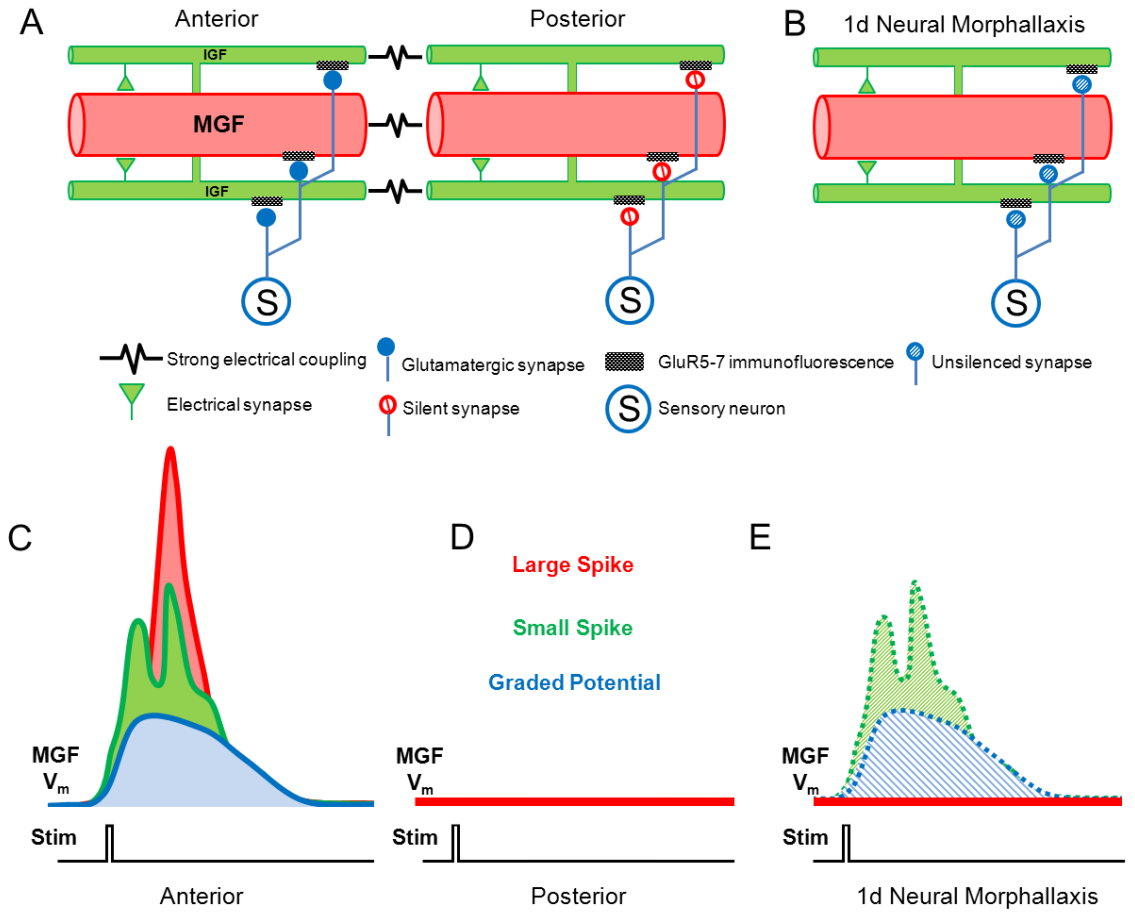

Figure 18. Functional unsilencing of glutamatergic sensory input onto the MGF coupled network during neural morphallaxis. A) Schematic of the medial giant fiber (MGF) coupled network composed of a sensory interneuron, intermediate giant fibers (IGF, green) and the MGF (red). Anti-GluR5-7 staining was located on periaxonal regions of MGF and IGF in both anterior and posterior segments. There were functional glutamatergic synapses onto the MGF pathway, however in posterior segments these synapses were functionally silent. B) Following one day (1d) of neural morphallactic regeneration synaptic transmission was unsilenced. C) Summary of the electrophysiology evidence. In anterior segments, activation of sensory inputs drove a large spike in the MGF (red peak) and a small spike (green peak), hypothesized to be an action potential in the electrically couple sensory interneuron. A graded potential (blue peak) is recorded postsynaptic potentials in the MGF. D) In posterior segments, there are no PSPs or spikes recorded from the MGF. E) Small spikes and MGF PSPs return following 1d of neural morphallactic regeneration.

between glutamatergic sensory afferents and the IGF sensory interneurons (discussed further below).

In support of this silent synapse idea, no differences in dye coupling or GluR5-7 immunoreactivity were detected within the MGF coupled networks of anterior and posterior segments of intact worms or in the MGF networks of regenerating worm fragments following head or tail amputation. Still, although the most plausible mechanism of sensory field plasticity during neural morphallaxis remains the unsilencing of existing sensory to IGF glutamatergic connections, the precise identification of those transforming synapses remains undetermined. The recruitment of functionally silent synapses has been demonstrated in other neural circuits, including those of crustaceans (Jahromi and Atwood, 1974), insects (Atwood et al., 1993), fish (Faber et al., 1991) and mammals (Wall, 1977; Isaac et al., 1995; Malenka and Nicoll, 1997).

Similar to the highly plastic silent synapses of the mammalian CNS (Isaac et al., 1999; Philpot and Zukin, 2010), sensory synapses within the escape neural circuit of *Lumbriculus* appear highly adapted for rapid strengthening, a characteristic feature of morphallactic regeneration following fragmentation due to injury, fission during asexual reproduction, or self-autotomy (Drewes and Fourtner, 1990; Lesiuk and Drewes, 1999; Martinez et al., 2005; Martinez et al., 2006). Some of the established mechanisms of synapse unsilencing were discovered within escape neural networks. For example, unsilencing of inhibitory synapses onto Mauthner cells in the goldfish involves nonfunctional postsynaptic membranes becoming functional (Faber et al., 1991),

whereas silent synapses in crayfish become functional through changes in presynaptic mechanisms (Wojtowicz et al., 1991; Wojtowicz et al., 1994). In the *Lumbriculus* escape neural circuit, glutamatergic synaptic transmission associated with activation of the MGF coupled network was abolished by CNQX, an AMPA/kainate antagonist in vertebrates, but not by AP5, a vertebrate NMDA receptor antagonist. Furthermore, GluR5-7 immunoreactivity, but not that of the NR1 NMDA receptor antibody, was detected at periaxonal regions of MGF network. Thus, if silent synapses underlie the synaptic plasticity associated with neural morphallaxis in *Lumbriculus*, then it is not likely that conventional vertebrate mechanisms of unsilencing involving NMDA receptor-mediated postsynaptic potentiation are involved. Rather, it is possible that the glutamatergic synapses recognized by the GluR5-7 antibody are the sites of neural morphallactic plasticity. In support of this idea, immunoreactivity of the GluR antibody and the Lan3-2 antibody, an established molecular marker of *Lumbriculus* neural morphallaxis (Martinez et al., 2005), were co-localized of at the periaxonal sites of putative synaptic activation of the MGF coupled network.

Interneuronal sensory processing in escape neural networks

Escape reflexes are powerful, short-latency behaviors with a clear and critical adaptive value, increasing the survivability of an organism when attacked (Herberholz et al., 2004). The escape neural circuits that mediate a number of startle and rapid avoidance behaviors have been extensively studied. In the cockroach, escape behaviors

are mediated by a set of interneuronal pathways. Touch stimuli (Burdohan and Comer, 1996; Ye and Comer, 1996) and wind stimuli (Comer, 1985; Camhi and Levy, 1989) activate different sets of interneurons in the ventral nerve cord that trigger specific escape responses. In some fishes, auditory evoked escape behavior is mediated by giant interneurons, the Mauthner (M) cells, which when activated drive a C-start motor behavior that turns the fish away from the aversive sound (Korn and Faber, 1975). Along with afferents from the 8th cranial nerve, this escape neural network involves input from the lateral line (LL) system onto the M-cell. A component of this LL afferent input is electrotonic and it influences M-cell excitability and the initial directionality of the escape (Mirjany and Faber, 2011). In crayfish, the tail-flip escape behavior is activated by tactile stimuli via a well-documented escape circuit (Edwards et al., 1999). Mechanosensory afferents connect via cholinergic synapses to secondary sensory interneurons that, in turn, are electrically coupled to the lateral giant (LG) interneurons that trigger the tail-flip reflex (Zucker, 1972; Miller et al., 1992). Rostral stimuli, by exciting the secondary interneurons, bring the LGs closer to threshold, thus priming the tail-flip pathway for activation (Liu and Herberholz, 2010). The intermediate giant interneurons of the *Lumbriculus* MGF escape neural circuit may function in a similar capacity through their priming of GF excitability.

IGF-mediated sensory processing may enhance intersegmental integration of afferent inputs, thereby contributing to spatial summation and synchrony of MGF activation. With the characteristic long space constant of giant fiber pathways, the electrically coupled sensory interneurons may serve as a distributor of inputs from many

neighboring segments to multiple collateral processes. In so doing, the synchronous inputs would create less shunting (loading) of currents between input sites, effectively increasing input resistance and making PSP amplitude larger and longer. The transmission of sensory signals to giant fibers in annelids is a highly labile process, providing for rapid habituation to repeated stimuli (Drewes, 1984). During studies of earthworm senory-to-giant fiber processing, Smith and Mittenthal (1980) suggested the likely existance of an interposed interneuron between touch sensory neurons and the MGF to explain the plasticity (facilitation and depression) and variation observed in the amplitude of evoked PSPs. Similarly, the S-cell network of the leech, which is a through conducting system along the ventral nerve cord, receives sensory inputs from touch neurons via a pair of small interneurons electrically coupled to the S-cell (Muller and Scott, 1981). The importance of these interposed interneurons, and those of *Lumbriculus*, might be contextual, such that they function to appropriately modulate the efficacy of sensory-to-giant fiber network communication.

Escape neural circuits exist in a wide range of animals, from annelids and arthropods and mollusks to chordates. Within those neural networks, some structural features that promote processing speed have evolved independently in muliple taxa. These include axonal gigantism and glial myelination (Schweigreiter et al., 2006; Hartline and Colman, 2007). Some aspects of synaptic structure and function are also consistently present within escape circuits, including gap junctions and electrical coupling for their speed in transmitting neural signals. The escape neural circuit we have described here for *Lumbriculus* possesses each of these features: giant axons, myelinated

fibers, and electrical synapses. The presence of sensory processing interneurons, similar to those described for the crayfish escape network (Edwards et al., 1999), are also present in *Lumbriculus* and these interneurons may be representative of yet another common characteristic of escape neural networks that function in aspects of circuit plasticity, such as regulating giant fiber excitability (priming), mediating the distribution of sensory inputs (unloading) and modulating of sensory-to-giant fiber neurotransmission (signaling).

Summary

Lumbriculus variegatus undergoes a rapid regenerative transformation of its escape neural circuits following body fragmentation. This form of nervous system plasticity, called neural morphallaxis, involves the remodeling of the giant fiber pathways that mediate rapid head and tail withdrawal behaviors. Sensory-to-intermediate giant fiber connections were the likely sites of morphallactic synaptic plasticity, an unsilencing of glutamatergic synapses, since strong IGF to MGF electrical synapses exit prior neural circuit morphallaxis. These sensory interneurons of the escape network are suggested to be potential sites of sensory input integration and modulation, as well as morphallactic transformation. Their commonalities with interneurons of other animal systems suggest that interneuronal sensory processing might be a characteristic feature of escape neural circuits, which have likely evolved independently across multiple taxa. Therefore, understanding morphallactic and other forms of neural plasticity within

escape neural circuits provides insight into the general principles of sensory processing and network modulation that are common to diverse groups of animals and their nervous systems, but in the context of behaviors critical to the organism's survival.

CHAPTER IV

ELECTRICAL SYNAPTIC PLASTICITY OF THE MEDIAL GIANT FIBER DURING NEURAL MORPHALLAXIS IN *Lumbriculus variegatus*

Introduction

Escape behaviors are short-latency and powerful motor responses to environmental stimuli. These behaviors are mediated by rapid neural reflexes, which ensure the successful escape from predators or withdrawal from noxious stimuli. Since the discovery of giant nerve fibers of cephalopods (Young, 1939), axons of large diameter ('giant axons') had been found to mediate rapid escape reflexes in a range of animal phyla (Hartline and Colman, 2007). The startle response in the squid, *Loligo opalescens,* is driven by activation of giant motor axons (Otis and Gilly, 1990). In crayfish, activation of giant interneurons initiates tail-flip escape behavior (Edwards et al., 1999). Cockroach escape responses are triggered by wind cues or touch stimuli, which are mediated by sets of giant interneurons within the ventral nerve cord (Comer, 1985; Ye and Comer, 1996). Even in vertebrates, for example the goldfish, startle behaviors are activated by excitation in Mauthner cell giant axons (Korn and Faber, 2005). In each of these escape neural reflexes, the giant axons serve to rapidly propagate action potentials along various paths of the neural circuit, effectively reducing the response time between sensory activation and motor behavior.

The escape behavior of *Lumbriculus variegatus,* an aquatic annelid worm, has been well characterized (Zoran and Martinez, 2009) and involves a set of dorsal giant axons that are highly conserved among oligochaete worms (Zoran and Drewes, 1987). In *Lumbriculus*, like other oligochaetes, tactile stimulation to anterior segments activates a medial giant fiber (MGF) pathway that drives motor responses for anterior shortening (head withdrawal) behavior. Likewise, stimulation to tail segments activates a lateral giant fiber (LGF) pathway and posterior shortening (tail withdrawal) behavior. Each of these giant fiber pathways is composed a chain of giant axons located within the dorsal region of the ventral nerve cord. The giant axon of each segment is electrically coupled at sites of contact between the giant axons of neighboring segments (Jamieson, 1981; Zoran and Martinez, 2009). These giant axon pathways are activated by tactile or photic stimulation and these afferent inputs are organized into anterior MGF and posterior LGF sensory fields (Drewes and Fourtner, 1990). Recent studies indicate that glutamatergic inputs to the MGF pathway involve a pair of sensory interneurons, which are electrically coupled to dorsal giant axons (Lybrand et al., 2012); see Chapter 2). The escape reflex pathways of *Lumbriculus variegatus* are quite plastic in adult worms and switch from LGF- to MGF-mediated behaviors during asexual reproduction and regenerative responses to injury (Martinez et al., 2005; Martinez et al., 2006), a rare type of behavioral plasticity called neural morphallaxis.

Neural morphallaxis (NM) in *Lumbriculus variegatus* is characterized by gradual changes, over many weeks, in giant fiber physiology and morphology (Drewes and Fourtner, 1990; Martinez et al., 2005; 2006). Several studies of neural morphallaxis in *L.*

variegatus have defined aspects of the transformation of escape neural circuits, particularly plasticity of the sensory-to-giant interneuron path (Lybrand and Zoran, 2012; see Chapter 1; Lybrand et al., 2012; see Chapter 2). Although it is known that giant axons change dramatically in size during morphallaxis (Drewes and Fourtner, 1990), little is known regarding the plasticity of electrical synapses between interneuronal axons of the giant fiber pathways. Here we demonstrate that the conduction velocity of the MGF pathway rapidly decreases during the first days of neural morphallaxis following body segment amputation, but this reduction in spike propagation rate is transient and recovers by the seventh day of regeneration. Electrophysiological and dye coupling approaches were used to determine the potential role of giant fiber electrical synaptic plasticity in morphallactic changes in axonal conduction velocity.

Materials and methods

Animals and maintenance

Aquatic oligocheate worms, *L. variegatus*, were purchased from Flinn Scientific (Batavia, IL). Worms were housed in plastic bins containing aerated, aged freshwater and squares of brown paper toweling. A constant temperature of 16^{o}C was maintained. Worms were fed powdered Algae-Feast™ Spirulina (Aquatic Eco-Systems Inc., Apoka, FL) weekly. Amputation of tail segments was conducted using microdissection scissors to generate fragments of desired segmental identity. For the present studies, experiments were performed from three proportionally sized regions of the worm: anterior, middle,

and posterior. Worms of about 120 total segments were used in these studies (see Fig. 17A). Thus, the anterior region was the first 30-40 segments, the middle regions was segments 40-80, and posterior were segments 80-120. To create fragments within the LGF sensory field, a cut was made either 10 segments posterior (dotted line b) or 30 segments posterior (dotted line c) to the anterior region (solid line a). Following amputation, worm fragments were maintained in fresh spring water (Ozarka, Oklahoma City, OK) until used for experiments.

Electrophysiological recording

Non-invasive electrophysiology

Conduction velocity of the medial giant fiber (MGF) and lateral giant fibers (LGF) were recorded using a non-invasive electrode grid (O'Gara et al., 1982; Lybrand and Zoran, 2012; Chapter 2). Worms were placed on recording grid and tactile stimulated with a handheld probe on either a head segment or a tail segment. MGF or LGF spikes were recorded using the printed circuit board electrode grid with positive and negative electrodes placed 1mm apart. Extracellular voltage changes were preamplified with a differential recording amplifier (100x gain, AC-coupled differential inputs) and digitized with a Powerlab A-D/4ST conversion system (ADInstruments, Inc., Colorado Springs, CO) at a sampling rate of 40kbs with 20kHz lowpass filtering. Waveforms were analyzed on a PowerMac G4 (Apple Inc., Cupertino, CA) using the Powerlab Chart.4.1 software. Conduction velocity was calculated by dividing the latency

of the GF spikes by the distance between the two recording electrodes placed 10mm apart.

Invasive electrophysiology

Dual current clamp recordings were performed on reduced preparations of *Lumbriculus variegatus.* Worms were immobilized in worm saline solution containing 0.25 mM nicotine and dissected out as described in previous chapters (Chapter II and II). Borosilicate glass microelectrodes (10-25MΩ tip resistance) filled with 1.5KCl were used to penetrate neighboring axons of the MGF. To measure electrical coupling, electrodes were placed in neighboring segments and stable resting membrane potentials were recorded. A large enough hyperpolarizing current was injected into the presynaptic (Pre) segment until a voltage change was recorded in the postsynaptic segment (Post) (see Fig. 18A). Change in membrane potential (both pre and post-synaptically) were amplified using a bridge-balance electrometer (Getting Instrumental Inc.), digitized using the Powerlab A-D/4ST and recorded using Powerlab Chart 4.1 (ADInstruments, Inc.) software on a PowerMac G4 (Apple Inc.). Electrical coupling was calculated as a ratio of postsynaptic to presynaptic voltage changes (Bennett, 1977). For all data measurements were taken 1s from the onset of the hyperpolarizing current injection.

Dye injections and dye coupling

For dye injections worms were immobilized, dissected and pinned as described previously (Chapter III). Medial giant fiber axons were injected with 3% lucifer yellow

and 3% rhodamine dextran (Molecular Probes) using a picospritzer (General Valve). Injected preparations were incubated in worm saline for 30 minutes to allow diffusion of the dye. Whole mount preparations were then imaged using an Olympus IX70 inverted microscope and CoolSnapHQ camera (Actimetrics, Wilmette, IL). Fluorescent intensity was measured using Simple PCI6.0 imaging software (Compix, Inc., Cranberry Township, PA). Dye coupling was calculated as a ratio of LYCH intensity from two neighboring segments. For all fluorescent intensity data presented, the average background intensity was subtracted from all intensity values.

Statistics

Statistical significance was analyzed using a Student's t-test (Excel 2010, Microsoft) and presented as $p<0.01$ or $p<0.05$ where indicated. Variation was presented as standard error of the mean (SEM).

Results

Medial giant fiber conduction velocity decreases during early neural morphallaxis

Lumbriculus neural morphallaxis (NM) is characterized by a gradual increase in GF diameter and conduction velocity, which requires many weeks to complete (Drewes and Fourtner, 1990; Martinez et al., 2005; 2006). More rapid changes in sensory field organization of the GF pathways occur early, in the first days, of NM (Lybrand and Zoran, 2012; see Chapter 1). A series of experiments were conducted to determine if early NM of the escape neural circuit involved changes in giant axon physiology.

Specifically conduction velocity during the first three weeks of NM was measured using non-invasive electrophysiological methods. In this first set of experiments, tail fragments were generated by complete transection of a worm's body at the interface between the anterior and the middle one-thirds of the animal's segments. A further 10, or in some cases 30, segments were removed from the anterior end of these posterior fragments to ensure that the remaining segments were entirely within the lateral giant fiber (LGF) sensory field (n=24; Fig. 19A). The conduction velocity of the LGF in middle body segments during the first 28 days of NM showed no significant changes (Fig. 19B). However, MGF conduction velocity significantly decreased from 12.9±0.5 m/s prior to amputation (D0; n=24) to 9.3±0.4 m/s one day following fragmentation (D1; n=13; $p<0.01$; Fig. 19B). By the fourth day post-amputation, conduction velocity in the MGF began to increase (D4; 10.9±0.3 m/s; n=23) and had fully recovered to intact speed by the seventh day post-amputation (D7; 12.7±0.5 m/s; n=23).

To test for a gradient in conduction velocity and its plasticity along the body-axis during NM, measurements were conducted at two different segmental levels more posterior within the middle body region (Fig. 19A). After one day of NM regeneration, MGF conduction velocity was reduced by 23.9±4.9% in fragments cut 10 segments into the middle body region of the worm (D1+10; n=5; Fig. 19C). However, in fragments produced by amputation at a site 20 segments more posterior, MGF conduction velocity was reduced even more by day one (D1+30; 31.4±3.2%; n= 5; p=0.1). Thus, the conduction velocity of the MGF decreased rapidly within the first day of NM following injury and was reduced to a greater degree the more posterior the site of amputation.

This plasticity in MGF conduction velocity was coincident with the time period of shifting sensory fields previously reported during NM at these segmental sites (Lybrand and Zoran, 2012; see Chapter 1).

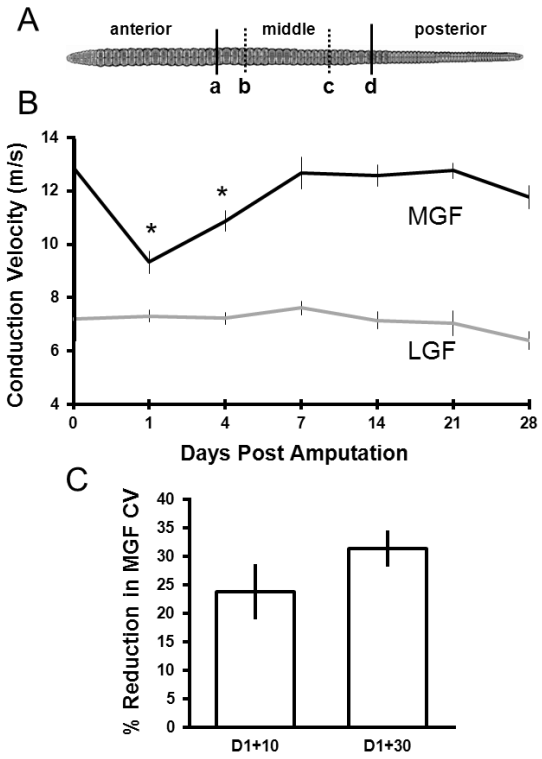

Figure 19. MGF conduction velocity reduction in early neural morphallaxis. A) Tactile stimulation to segments within the anterior one-third (anterior) of the worm activated the MGF pathway. Similarly, stimulation of the posterior two-thirds of the animal, the middle and posterior regions, activated the LGF pathway. Cuts (solid lines) were made such that fragments were generated for NM regeneration taken from the middle and posterior regions. In some experiments, middle section cuts (dotted lines) were made further posterior into the fragment. B) MGF, but not LGF, conduction velocity in middle region fragments exhibited a transient reduction during the first days of NM. C) On day one of NM, the conduction velocity of the MGF from fragments cut 10 segments (D1 +10; dotted line b) and 30 segments (D1 +30; dotted line c) more posteriorly into the middle region was measured. Greater reduction in conduction was observed in more posterior fragments. Asterisk (*) indicates statistical significance of $p<0.01$. Error bars represent standard error of the mean.

MGF electrical coupling does not change during early neural morphallaxis

Differences in giant fiber conduction speed in annelid worms are dependent on the extent of myelination and the axon's diameter (Drewes, 1984). These chains of giant interneuronal axons are also coupled segmentally via gap junctions (Gunther, 1975; Oesterle and Barth, 1981). In the next set of experiments, MGF electrical coupling coefficient (ECC) was measured using dual current-clamp recordings from neighboring giant interneuron axons within the middle body region of intact and regenerating worms (Fig. 20A). The voltage change elicited by a hyperpolarizing current injection was recorded in both the presynaptic and postsynaptic interneurons and ECC was calculated (see Materials and Methods). MGF electrical coupling was not significantly different between D0 (n=4) and D1 (n=2; Fig. 20 B and C), suggesting that the rapid and marked change in conduction velocity one day after fragmentation was not due to transient changes in electrical coupling between MGF axons. Furthermore, no significant differences in the amplitude of MGF membrane potential changes elicited by injection of hyperpolarizing current were detected (Fig. 20D), further indicating a lack of rapid alterations in MGF passive electrical properties.

MGF dye coupling is plastic during late, but not early, neural morphallaxis

Medial giant fibers within the three body regions tested (Fig. 19A) were injected with the fluorescent dyes lucifer yellow (LYCH) and rhodamine dextran (RHDX). RHDX, with a large molecular weight (10,000 kDa) did not pass between MGF axons of

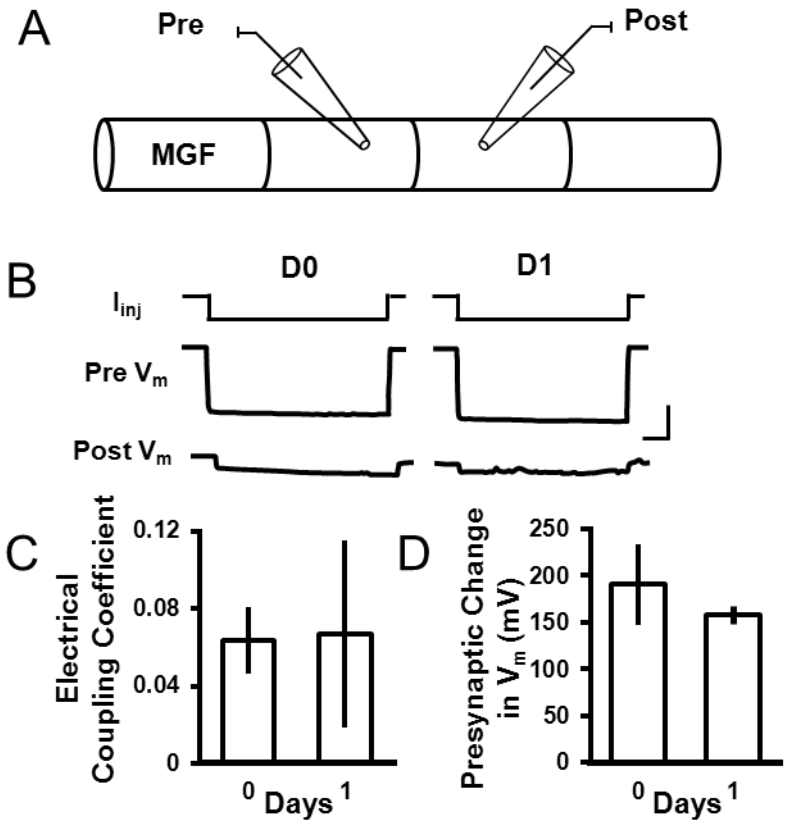

Figure 20. MGF electrical coupling during early neural morphallaxis. A) Neighboring axon segments of the MGF were simultaneously penetrated with microelectrodes. A hyperpolarizing current was injected into the presynaptic segment and the voltage change in both the pre- and postsynaptic cell was recorded. The electrical coupling coefficient was calculated by dividing the magnitude of the change in membrane potential of the neighboring cell (post) by the change in membrane potential of the injected cell (pre). B) Representative traces from the pre- and postsynaptic interneurons show the changes in membrane potential of a non-regenerating, intact worm (D0) and of a worm fragment one day after amputation (D1). C) Quantification of the electrical coupling coefficient from D0 to D1 preparations demonstrated no significant difference in MGF electrical coupling. D) No differences in the membrane responses to current injection were detected between D0 and D1 preparations. Scale bars in B represent 5ms and 50mV. Error bars represent SEM.

neighboring body segments in any body region of intact animal or during NM (Fig. 21A-D). However, lucifer yellow, a dye with a much smaller molecular weight (500 kDa), diffused bidirectionally between neighboring MGF axons. Furthermore, LYCH readily diffused along many segments of MGF axon in both posterior segments of intact animals (Fig. 21E) and in fragments produced from similar regions following 4 weeks of NM (Fig. 21F). As with electrical coupling studies, no obvious differences in dye coupling were observed in early stages (day one) of NM (data not shown). However, dye coupling coefficient (DCC), calculated from fluorescence intensity measurements (see Materials and Methods), was significantly increased between MGF axons of posterior (n=5), but not anterior (n=5; $p<0.05$), body segments following 4 weeks of neural morphallaxis (Fig. 21G). Thus, the MGF of *Lumbriculus* was septate along the length of the body, as demonstrated by the lack of RHDX diffusion across segmental boundaries, even during neural morphallaxis. Furthermore, rapid reduction in MGF conduction velocity during early NM was not correlated with changes in dye coupling, but long-term changes in spike conduction may be a product of similar long-term enhancement of MGF axon electrical coupling.

Discussion

Neural morphallaxis in the aquatic oligochaete worm, *Lumbriculus variegatus*, involves transformations in neurobehavioral substrates as body fragments regenerate short heads and long tails and acquire new positional identity (Drewes and Fourtner, 1990; Martinez et al., 2005). Multiple cellular and molecular mechanisms associated

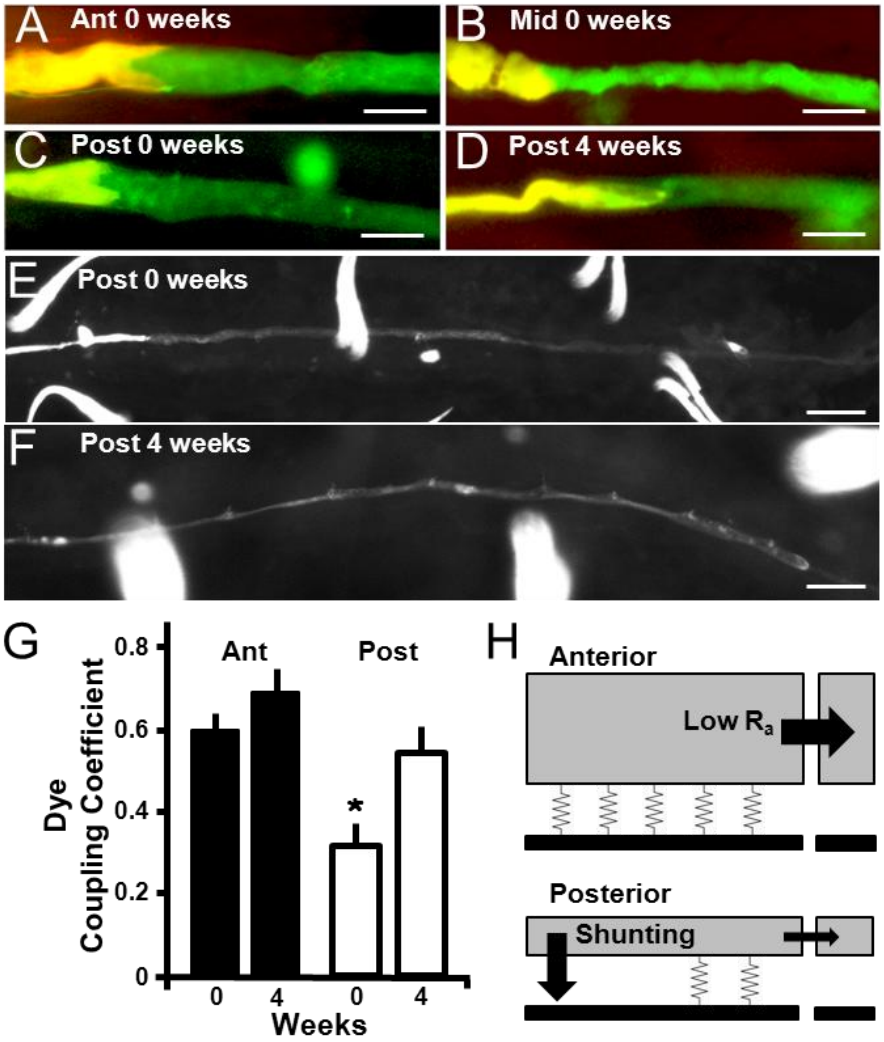

Figure 21. MGF dye coupling during late neural morphallaxis. Fluorescent dye was injected into the MGF in anterior (A), middle (B) and posterior (C) segments. Rhodamine dextran (RHDX; ~10,000Da), seen in red, was too large to pass through gap junctions at the septal boundary and was used to identify the injected segment. At a smaller molecular weight, lucifer yellow (LYCH; ~500Da), in green, passed readily between the giant interneuronal axons. Injected segments appear yellow in the merged images, as they contain both RHDX and LYCH. D) MGF dual-injected with RHDX and LYCH in a posterior fragment at 4 weeks of regeneration. Much like the non-regenerating MGF images, at 4 weeks of NM the MGF was septate and LYCH passed readily across the septum. E-F) LYCH passed along many segments of MGF in intact (E) and regenerating (F) worms. Autofluorescent setae pairs, located within each body segment, indicate the distance of dye diffusion from the site of injection (extreme left of images). Scale bars equivalent to 10 µm (A-D), E and F equals 50 µm. G) Dye coupling coefficient was measured from the fluorescent intensity of neighboring segments in non-regenerating worms and worms after four weeks of regeneration. Quantification of MGF dye coupling coefficient data demonstrated a increased coupling in posterior, but not anterior, fragments after four weeks of NM. Error bars represent SEM, $p<0.05$. H) Illustration of the relative size of MGF axons (gray rectangles) and sensory interneurons (black rectangles) in anterior and posterior body segments. We predict that the lower axial resistance (R_a) of the large MGF axons of anterior segments will be associated with great current flow along the MGF. Relatively greater resistance (indicated by resistor symbols) at electrical synapses connecting the sensory interneurons will limit shunting of MGF currents. In posterior segments, the smaller diameter MGF will generate a higher resistance to current flow along the pathway, consequently reducing resistance between the MGF and sensory interneurons and enhancing current shunting.

with neural morphallaxis underlie changes in giant interneuronal structure and function, as fragments transform their escape reflexes into circuits appropriate for a new segmental identity. The giant interneuronal pathways in *Lumbriculus*, like those of most other oligochaete worms (Zoran and Drewes, 1987), are chains of segmental giant axons that mediate two independent escape circuits: the medial giant fiber (MGF) pathway that regulates head withdrawal and the lateral giant fiber (LGF) pathway that regulates tail withdrawal. As in many other animal phyla that have evolved giant axons (Hartline and Colman, 2007), the GF pathways of oligochaete worms confer a reduced axial resistance to current flow and therefore allow for rapid action potential propagation along the length of the animal's body (Drewes, 1984). Transforming segments from the posterior body region acquire an increased MGF conduction velocity by 3 weeks of regeneration (Drewes and Fourtner, 1990; Martinez et al., 2005; Martinez et al., 2006). These functional changes in the MGF were accompanied by structural changes in giant fiber diameter. From three to nine weeks of regeneration, MGF diameter increased significantly, while the diameter of the LGFs decreased (Drewes and Fourtner, 1990; Martinez et al., 2006). Because neural circuit speed is critical for rapid escape reflexes, electrical coupling of the giant axon elements, via gap junctions, facilitates rapid GF

spike conduction (Mulloney, 1970; Brink and Ramanan, 1985). Changes in giant axon electrical coupling were demonstrated here to underlie, in part, increased speed of MGF spike propagation during late stages of NM. Dye coupling coefficients, based on Lucifer yellow, a fluorescent dye small enough to pass through MGF gap junctions, were significantly increased over 4 weeks of NM. This time frame is similar to that reported for GF diameter changes during NM (Drewes and Fourtner, 1990; Martinez et al., 2005). Thus, late stages of NM involve multiple mechanisms of neural plasticity to facilitate changes in giant axon structure and function.

Interestingly, MGF conduction velocity rapidly decreased during the first 24 hours of NM and this reduced velocity was not a function of decreased electrical coupling between MGF axons. We considered it unlikely that changes in MGF diameter or myelination were responsible for these rapid and transient changes in conduction velocity, since they would require substantial time and no evidence for such changes had previously been observed (Drewes and Fourtner, 1990). Recent studies identified a sensory interneuronal pathway in *Lumbriculus* that is electrically coupled to the MGF (Lybrand et al., 2012; see Chapter 2). Although dye coupling between sensory interneurons and the MGF does not appear to changes during NM, it is not known if electrical coupling at these synaptic contacts varies. If these electrical synapses are a site of plasticity, transient increases in electrical coupling between the MGF and sensory interneurons could influence MGF conduction velocity by the shunting more current into the sensory interneurons, thereby increasing axial resistance. In support of this idea, reduction in MGF conduction velocity during early NM was greater in regenerating

fragments from more posterior regions. In these fragments, medial giant interneurons axons are smaller in diameter (Drewes and Fourtner, 1990) and therefore differences in axon diameter between medial giant interneurons and sensory interneurons would be less. These differences in relative diameter of the electrically coupled elements of the MGF network would favor greater current shunting in more posterior segments (Fig. 21H). Additional electrophysiology is necessary to test this prediction. Nonetheless, plasticity in MGF conduction velocity during NM involves an early and transient suppression followed by a late and sustained enhancement. The late phase of MGF conduction plasticity involved increased coupling at giant axon electrical synapses, while early phase plasticity did not.

A relatively common feature of the oligochaete lifestyle is the need for rapid behavioral responses to potential predatory attacks. Consequently, giant axons that traverse the worm's longitudinal axis and regulate rapid withdrawals are ubiquitous. Although a marked diversity in the number, size and arrangement of GFs within polychaetes exists (Bullock, 1948; Nicol, 1948; Bullock, 1965), a conserved feature of most oligochaete worms is the presence of three GFs (Zoran and Drewes, 1987). Dye fills of the *Lumbriculus* MGF pathway demonstrated the septate nature of these giant axons. That is, these axons are separated by a membranous septum, as opposed to a syncytial fusion. Both forms of connectivity exist among annelid worms (Mulloney, 1970; Gunther, 1975). The septate boundaries of annelid giant fibers are the sites of high-density clusters of gap junctions (Gunther, 1975; Osterle and Barth, 1981) and presumably the sites of dye transfer along the MGF. The early and late phases of giant

axon plasticity described here add to the characteristic features of NM in *Lumbriculus*. Furthermore, early phase changes in giant axon function are rapid, transient and suppressive, while late phase changes are gradual, sustained and facilitative. Thus, GF functional changes exhibit a duality in NM plasticity, which may be critical to the appropriate transformation of the escape neural circuitry.

CHAPTER V

GENERAL CONCLUSIONS

At the outset of my dissertation research, I proposed to gain a further understanding of the mechanisms underlying the regenerative processes in the nervous system of *Lumbriculus variegatus* that lead to changes in its escape neural circuit, a form of neural plasticity where one circuit transforms to produce a new circuit in a short period of time. I hypothesized that this rare form of neural plasticity, called neural morphallaxis, was mediated by a concerted silencing and unsilencing of sensory inputs onto the giant fiber pathway, a through-conducting circuit of interneurons that govern rapid escape reflexes. The similarities in neural morphallaxis with other forms of plasticity such as learning and memory suggest that the underlying mechanism might be conserved across a wide-range of animal phyla. Therefore, the implications of this research not only span basic areas of neuroscience, like neural plasticity and recovery of function following injury, but also the evolution of their underlying processes.

Silent synapses and neural morphallaxis

Non-invasive extracellular electrophysiology showed that transforming posterior segments switched their patterns of sensory activation from the lateral giant fiber (LGF) pathway to the medial giant fiber (MGF) pathway in less than a day following head amputation. This pathway transformation occurred much more rapidly than the overt

changes in escape reflex behavior from tail to head withdrawal. Also, there was a transient period of dual activation of the LGF and MGF pathways within the first 6 hours of neural morphallactic regeneration, suggesting that as the MGF pathway gained functionality, LGF pathway escape circuit function was also temporarily maintained in those segments (Lybrand and Zoran, 2012; Chapter II). The speed with which the MGF pathway gained functional activation suggested a mechanism of unsilencing of previously ineffective sensory inputs onto this interneuronal pathway.

Intracellular current clamp recordings were used to demonstrate that sensory input onto the MGF was, in fact, functionally silent prior to neural morphallactic regeneration. Functional synaptic transmission was readily detected in anterior segments, whereas recordings from MGF interneurons in posterior segments failed to demonstrate functional synaptic transmission. However, 24 hours after regeneration, recovery of functional synaptic transmission was present in transforming segments (Lybrand and Zoran, 2012; Chapter II). These experiments demonstrated that sensory input onto the MGF pathway was indeed functionally silent prior to neural morphallaxis and that the awakening of these ineffective synapses could occur in a matter of hours following injury. These results are the first demonstration of such rapid unsilencing of a sensory afferent pathway following injury, in an escape reflex or any other, and the first demonstration of synaptic plasticity in the context of morphallactic regeneration.

Stimulation of sensory inputs activated large spikes, small spikes and graded postsynaptic potentials (PSP) in the MGF. Large spikes were determined to be the MGF action potential necessary for the activation of escape motor outputs. Small MGF spikes

were recorded both in synchrony and preceding the large spikes temporally. Interestingly, following morphallactic regeneration, initial activation of the MGF recruited small spikes and graded PSPs. I initially hypothesized that the origin of the small spikes was action potentials generated in interneurons strongly coupled the MGF (Lybrand and Zoran, 2012; Chapter II). This hypothesis was later confirmed with the discovery of a bilaterally paired set of sensory interneurons dye coupled to the MGF (Chapter III). Thus, the transformation of sensory inputs onto the MGF neural circuit during neural morphallaxis likely involves initial unsilencing of these inputs to the strongly coupled sensory interneurons.

To demonstrate that sensory-to-giant fiber afferents were in fact silent synapses, it was necessary to demonstrate that they were physically (structurally) present. Injections of the nerve tracer, neurobiotin, NB, into the MGF identified the cellular nature of the electrically coupled MGF network. In total, nine cell bodies and their processes, including the medial giant interneuron and a bilateral pair of intermediate giant fiber (IGF) sensory interneurons, were labeled with NB dye (Chapter III). These sensory interneurons were likely the origin of the small spikes from the electrophysiological studies. Previous anatomical studies of the oligocheate nervous system also suggested the existence of sensory bundles associated with unmyelinated giant interneurons of the ventral cord as a potential source for dorsal giant fiber activation (Drewes, 1984; Gunther and Schurmann, 1973). My dissertation studies have identified for the first time the entirety of the MGF coupled network and have implicated the unmyelinated, IGF

sensory interneurons as the likely site of sensory input plasticity during neural morphallaxis.

A number of small projections through the myelin-like sheath of annelid dorsal giant fibers were previously identified and these unmyelinated regions of membrane have been proposed to be the sites of GF action potential initiation and propagation, sensory synaptic inputs and motor synaptic outputs (Gunther, 1976; Drewes, 1984; Martinez et al., 2005). Serial transmission electron microscopy of MGF collaterals in *Lumbriculus* failed to identify evidence of synaptic input. However, large clusters of synaptic vesicles within the collaterals provided clear support for synaptic outputs of the MGF, likely synapses upon motor neurons. Similar output synapses in the earthworm, *Lumbricus terrestris,* have been described and exist in close association with mitochondria near pre- and post-synaptic densities (Jamison, 1981). Although no obvious synaptic inputs were detected onto the MGF, synaptic structures onto the sensory interneurons of the IGF bundles were apparent (Chapter III). Serial TEM sections also confirmed cross-bridge structures between the IGF bundles and the MGF collaterals. These discoveries of the sites of chemical synaptic contact of the IGFs and their electrical synaptic contact with the MGF were important in that they identified the likely morphological substrates of the physiological elements I previously described for the escape neural circuit in *Lumbriculus variegatus*.

Intracellular current clamp recordings where conducted on MGF interneurons while different glutamatergic antagonists were applied to determine the nature of the synaptic physiology of the sensory afferents to the MGF coupled network. CNQX, an

AMPA/kainate receptor antagonist, abolished all electrical signaling in the MGF evoked by body wall stimulation, including large spikes, small spikes, and graded potentials. However, AP5, a NMDA receptor antagonist, had no effect on the MGF responses to stimulation (Chapter III). Glutamatergic sensory synapses have been identified in other annelid worms such as the leech *Hirudo*, where CNQX was shown to abolish neurotransmission at the pressure mechanosensory-to-interneuron synapses (Baccus et al., 2000). Because of these synaptic physiology results, I used a number of glutamate receptor antibodies to identify the location of glutamate receptors within the ventral nerve cord of *Lumbriculus*. Staining with a GluR5-7 antibody, which recognizes the 5,6, and 7 subunits of the AMPA/kainate receptors, revealed punctate patterns of immunoreactivity throughout the nerve cord. Periaxonal regions of the MGF and sensory interneuronal IGF bundles in both anterior and posterior segments showed clusters of even more intense punctate staining. That glutamate receptor staining was localized around the putative sites of sensory input to the MGF coupled network in posterior segments is further evidence of structural afferent synapses being present prior to neural morphallaxis. Therefore, I have demonstrated that sensory inputs onto the MGF coupled network (MGF plus their coupled sensory interneurons) are glutamatergic and that no obvious differences in GluR expression were detected at presumptive synaptic sites between anterior and posterior body segments. Taken together, these results suggest that silent sensory synapses are a pervasive element of *Lumbriculus* escape neural circuits and, following injury or fragmentation associated with asexual reproduction, vast numbers of synapses along the axial length of giant fiber systems

rapidly transition from a functionally silent state into an effective activator of system excitation.

Sensory interneurons and afferent processing

Electrically coupled sensory interneurons are a conserved feature of the neural circuits that mediate many animal escape and startle responses. In cockroaches, different startle behaviors are triggered by activation of alternate sets of interneurons in response to either wind stimuli (Comer, 1985; Camhi and Levy, 1989) or touch stimuli (Ye and Comer, 1996; Burdohan and Comer, 1996). The information encoded in the activity of these interneurons is then transmitted to other sets of interneurons for the regulation of escape behaviors, either running or flight. The contralateral-start, or C-start, in some fishes is triggered upon activation of a pair of identifiable hindbrain neurons called Mauthner cells (M-cells) (Korn and Faber, 2005). This Mauthner escape neural network receives input from the lateral line system and a number of interneurons have been implicated in the modulation of M-cell excitability and, thereby, initiation of the C-start (Mirjay and Faber, 2011). In crayfish, lateral giant (LG) interneurons that mediate tail flip escape reflexes receive input from sensory interneurons that too modulate the excitability of the LG command interneurons (Zucker, 1972; Liu and Herberholz, 2010). It is likely the IGF sensory interneurons I have identified in *Lumbriculus variegatus* function similarly to integrate and modulate afferent inputs.

A monoclonal antibody, Lan3-2, that recognizes a conserved glycoepitope involved in the cell-type-specific glycosylation of neural cell adhesion molecules was co-localized

with GluR staining to synaptic sites of the MGF and IGF interneurons. This glycoepitope is associated with the ectodomains of leechCAM and tractin, homologues of NCAM, ApCAM and FASII, all members of the conserved family of cell adhesion molecules (CAM) implicated in a number of developmental and modulatory events, including synaptogenesis and synaptic plasticity (Huang et al., 1997; Zipser, 1995). Temporal changes in expression of the Lan3-2 epitope on multiple *Lumbriculus* proteins during morphallaxis and their expression patterns with the ventral nerve cord implicated this glycoepitope antibody as a molecular marker of neural morphallaxis (Martinez et al., 2006). Colocalization of Lan3-2 with glutamate receptors suggested that neural morphallactic plasticity occurs at these sites of glutamatergic synaptic inputs onto the coupled IGF sensory interneurons in *Lumbriculus.* Thus, sensory interneurons not only play an important role in the processing of sensory information within the escape neural circuit of *Lumbriculus*, as they do in many other escape systems, but they are also likely the sites of neural modifications to their sensory inputs during morphallactic plasticity.

Early and late plasticity in giant axon spike conduction

Neural morphallaxis in *Lumbriculus variegatus* was also characterized by plasticity of giant axon physiology (Chapter IV). Noninvasive extracellular electrophysiological recordings showed a reduction in the conduction velocity of the MGF during early phases of neural morphallactic plasticity. This early giant axon plasticity (~1-2 days after injury) was characterized by the coincidence of rapid and transient modifications in both conduction velocity and effective, but not intrinsic, excitability. Dual intracellular

recordings demonstrated that this early phase plasticity was not a change in the electrical coupling between giant axons. However, a late phase of morphallactic plasticity (>3 weeks after injury) was characterized by morphological and functional increases in giant fiber diameter and conduction velocity (Drewes and Fourtner, 1990; Martinez et al., 2006; Chapter IV). Fluorescent dye fills of the MGF demonstrated the plasticity of late phase neural morphallaxis was accompanied by an increased coupling between giant fiber axons. Therefore, it remains to be determined if early plasticity in MGF conduction velocity is due to changes sensory interneuron-to-MGF electrical coupling, however, I have made an argument for this potential relationship (Chapter IV). Nonetheless, it is clear that electrical synapse plasticity is an important, although late occurring, aspect of giant axon morphallaxis following injury.

Mechanism of sensory synapse unsilencing

While I do not fully understand the mechanism by which glutamatergic sensory inputs onto the sensory interneurons of *Lumbriculus* become unsilenced during morphallaxis, the present studies provide insight into the nature of the plasticity likely involved. One silent synapse mechanism initially proposed was involving a form of NMDA-dependent long-term potentiation (LTP) and depression (LTD) similar to that described in many forms of developmental and learning-like plasticity (Atwood and Wojtowicz, 1999). My discovery of the glutamatergic nature of the sensory synaptic transmission gave support to such a mechanism. However, my subsequent determinations that NMDA antagonists have no effect on this synapse and that no

NMDA-like immunoreactivity is present in the *Lumbriculus* VNC made this proposed mechanism unlikely.

Another potential mechanism for the plasticity was the upregulation of a critical electrical synapse within the escape neural circuit. My demonstration of the entirety of the electrically coupled network and its lack of variation along the length of the VNC strongly suggest that changes in gap junction protein expression or clustering during early phases of neural morphallaxis cannot account for synaptic unsilencing. Furthermore, electrophysiological data demonstrating that application of CNQX completely abolishes sensory input to the MGF network, essentially mimicking the pre-morphallaxis state of synaptic silence, suggest the lack of substantial involvement of electrical synaptic plasticity.

One possible mechanism I had initially proposed, but has yet to be experimentally addressed, is the role of an inhibitory modulator as the synaptic silencing agent. Based on my discovery of the neural circuit architecture, the afferent sensory neurons, the IGF sensory interneurons, or the dorsal giant fiber itself could be the site of such prolonged and profound inhibition of excitability. If the giant fiber coupled networks were under a constant state of depression by inhibitory interneurons, then the removal of this inhibition would effectively unsilence escape neural circuits. A perhaps informative future experiment to test this possibility would be to apply antagonists of known inhibitory neurotransmitters and assess the state of pathway depression. For example, bicuculline is antagonist of some gamma-aminobutyric acid (GABA) receptors, which mediate synaptic inhibition in vertebrates and invertebrates. Should functional synaptic

transmission emerge upon application of bicuculline, it would indicate the presence of an inhibitory modulating interneuron.

Other possible regulators of silent synaptic plasticity are a wide range of morphogenic and trophic signaling mechanisms known to be involved in synaptic development and plasticity. Although attempting any analysis of such signaling mechanism was beyond the scope of this dissertation research, or the capabilities of the *Lumbriculus* system, I have performed a series of studies based upon previous observations that β-catenin is highly upregulated in worm fragments following injury (Martinez, unpublished observation) and recent studies have implicated β-catenin and Wnt signaling in the process of synaptic plasticity, as well as synapse formation, in multiple nervous systems (Budnik and Salinas, 2011). I demonstrated that β-catenin was expressed in the regenerating head-bud and ventral nerve cord of *Lumbriculus variegatus* body fragments during neural morphallactic regeneration (Fig. 22). β-catenin is an armadillo family protein and a major component in the canonical Wnt signaling pathway. Thus, Wnt signaling became a potential regulator of neural morphallactic regeneration and plasticity. I tested a number of pharmacological agents that either activate or inhibit the Wnt signaling pathway. Tail fragments were placed in solutions of these drugs (Table 1) and assessed for bud formation and morphallactic transformation in escape reflex behavior. There were no morphallactic changes in reflex behavior produced by any drugs. Lithium chloride (LiCl) induced marked changes in the generation of new head and, particularly, new tail segments. A reduction in head bud segments of about 25% and a greater reduction of about 90% in new tail segments were

present. Therefore, LiCl disrupted epimorphic, but not morphallactic, regeneration in *Lumbriculus*.

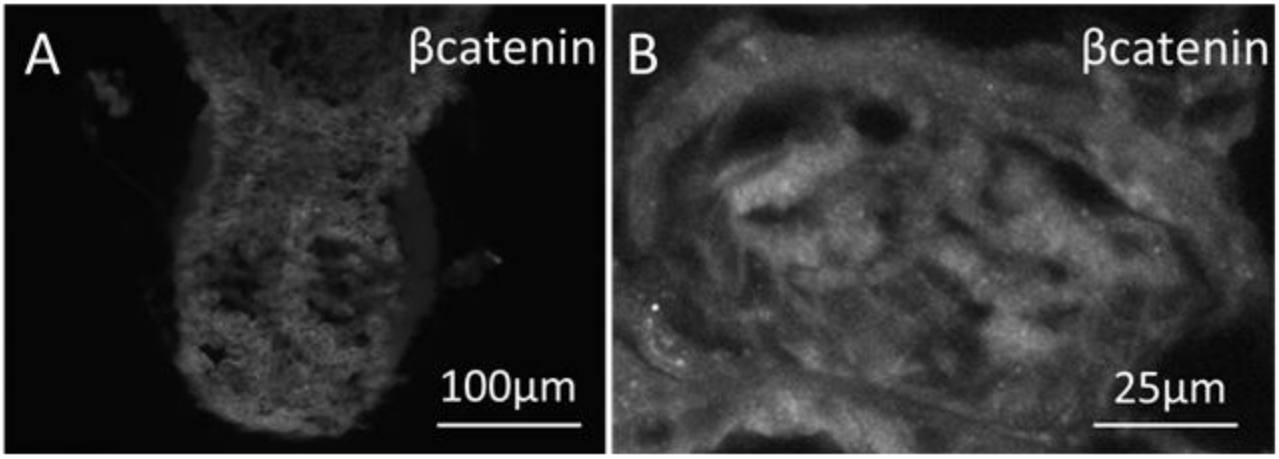

Figure 22. βcatenin expression during regeneration. A) βcatenin antibody was located in the regenerating head bud following segmental amputation. B) βcatenin staining was located within the ventral nerve cord in transforming segments during neural morphallaxis.

Comparative and evolutionary considerations

Neural circuits that mediate rapid escape reflexes are prominent in a wide range of animals. Commonalities among these neural circuits include axonal gigantism, myelination, and electrical synapses that each aid in the rapid conduction of neural signals. Furthermore, all of these features can be found in the escape neural circuitry of *Lumbriculus variegatus*. Sensory processing interneurons, similar to those identified

within the escape neural circuitry in other organisms, have been identified here for the escape circuit of *Lumbriculus*. This observation suggests that such interneuronal processing may be a common feature of escape neural circuits. However, since these escape networks have evolved many times independently within oligochaetes and polychaetes (Zoran and Martinez, 2009), and across many phyla, it is likely that many of these common features of escape circuits represent convergent evolution. In annelids, regeneration of body parts after injury is widespread. Even regeneration of lost heads, a trait not found in many animals, is not rare in annelid worms (Zoran and Martinez, 2009). It is quite possible that the evolution of regenerative abilities in annelids gave rise to new capabilities such as morphallaxis and asexual reproduction. In turn, neural mechanisms for rapid plasticity, such as pervasive silent synapses and their associated abilities for unsilencing were highly adaptive.

Table 1. Pharmacological agents of the wnt signaling pathway

Drug	Target	Wnt pathway	Reference
BIO	GSK3 inhibitor	activates	Sato et al,2004
DCA	βcatenin activator	activates	Pai et al, 2004
Lithium Chloride	GSK3 inhibitor	activates	Klein and Melton, 1996
Niclosamide	Frizzled inhibitor	inhibits	Chen 2009
Quercetin	TCF inhibitor	inhibits	Park et al, 2005

In a broader sense, the discovery of wide-spread silent synapses in this annelid worm and their awakening during recovery of function following injury could have future importance for mammalian nervous system recovery of function. The first identification of silent synapses occurred in the 1970's by Patrick Wall and Eugene Merrill. They demonstrated that primary sensory afferent processes were ineffective in activating spinal cord neurons, but after cord transection of sensory afferent fibers, some previously silent synapses became functional. Silent synapses are present in a wide range of animals and it has been suggested that they may be pervasive in many nervous systems (Atwood and Wojtowicz, 1999). If this is true, as it is for *Lumbriculus*, and regenerative mechanisms can be discovered that awaken these intact, but silent pathways, the implications for spinal cord and brain recovery of function following trauma are many. This, I believe, is the importance of continuing to pursue comparative neuroscience research and the potential benefits that would be lost should such research fall silent.

Summary

In conclusion, the speed by which early aspects of neural morphallaxis are consolidated into changes in escape neural networks implicates a mechanism of synaptic unsilencing. Gain of function at glutamatergic sensory synapses onto a system of electrical coupled giant interneurons occurs in as short as 6 hours following injury. This synaptic plasticity likely occurs at an afferent input to an integrating sensory interneuron that is strongly coupled by electrical synapses to the dorsal giant axons of the escape

neural network. This early phase of neural morphallaxis coincides with changes in giant axon physiology, including a transient reduction in conduction velocity. While the mechanisms of synaptic unsilencing have yet to be determined, these studies provide the functional and structural basis for future studies in understanding the plasticity in the rapid escape reflexes in *Lumbriculus variegatus* and comparative studies into the evolution of neural circuits and their inherent plasticity.

REFERENCES

Alvarado AS (2000) Regeneration in the metazoans: why does it happen? BioEssays 22:578-590.

Atwood HL, Wojtowicz JM (1999) Silent synapses in neural plasticity: current evidence. Learn Mem 6:542-571.

Atwood HL, Govind CK, Wu CF (1993) Differential ultrastructure of synaptic terminals on ventral longitudinal abdominal muscles in Drosophila larvae. J Neurobiol 24:1008-1024.

Baccus SA, Burrell BD, Sahley CL, Muller KJ (2000) Action potential reflection and failure at axon branch points cause stepwise changes in EPSPs in a neuron essential for learning. J Neurophysiol 83:1693-1700.

Bajt ML, Schmitz B, Schachner M, Zipser B (1990) Carbohydrate epitopes involved in neural cell recognition are conserved between vertebrates and leech. J Neurosci Res 27:276-285.

Baudry M, Davids J, Thompson R (1999) Advances in synaptic plasticity. Cambridge MA: MIT Press.

Bely AE (1999) Decoupling of fission and regenerative capabilities in an asexual oligochaete. Hydrobiologia 406:243-251.

Bely AE (2006) Distribution of segment regeneration ability in the Annelida. Integr Comp Biol 46:508-518.

Bely AE, Wray GA (2001) Evolution of regeneration and fission in annelids: insights from engrailed- and orthodenticle-class gene expression. Development 128:2781-2791.

Bennett MVL (1977) Electrical Transmission: A Functional Analysis and Comparison to Chemical Transmission. In: Comprehensive Physiology: John Wiley & Sons, Inc.

Berrill NJ (1952) Regeneration and budding in worms. Biological Reviews 27:401-438.

Bourne JA (2010) Unravelling the development of the visual cortex: implications for plasticity and repair. J Anat 217:449-468.

Brink PR, Ramanan SV (1985) A model for the diffusion of fluorescent probes in the septate giant axon of earthworm. Axoplasmic diffusion and junctional membrane permeability. Biophys J 48:299-309.

Brinkhurst RO, Jamieson BGMja (1971) Aquatic oligochaeta of the world Edinburgh, :: Oliver and Boyd.

Bullock TH (1948) Non-integrative synapses. Biol Bull 95:249.

Bullock TH (1965) Comparative Aspects of Superficial Conduction Systems in Echinoids and Asteroids. Am Zool 5:545-562.

Burdohan JA, Comer CM (1996) Cellular organization of an antennal mechanosensory pathway in the cockroach, Periplaneta americana. J Neurosci 16:5830-5843.

Burrell BD, Sahley CL (2004) Multiple forms of long-term potentiation and long-term depression converge on a single interneuron in the leech CNS. J Neurosci 24:4011-4019.

Burrell BD, Li Q (2008) Co-induction of long-term potentiation and long-term depression at a central synapse in the leech. Neurobiology of learning and memory 90:275-279.

Camhi JM, Levy A (1989) The code for stimulus direction in a cell assembly in the cockroach. J Comp Physiol A 165:83-97.

Comer CM (1985) Analyzing cockroach escape behavior with lesions of individual giant interneurons. Brain Res 335:342-346.

Cooper RL, Hampson DR, Atwood HL (1995) Synaptotagmin-like expression in the motor nerve terminals of crayfish. Brain Res 703:214-216.

Dagan D, Parnas I (1974) After effects of spikes in cockroach giant axons. J Neurobiol 5:95-105.

DeFelipe J (2006) Brain plasticity and mental processes: Cajal again. Nat Rev Neurosci 7:811-817.

Dennis MJ, Ziskind-Conhaim L, Harris AJ (1981) Development of neuromuscular junctions in rat embryos. Dev Biol 81:266-279.

Drewes C, D. (1984) Escape reflexes in earthworms and other annelids. In: Neural mechanisms of startle behavior. (Eaton RC, ed), pp 43-91: Plenum Press.

Drewes CD, Fourtner CR (1990) Morphallaxis in an aquatic oligochaete, Lumbriculus variegatus: reorganization of escape reflexes in regenerating body fragments. Dev Biol 138:94-103.

Edwards DH, Heitler WJ, Krasne FB (1999) Fifty years of a command neuron: the neurobiology of escape behavior in the crayfish. Trends Neurosci 22:153-161.

Faber DS, Lin JW, Korn H (1991) Silent synaptic connections and their modifiability. Ann N Y Acad Sci 627:151-164.

Fischbach GD, Frank E, Jessell TM, Rubin LL, Schuetze SM (1978) Accumulation of acetylcholine receptors and acetylcholinesterase at newly formed nerve-muscle synapses. Pharmacol Rev 30:411-428.

Grey KB, Burrell BD (2010) Co-induction of LTP and LTD and its regulation by protein kinases and phosphatases. J Neurophysiol 103:2737-2746.

Gunther J (1975) Neuronal syncytia in the giant fibres of earthworms. J Neurocytol 4:55-62.

Gunther J (1976) Impulse conduction in the myelinated giant fibers of the earthworm. Structure and function of the dorsal nodes in the median giant fiber. J Comp Neurol 168:505-531.

Gunther J, Schurmann FW (1973) Ultrastructure of the dorsal giant fibre system in the ventral nerve cord of the earthworm. II. Synaptic connections of the proximal collaterals of the giant fibres. Zeitschrift fur Zellforschung und mikroskopische Anatomie 139:369-396.

Günther J, Walther JB (1971) Funktionelle Anotomie der dorsalen Riesenfaser-Systeme von *Lumbriculus terrestris*. Z Morphol Tiere 70:253-280.

Harel NY, Strittmatter SM (2006) Can regenerating axons recapitulate developmental guidance during recovery from spinal cord injury? Nat Rev Neurosci 7:603-616.

Hartline DK, Colman DR (2007) Rapid conduction and the evolution of giant axons and myelinated fibers. Curr Biol 17:R29-35.

Hensch TK (2005) Critical Period Mechanisms in Developing Visual Cortex. Current Topics in Developmental Biology Volume 69:215-237.

Herberholz J, Sen MM, Edwards DH (2004) Escape behavior and escape circuit activation in juvenile crayfish during prey-predator interactions. J Exp Biol 207:1855-1863.

Huang L, Hollingsworth RI, Haslam SM, Morris HR, Dell A, Zipser B (2008) The Lan3-2 glycoepitope of Hirudo medicinalis consists of beta-(1,4)-linked mannopyranose: cell type-specific glycans of H. medicinalis. J Neurochem 107:1448-1456.

Hubel DH, Wiesel TN (1970) The period of susceptibility to the physiological effects of unilateral eye closure in kittens. J Physiol 206:419-436.

Isaac JT, Nicoll RA, Malenka RC (1995) Evidence for silent synapses: implications for the expression of LTP. Neuron 15:427-434.

Isaac JT, Nicoll RA, Malenka RC (1999) Silent glutamatergic synapses in the mammalian brain. Can J Physiol Pharmacol 77:735-737.

Jahromi SS, Atwood HL (1974) Three-dimensional ultrastructure of the crayfish neuromuscular apparatus. J Cell Biol 63:599-613.

James W (1890) The principles of psychology: H. Holt and company.

Jamieson BGM (1981) The ultrastructure of the oligochaeta: Academic Press.

Kensler RW, Brink PR, Dewey MM (1979) The septum of the lateral axon of the earthworm: a thin section and freeze-fracture study. J Neurocytol 8:565-590.

Kerchner GA, Nicoll RA (2008) Silent synapses and the emergence of a postsynaptic mechanism for LTP. Nat Rev Neurosci 9:813-825.

Korn H, Faber DS (1975) An electrically mediated inhibition in goldfish medulla. J Neurophysiol 38:452-471.

Kullberg RW, Lentz TL, Cohen MW (1977) Development of the myotomal neuromuscular junction in Xenopus laevis: an electrophysiological and fine-structural study. Dev Biol 60:101-129.

Kullmann DM, Lamsa KP (2007) Long-term synaptic plasticity in hippocampal interneurons. Nat Rev Neurosci 8:687-699.

Kullmann DM, Erdemli G, Asztely F (1996) LTP of AMPA and NMDA receptor-mediated signals: evidence for presynaptic expression and extrasynaptic glutamate spill-over. Neuron 17:461-474.

Lesiuk NM, Drewes CD (1999) Autotomy reflex in a freshwater oligochaete, Lumbriculus variegatus (Clitellata: Lumbriculidae). Hydrobiologia 406:253-261.

Lesiuk NM, Drewes CD (2001a) Behavioral plasticity and central regeneration of locomotor reflexes in the freshwater oligochaete, Lumbriculus variegatus. I: Transection studies. Invertebrate Biology 120:248-258.

Lesiuk NM, Drewes CD (2001b) Behavioral plasticity and central regeneration of locomotor reflexes in the freshwater oligochaete, Lumbriculus variegatus. II: Ablation studies. Invertebrate Biology 120:259-268.

Levine RB, Truman JW (1982) Metamorphosis of the insect nervous system: changes in morphology and synaptic interactions of identified neurones. Nature 299:250-252.

Li Q, Burrell BD (2011) Associative, bidirectional changes in neural signaling utilizing NMDA receptor- and endocannabinoid-dependent mechanisms. Learn Mem 18:545-553.

Liao D, Hessler NA, Malinow R (1995) Activation of postsynaptically silent synapses during pairing-induced LTP in CA1 region of hippocampal slice. Nature 375:400-404.

Liao D, Scannevin RH, Huganir R (2001) Activation of silent synapses by rapid activity-dependent synaptic recruitment of AMPA receptors. J Neurosci 21:6008-6017.

Liu YC, Herberholz J (2010) Sensory activation and receptive field organization of the lateral giant escape neurons in crayfish. J Neurophysiol 104:675-684.

Lu W, Man H, Ju W, Trimble WS, MacDonald JF, Wang YT (2001) Activation of synaptic NMDA receptors induces membrane insertion of new AMPA receptors and LTP in cultured hippocampal neurons. Neuron 29:243-254.

Lybrand ZR, Zoran MJ (2012) Rapid neural circuit switching mediated by synaptic plasticity during morphallactic regeneration. Dev Neurobiol.

Lybrand ZR, Martinez VG, Zoran MJ (2012) Glutamatergic synapstic plasticity mediates rapid escape reflex transformation during morphallactic regeneration in the annelid worm, *Lumbriculus variegatus*. In preparation.

Malenka RC, Nicoll RA (1997) Silent synapses speak up. Neuron 19:473-476.

Martinez VG, Menger GJ, 3rd, Zoran MJ (2005) Regeneration and asexual reproduction share common molecular changes: upregulation of a neural glycoepitope during morphallaxis in Lumbriculus. Mech Dev 122:721-732.

Martinez VG, Reddy PK, Zoran MJ (2006) Asexual reproduction and segmental regeneration, but not morphallaxis, are inhibited by boric acid in Lumbriculus variegatus (Annelida: Clitellata: Lumbriculidae). Aquatic Oligochaete Biology IX 186:73-86.

Martinez VG, Manson JM, Zoran MJ (2008) Effects of nerve injury and segmental regeneration on the cellular correlates of neural morphallaxis. J Exp Zool B Mol Dev Evol 310:520-533.

Merrill EG, Wall PD (1972) Factors forming the edge of a receptive field: the presence of relatively ineffective afferent terminals. J Physiol 226:825-846.

Miller MW, Vu ET, Krasne FB (1992) Cholinergic transmission at the first synapse of the circuit mediating the crayfish lateral giant escape reaction. J Neurophysiol 68:2174-2184.

Mirjany M, Faber DS (2011) Characteristics of the anterior lateral line nerve input to the Mauthner cell. J Exp Biol 214:3368-3377.

Morgan TH (1901) Regeneration and Liability to Injury. Science 14:235-248.

Muller KJ, Scott SA (1981) Transmission at a 'direct' electrical connexion mediated by an interneurone in the leech. J Physiol 311:565-583.

Mulloney B (1970) Structure of the giant fibers of earthworms. Science 168:994-996.

Munno DW, Syed NI (2003) Synaptogenesis in the CNS: an odyssey from wiring together to firing together. J Physiol 552:1-11.

Nicol JA (1948) The giant axons of annelids. Q Rev Biol 23:291-323.

O'Gara B, Vining EP, Drewes CD (1982) Electrophysiological correlates of rapid escape reflexes in intact earthworms, Eisenia foetida. I. Functional development of giant nerve fibers during embryonic and postembryonic periods. J Neurobiol 13:337-353.

Oesterle D, Barth FG (1981) Dorsal giant fibre septum of earthworm. Fine structural details and further evidence for gap junctions. Tissue Cell 13:9-18.

Onifer SM, Smith GM, Fouad K (2011) Plasticity after spinal cord injury: relevance to recovery and approaches to facilitate it. Neurotherapeutics 8:283-293.

Otis TS, Gilly WF (1990) Jet-propelled escape in the squid Loligo opalescens: concerted control by giant and non-giant motor axon pathways. Proc Natl Acad Sci U S A 87:2911-2915.

Peinado A, Macagno ER, Zipser B (1987) A group of related surface glycoproteins distinguish sets and subsets of sensory afferents in the leech nervous system. Brain Res 410:335-339.

Philpot BD, Zukin RS (2010) Synapse-specific metaplasticity: to be silenced is not to silence 2B. Neuron 66:814-816.

Pickard L, Noel J, Duckworth JK, Fitzjohn SM, Henley JM, Collingridge GL, Molnar E (2001) Transient synaptic activation of NMDA receptors leads to the insertion of native AMPA receptors at hippocampal neuronal plasma membranes. Neuropharmacology 41:700-713.

Racca C, Stephenson FA, Streit P, Roberts JD, Somogyi P (2000) NMDA receptor content of synapses in stratum radiatum of the hippocampal CA1 area. J Neurosci 20:2512-2522.

Redondo RL, Morris RG (2011) Making memories last: the synaptic tagging and capture hypothesis. Nat Rev Neurosci 12:17-30.

Renger JJ, Egles C, Liu G (2001) A developmental switch in neurotransmitter flux enhances synaptic efficacy by affecting AMPA receptor activation. Neuron 29:469-484.

Roberts AC, Glanzman DL (2003) Learning in Aplysia: looking at synaptic plasticity from both sides. Trends in Neurosciences 26:662-670.

Rogge RW, Drewes CD (1993) Assessing sublethal neurotoxicity effects in the freshwater oligochaete, Lumbriculus variegatus. Aquatic Toxicology 26:73-89.

Schweigreiter R, Roots BI, Bandtlow CE, Gould RM (2006) Understanding myelination through studying its evolution. Int Rev Neurobiol 73:219-273.

Smith PH, Mittenthal JE (1980) Intersegmental variation of afferent pathways to giant interneurons of the earthworm *Lumbricus terrestris*. Journal of Comparative Physiology A: Neuroethology, Sensory, Neural, and Behavioral Physiology 140:351-363.

Tai MH, Zipser B (1998) Mannose-specific recognition mediates two aspects of synaptic growth of leech sensory afferents: collateral branching and proliferation of synaptic vesicle clusters. Dev Biol 201:154-166.

Takumi Y, Ramirez-Leon V, Laake P, Rinvik E, Ottersen OP (1999) Different modes of expression of AMPA and NMDA receptors in hippocampal synapses. Nat Neurosci 2:618-624.

Thorogood MS, Almeida VW, Brodfuehrer PD (1999) Glutamate receptor 5/6/7-like and glutamate transporter-1-like immunoreactivity in the leech central nervous system. J Comp Neurol 405:334-344.

Vansteenhouse HC, Horton ZA, O'Hagan R, Tai MH, Zipser B (2010) Phylogenetic conservation of the cell-type-specific Lan3-2 glycoepitope in Caenorhabditis elegans. Dev Genes Evol 220:77-87.

Voronin LL, Cherubini E (2004) 'Deaf, mute and whispering' silent synapses: their role in synaptic plasticity. J Physiol 557:3-12.

Wall PD (1977) The presence of ineffective synapses and the circumstances which unmask them. Philos Trans R Soc Lond B Biol Sci 278:361-372.

Walther JB (1971) Funktionelle anatomie der dorsalen riesenfaser-systeme von Lumbricus terrestris L. (Annelida, Oligoehaeta). Zoomorphology 70:253-280.

Westin J, Ritzmann RE, Goddard DJ (1988) Wind-activated thoracic interneurons of the cockroach: I. Responses to controlled wind stimulation. J Neurobiol 19:573-588.

Wine JJ, Krasne FB (1972) The organization of escape behaviour in the crayfish. J Exp Biol 56:1-18.

Wittenberg GF (2010) Experience, cortical remapping, and recovery in brain disease. Neurobiol Dis 37:252-258.

Wojtowicz JM, Smith BR, Atwood HL (1991) Activity-dependent recruitment of silent synapses. Ann N Y Acad Sci 627:169-179.

Wojtowicz JM, Marin L, Atwood HL (1994) Activity-induced changes in synaptic release sites at the crayfish neuromuscular junction. J Neurosci 14:3688-3703.

Wolszon LR, Faber DS (1989) The effects of postsynaptic levels of cyclic AMP on excitatory and inhibitory responses of an identified central neuron. J Neurosci 9:784-797.

Xu YZ, Ji Y, Zipser B, Jellies J, Johansen KM, Johansen J (2003) Proteolytic cleavage of the ectodomain of the L1 CAM family member Tractin. J Biol Chem 278:4322-4330.

Ye S, Comer CM (1996) Correspondence of escape-turning behavior with activity of descending mechanosensory interneurons in the cockroach, Periplaneta americana. J Neurosci 16:5844-5853.

Young JZ (1939) Fused Neurons and Synaptic Contacts in the Giant Nerve Fibres of Cephalopods. Philosophical Transactions of the Royal Society of London Series B, Biological Sciences 229:465-503.

Zipser B, McKay R (1981) Monoclonal antibodies distinguish identifiable neurones in the leech. Nature 289:549-554.

Zipser K, Erhardt M, Song J, Cole RN, Zipser B (1994) Distribution of carbohydrate epitopes among disjoint subsets of leech sensory afferent neurons. J Neurosci 14:4481-4493.

Zoran MJ, Drewes CD (1987) Rapid escape reflexes in aquatic oligochaetes: variations in design and function of evolutionarily conserved giant fiber systems. Journal of Comparative Physiology A: Neuroethology, Sensory, Neural, and Behavioral Physiology 161:729-738.

Zoran MJ, Drewes CD (1988) The Rapid Tail Withdrawal Reflex of the Tubificid Worm, Branchiura Sowerbyi. Journal of Experimental Biology 137:487-500.

Zoran MJ, Martinez VG (2009) *Lumbriculus variegatus* and the Need for Speed: A Model System for Rapid Escape, Regeneration and Asexual Reproduction, in Annelids in Modern Biology. In: Annelids in Modern Biology (Shain DH, ed). Hoboken, NJ: John Wiley & Sons, Inc.

Zoran MJ, Drewes CD, Fourtner CR, Siegel AJ (1988) The lateral giant fibers of the tubificid worm, Branchiura sowerbyi: structural and functional asymmetry in a paired interneuronal system. J Comp Neurol 275:76-86.

Zottoli SJ (1977) Correlation of the startle reflex and Mauthner cell auditory responses in unrestrained goldfish. J Exp Biol 66:243-254.

Zucker RS (1972) Crayfish escape behavior and central synapses. I. Neural circuit exciting lateral giant fiber. J Neurophysiol 35:599-620.